U.S. Department
of Transportation
Federal Railroad
Administration

Office of Research,
Development and Technology
Washington, DC 20590

Modeling the Effects of Top-of-Rail Products on Creep Forces in the Wheel-Rail Interface

DOT/FRA/ORD-24/42

Final Report | September 2024

NOTICE

This document is disseminated under the sponsorship of the Department of Transportation in the interest of information exchange. The United States Government assumes no liability for its contents or use thereof. Any opinions, findings and conclusions, or recommendations expressed in this material do not necessarily reflect the views or policies of the United States Government, nor does mention of trade names, commercial products, or organizations imply endorsement by the United States Government. The United States Government assumes no liability for the content or use of the material contained in this document.

NOTICE

The United States Government does not endorse products or manufacturers. Trade or manufacturers' names appear herein solely because they are considered essential to the objective of this report.

REPORT DOCUMENTATION PAGE

Form Approved
OMB No. 0704-0188

1. REPORT DATE *(DD-MM-YYYY)*	**2. REPORT TYPE**	**3. DATES COVERED** *(From - To)*
26/09/2024	Technical Report	Oct 2017 – June 2020

4. TITLE AND SUBTITLE

Modeling the Effects of Top-of-Rail Products on Creep Forces in the Wheel-Rail Interface

5a. CONTRACT NUMBER
DTFR5317C00009

5b. GRANT NUMBER

5c. PROGRAM ELEMENT NUMBER

6. AUTHOR(S)

Zing Lee: ORCID #0000-0002-4140-1113

Roger Lewis: ORCID #0000-0002-4300-0540

Gerald Trummer: ORCID #0000-0001-7317-8879

Klaus Six: ORCID #0000-0002-1005-8041

5d. PROJECT NUMBER

5e. TASK NUMBER

5f. WORK UNIT NUMBER

7. PERFORMING ORGANIZATION NAME(S) AND ADDRESS(ES)

The University of Sheffield, Mappin Street, Sheffield/South Yorkshire S1 3JD, UK

Virtual Vehicle Research GmbH, Inffeldgasse 21a, 8010 Graz, Austria

8. PERFORMING ORGANIZATION REPORT NUMBER

9. SPONSORING/MONITORING AGENCY NAME(S) AND ADDRESS(ES)

U.S. Department of Transportation
Federal Railroad Administration
Office of Research, Development, and Technology
1200 New Jersey Avenue, SE
Washington, DC 20590

10. SPONSOR/MONITOR'S ACRONYM(S)

11. SPONSOR/MONITOR'S REPORT NUMBER(S)
DOT/FRA/ORD-24/42

12. DISTRIBUTION/AVAILABILITY STATEMENT

This document is available to the public through the FRA website.

13. SUPPLEMENTARY NOTES

COR: Abe Meddah

14. ABSTRACT

The main aim of this project was to develop a wheel-rail creep force model that accounts for the effects of third-body layers resulting from the application of a range of top-of-rail (TOR) materials. Initially, researchers carried out experimental assessments of different types of TOR products to assess the pick-up, carry-on, and friction performance of each. They conducted these tests across several scales using a twin-disc simulation of the wheel/rail interface, a scaled wheel rig, and a full-scale rig. The data from the tests were used to inform the development of models for TOR product pick-up and consumption. The team created a graphical user interface (GUI) that allows easy use of the TOR product model and provides access to the main model variables. The GUI can be used to explore the model behavior with respect to field operation in a variety of ways. However, model predictions are extrapolations based on laboratory experiments from small-scale twin-disc tests and full-scale wheel-rail rig tests. The evolution of the friction conditions along the rail in the model predictions for the field are determined by two main processes: the pick-up of TOR product at the application site followed by a steady redistribution of TOR product between wheel and rail, and the consumption behavior of the TOR product as a result of the wheel/rail interaction.

15. SUBJECT TERMS

Wheel/rail interface; friction management; top-of-rail products; friction measurement; friction modelling

16. SECURITY CLASSIFICATION OF:			**17. LIMITATION OF ABSTRACT**	**18. NUMBER OF PAGES**	**19a. NAME OF RESPONSIBLE PERSON**
a. REPORT	**b. ABSTRACT**	**c. THIS PAGE**		89	**19b. TELEPHONE NUMBER** *(Include area code)*

METRIC/ENGLISH CONVERSION FACTORS

ENGLISH TO METRIC	METRIC TO ENGLISH
LENGTH (APPROXIMATE)	**LENGTH (APPROXIMATE)**
1 inch (in) = 2.5 centimeters (cm)	1 millimeter (mm) = 0.04 inch (in)
1 foot (ft) = 30 centimeters (cm)	1 centimeter (cm) = 0.4 inch (in)
1 yard (yd) = 0.9 meter (m)	1 meter (m) = 3.3 feet (ft)
1 mile (mi) = 1.6 kilometers (km)	1 meter (m) = 1.1 yards (yd)
	1 kilometer (km) = 0.6 mile (mi)
AREA (APPROXIMATE)	**AREA (APPROXIMATE)**
1 square inch (sq in, in^2) = 6.5 square centimeters (cm^2)	1 square centimeter (cm^2) = 0.16 square inch (sq in, in^2)
1 square foot (sq ft, ft^2) = 0.09 square meter (m^2)	1 square meter (m^2) = 1.2 square yards (sq yd, yd^2)
1 square yard (sq yd, yd^2) = 0.8 square meter (m^2)	1 square kilometer (km^2) = 0.4 square mile (sq mi, mi^2)
1 square mile (sq mi, mi^2) = 2.6 square kilometers (km^2)	10,000 square meters (m^2) = 1 hectare (ha) = 2.5 acres
1 acre = 0.4 hectare (he) = 4,000 square meters (m^2)	
MASS - WEIGHT (APPROXIMATE)	**MASS - WEIGHT (APPROXIMATE)**
1 ounce (oz) = 28 grams (gm)	1 gram (gm) = 0.036 ounce (oz)
1 pound (lb) = 0.45 kilogram (kg)	1 kilogram (kg) = 2.2 pounds (lb)
1 short ton = 2,000 pounds (lb) = 0.9 tonne (t)	1 tonne (t) = 1,000 kilograms (kg) = 1.1 short tons
VOLUME (APPROXIMATE)	**VOLUME (APPROXIMATE)**
1 teaspoon (tsp) = 5 milliliters (ml)	1 milliliter (ml) = 0.03 fluid ounce (fl oz)
1 tablespoon (tbsp) = 15 milliliters (ml)	1 liter (l) = 2.1 pints (pt)
1 fluid ounce (fl oz) = 30 milliliters (ml)	1 liter (l) = 1.06 quarts (qt)
1 cup (c) = 0.24 liter (l)	1 liter (l) = 0.26 gallon (gal)
1 pint (pt) = 0.47 liter (l)	
1 quart (qt) = 0.96 liter (l)	
1 gallon (gal) = 3.8 liters (l)	
1 cubic foot (cu ft, ft^3) = 0.03 cubic meter (m^3)	1 cubic meter (m^3) = 36 cubic feet (cu ft, ft^3)
1 cubic yard (cu yd, yd^3) = 0.76 cubic meter (m^3)	1 cubic meter (m^3) = 1.3 cubic yards (cu yd, yd^3)
TEMPERATURE (EXACT)	**TEMPERATURE (EXACT)**
[(x-32)(5/9)] °F = y °C	[(9/5) y + 32] °C = x °F

QUICK INCH - CENTIMETER LENGTH CONVERSION

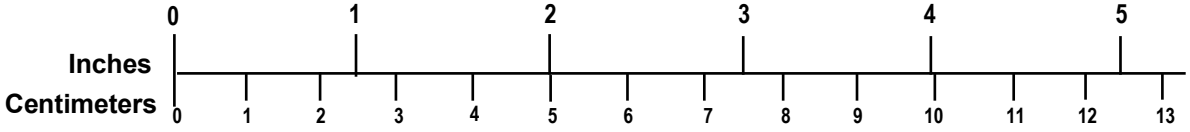

QUICK FAHRENHEIT - CELSIUS TEMPERATURE CONVERSIO

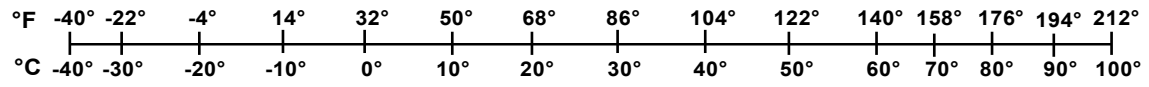

For more exact and or other conversion factors, see NIST Miscellaneous Publication 286, Units of Weights and Measures. Price $2.50 SD Catalog No. C13 10286

Updated 6/17/98

Contents

Illustrations

Tables

Executive Summary

The main aim of this project was to develop a wheel-rail creep force model that accounts for the effects of third-body layers resulting from the application of a range of top-of-rail (TOR) materials (such as TOR friction modifiers, TOR lubricants, etc., [see Stock et al., 2016 for full definitions of materials]) over a range of creepages.

Initially, researchers carried out experimental assessments of different types of TOR products, including TOR-FMs (water-based drying products), two TOR lubricants (TOR-oil and TOR-grease), and a hybrid product (TOR-hybrid) to assess the pick-up, carry-on, and friction performance of each. They conducted these tests across several scales using a twin-disc simulation of the wheel/rail interface, a scaled wheel rig, and a full-scale rig.

The research team drew these conclusions from the tests:

- Water-based, drying, TOR-FMs provided intermediate levels of friction, whereas TOR lubricants (oils and greases) showed much lower friction levels.
- TOR lubricants had a lower consumption rate than TOR-FMs but had a prolonged period of low friction.
- The TOR-hybrid (a mix of water- and oil-based product) showed mixed results behavior.
- Pick-up and carry-on were only investigated for two TOR-FMs. The behavior was largely dictated by the viscosity/tackiness of the product.

The tests themselves can be used in the future to assess new products' performance and benchmark them against the products trialed in this project. The data from the tests were used to inform the development of models for TOR product pick-up and consumption.

As part of the model development, the team created a graphical user interface (GUI) that allows easy use of the TOR product model and provides access to the main model variables. The GUI can be used to explore the model behavior with respect to field operation in a variety of ways. However, model predictions are extrapolations based on laboratory experiments from small-scale twin-disc tests and full-scale wheel-rail rig tests.

The evolution of the friction conditions along the rail in the model predictions for the field are determined by two main processes: the pick-up of TOR product at the application site followed by a steady redistribution of TOR product between wheel and rail, and the consumption behavior of the TOR product as a result of the wheel/rail interaction.

The model code can be integrated into other models, such as multi-body dynamics simulations, to facilitate assessment of TOR products on vehicle dynamic performance. The code can be obtained from FRA or University of Sheffield. University of Sheffield/Virtual Vehicle Research Center engineers can provide training in the model used for this project.

1. Introduction

This section gives an overview of the project background and the aim of the work.

1.1 Background

Previous research has shown that the traction-creepage characteristic of the wheel-rail interface is strongly influenced by increased temperatures in the contact patch due to high creepages (falling friction), the normal load in combination with the contact geometry, and the shearing behavior of third-body layers (see Stock, et al., 2016, for example). Current vehicle-track interaction (VTI) software packages are not able account for this sufficiently. They use either creep force models based on Kalker's theory (Kalker, 1967 and 1982), assuming a constant coefficient of friction (not able to predict falling friction) or models predicting more complex traction characteristics with empirical input parameters (Polach, 2005, Spiyagin, et al., 2013, Vollebregt, 2014) without appropriate connection to the physical phenomena behind it. These models do not account for specific third-body layers or the effect of heat at higher creep levels. This results in incorrect calculation of contact forces and, thus, vehicle dynamics, wear, and rolling contact fatigue (RCF) predictions are inaccurate. With current modelling approaches, it is also impossible to show the benefits of TOR material application and discriminate between different products (e.g., FMs, TOR lubricants). A new model is required that allows for TOR product performance to be incorporated into models of train performance.

1.2 Objectives

The main aim of the project was to develop a wheel-rail creep force model that takes account of the effects of third-body layers resulting from the application of a range of top-of-rail (TOR) materials (such as TOR friction modifiers, TOR lubricants, etc. [see Stock, et al., 2016 for full definitions of materials]) over a range of creepages.

1.3 Overall Approach

Researchers intended to provide a basis for assessing and utilizing the full benefits of TOR materials regarding all aspects of VTI. The development of the model was based on an understanding of the main physical phenomena occurring in the wheel-rail interface (the influence of temperature, elastic-plastic behavior of third-body layers, load dependency, etc.). The model was intended to be a MATLAB tool that could be integrated to any VTI software. The experimental work carried out to derive inputs for the model was also intended to provide a means to benchmark TOR materials prior to field application.

The research team began with a focus on wayside application devices. The target for the model was an ability to predict the creep force characteristics on the track, dependent on the distance from the applicator and the number of wheel passes after application (TOR carry-down and TOR consumption). This is complex because the application is typically every 8 to 48 axle passes; the model must account for product pick-up and transfer down the track, so the TOR deposit can be considered and then consumption of the TOR that occurs prior to the next application. This is shown schematically in Figure 1. The model was initially targeted at the industry stakeholders, shown in Table 1; possible applications are also listed.

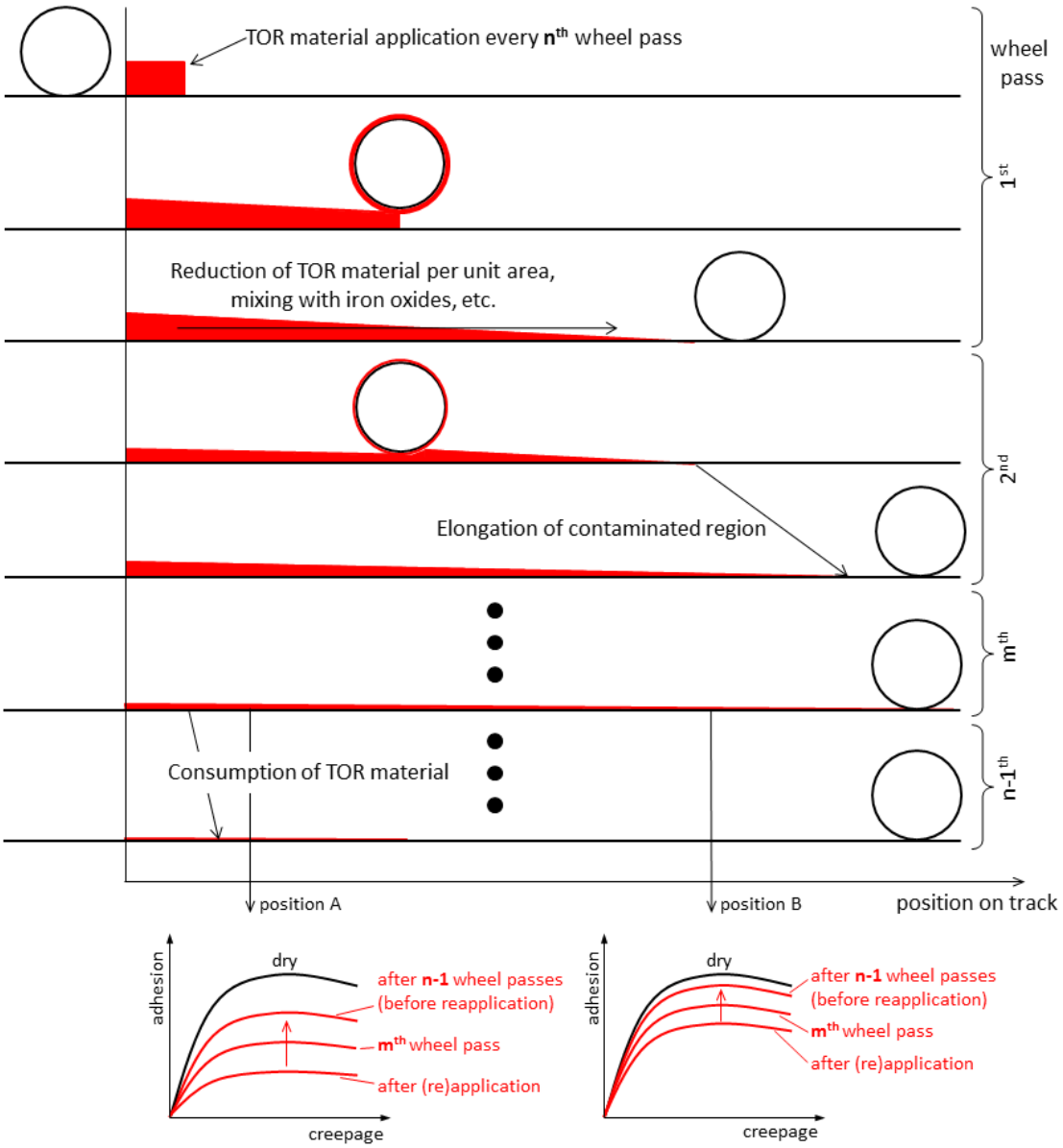

Figure 1. Effects of TOR carry-on and TOR consumption on TOR coverage as a function of position on the track and the number of wheel passes

Table 1. Industry stakeholders and ways to use the creep force model for TOR materials

Industry Stakeholder	Model Uses
TOR material suppliers	• In product development • In developing business case for use of TOR materials • To determine the best approach for product application dependent on operating conditions (load, curve radius, etc.) • Tribological test methods developed will also help in product benchmarking.
Infrastructure owners/maintainers	• Incorporated into VTI software, the model can help predict the impact of TOR material application on reducing wheel-rail forces and track damage (wear, RCF, corrugation, etc.) dependent on operating conditions (load, curve radius, etc.). • To determine which product to apply where in what amounts (field side application) • It could also be incorporated into a track access charging model to assess track-friendliness of trains applying TOR materials.

Industry Stakeholder	Model Uses
Train manufacturers/operators	• Incorporated into VTI software, the model can help predict the impact of TOR material application on reducing wheel-rail forces and wheel damage (wear, RCF, polygonization, etc.) dependent on operating conditions (load, curve radius, etc.). • To improve models of train performance taking account of third-body layers • To determine which product to apply where and in what amounts (on board systems) • To make the case for reduced track access charging due to improved track friendliness • To make the case for reduced energy consumption due to reduced curving resistance • To improve traction and braking control strategies
Wheel-rail interface researchers	• To improve models of train performance taking account of third-body layers • To improve development of creep force and damage models

1.4 Scope

The research team split this project into three work packages: Data Collection (WP1), Tribological Testing (WP2), and Friction Modifier (FM) Model Development (WP3); Figure 2.

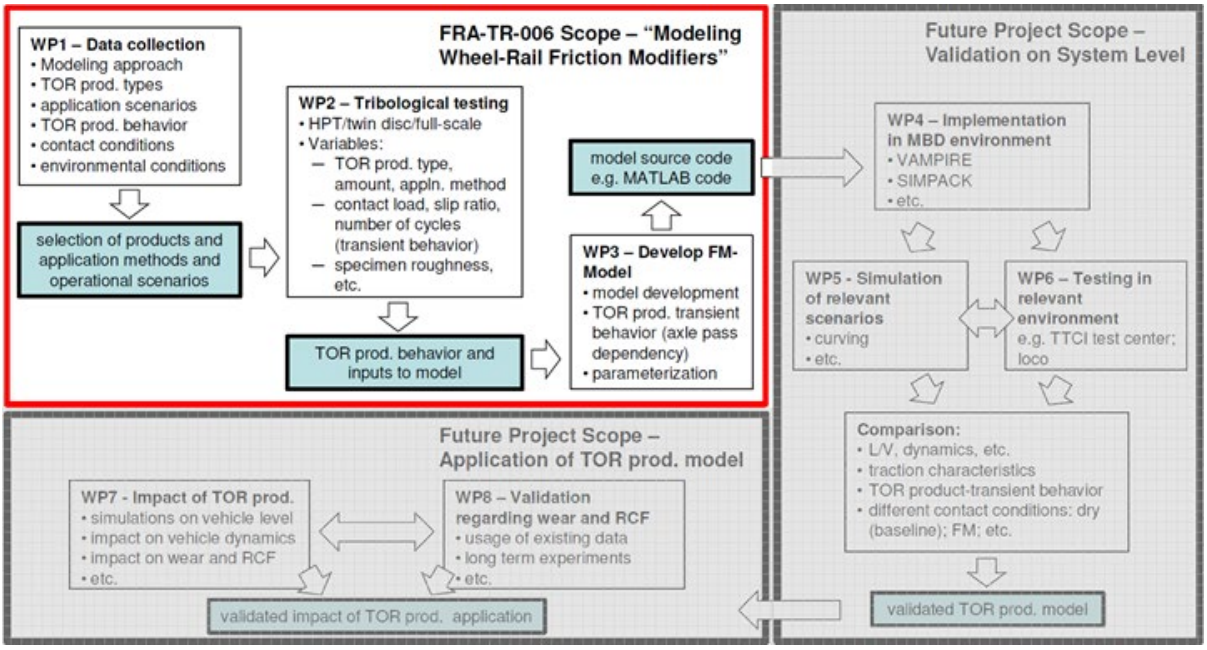

Figure 2. Project plan flow chart

1.5 Organization of the report

The report is split into sections, each of which report the activity carried out in relation to each of the three work packages: Data Collection (WP1), Tribological Testing (WP2), and Friction Modifier (FM) Model Development (WP3). The report sections were as follows:

- Data collection that aims to decide which modeling approach to use and to determine the key model inputs (e.g., TOR material type, variables associated with the operation of the wheel/rail interface, materials, and environmental conditions) and gather appropriate data relating to these inputs.
- Tribological testing to assess TOR Product performance, focusing on studying the essential behaviors of TOR products (pick-up, carry-on, and consumption) and how these affect the friction levels achieved in the wheel/rail interface.

- Development and validation of the wheel-rail creep model. The team divided it into a creep force model and TOR product model. The TOR product model includes a TOR product consumption model and a TOR product carry-on model. It uses the representative (steady-state) creep force curves provided by the creep force model and modifies them accordingly as a function of the number of axle passes and the distance to the applicator. The main output of the modeling approach is the value of adhesion (in form of a working point) along the track.

2. Data Collection

The aim of WP1 was to decide which modeling approach to use and to determine the key model inputs (e.g., TOR material type, variables associated with the operation of the wheel/rail interface, materials, and environmental conditions) and gather appropriate data relating to these inputs.

FRA and a group of academics and industrialists from the International Collaborative Research Initiative (ICRI) formed a stakeholder group, whose membership included most of the groups identified in Table 1.

The stakeholders provided their input/opinion by direct contact (face-to-face or via telephone) and through online questionnaires. Stakeholders helped in considering:

- The full range of TOR products with a view to selecting most appropriate for inclusion in the project
- Application methods (wayside or on-board)
- Operational scenarios (to establish how products are applied and in what amounts and relevant wheel-rail contact conditions)
- Uses for the model to help focus on the applications listed in Figure 2.

Initial work then focused on a critical review of available modeling approaches to select the most appropriate for the purpose of accommodating TOR material effects and meeting the key requirements of the stakeholder group.

2.1 Questionnaire and Responses

As mentioned above, the team drafted a questionnaire to gather stakeholders' input, focusing on TOR materials to be used, the operational and environmental conditions, and the expectations from the model. The full questionnaire created is shown in Appendix A.

Responses were collected from a range of stakeholders in academia and industry, such as engineers from railway infrastructure owners and maintainers, rolling stock operators, builders and maintainers, consultancies, and the industry's supply chain. Full details of responses for each question are available in Appendix B. In the following sections highlight some of the more important information that emerged.

2.1.1 Where Application of TOR Products Is Important

Figure 3 shows a summary of the industry areas stakeholders thought could benefit from the application of TOR products. Most stakeholders thought the application of TOR products would help in influencing wheel-rail damage levels, with vehicle dynamics as the second most popular choice. This was helpful in thinking about where the developed model might be used (as outlined in Section 2.1.3).

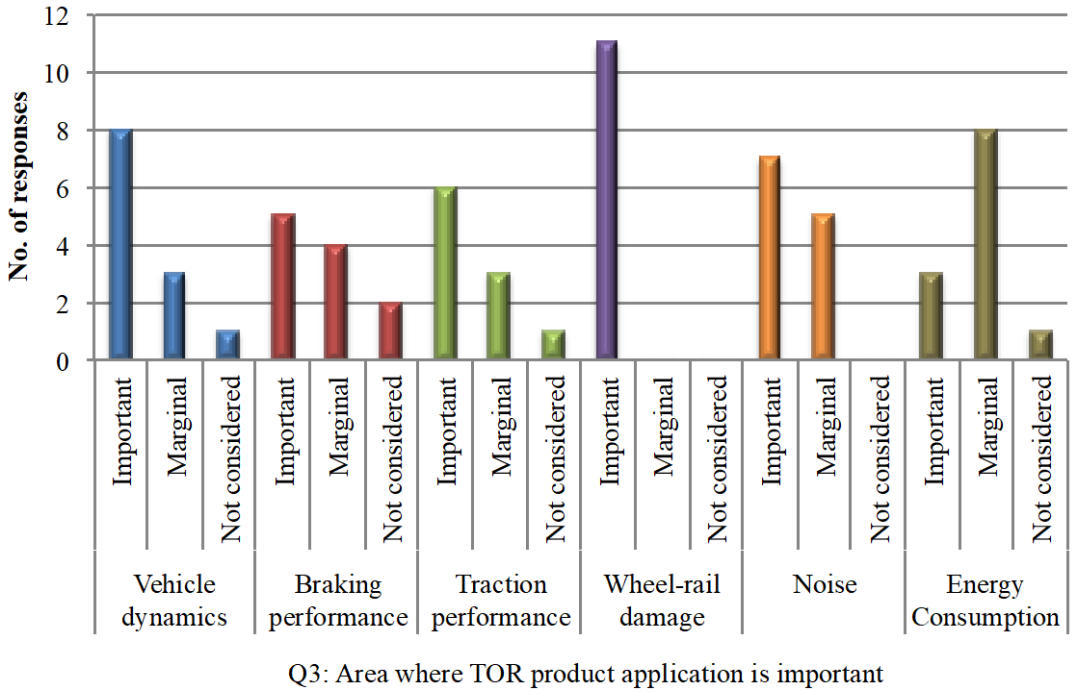

Figure 3. Industry areas that could benefit from the application of TOR products

Some stakeholders reported they already used TOR products in their respective roles. There was a range of different product types listed. It was clear that the team had to investigate the full range of TOR products in selecting those tested in the project. While the type of products mentioned had very diverse properties, they were typically applied to the rail head using wayside systems for the wheel to pick up and carry on the track. Only a few respondents used friction modifiers in onboard systems. This is clearly an emerging technology which is not currently used by many of respondents, so it was not considered for this project, but may be included in future research as usage grows.

2.1.2 Operational and Environmental Conditions

The average train speed ranged between 35 to 70 km/h and the axle load ranged from 45 to 354 kN per axle. The trains could operate under dry or rainy conditions with known temperature ranging from -25 to 60 °C, and the relative humidity ranged from 0 to 100 percent. Known wheel materials were ER7, ER8, C64M, pearlitic (B5T), Class A, B, or C (medium and high-carbon steel), and AAR Class C. Known rail materials were R350HT, R260, bainitic (nose-in switches), pearlitic (R260Mn), high-carbon steel, and AREMA Premium (high strength).

2.1.3 Model Usage

Most respondents expected the creep force model to be useful in improving the prediction of wheel/rail damage with mixed responses in other areas, as shown in Figure 4.

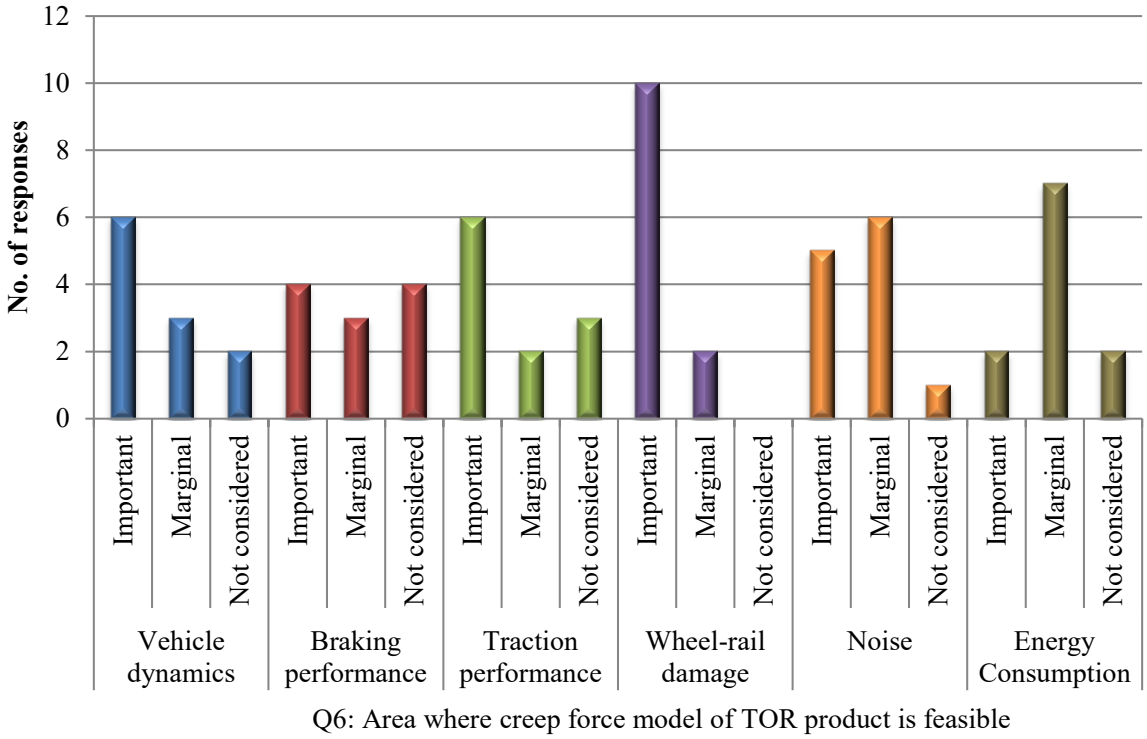

Figure 4. Industry areas that could benefit from the creep force model of TOR product

Three main model uses emerged from the stakeholder engagement:

- As a standalone tool to assess the effect of a TOR product at a particular track
- To determine the application amount of a TOR product (to maximize product performance without over-application)
- For implementation in multibody dynamics
    - This has various applications, including assessment of train performance, possibly as an input to a costing model, and for informing wheel and rail damage models (e.g., for wear or RCF).

These model uses are summarized in a flow chart in Figure 5.

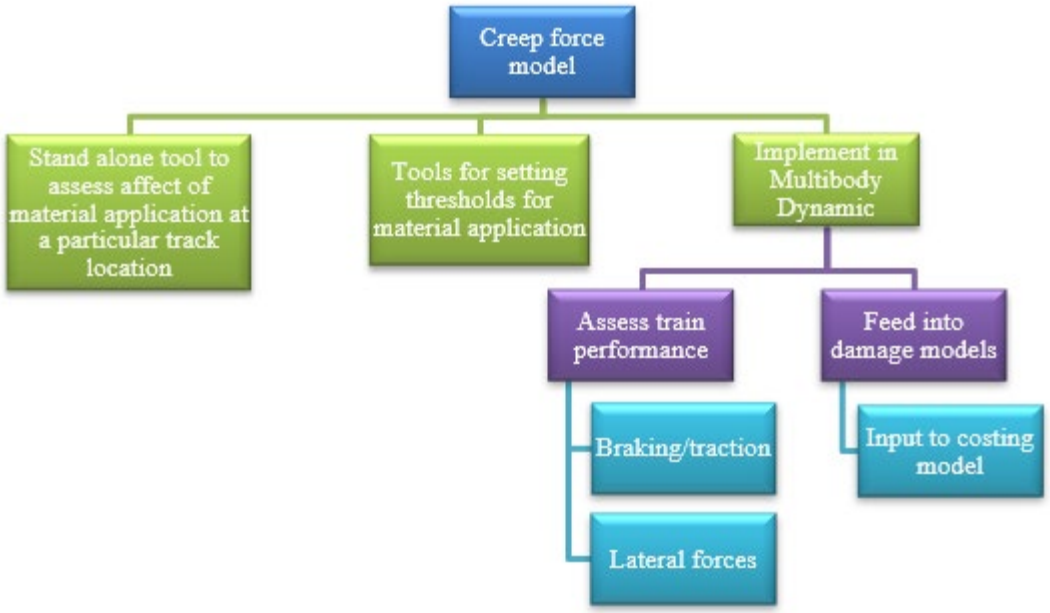

Figure 5. Flow chart of model uses

2.2 TOR Materials

After receiving the feedback from stakeholders regarding TOR product types, the researchers needed to ensure all types were considered. There is misunderstanding regarding terminology used for products applied to the wheel/rail interface, so it was important to carefully define the TOR product types. Descriptions of the main types from Stock, et al. (2016) will be used in this report and are defined below.

2.2.1 TOR Friction Modifier

A TOR friction modifier is "a material that specifically reduces the friction from high levels under dry conditions (0.5–0.8) to an intermediate coefficient of friction (COF) of 0.3–0.4" (Stock, et al., 2016; see Figure 6 for approximate friction ranges). "[A] TOR-FM also provides positive friction characteristics between the wheel and rail over an extended creepage range" (Suda, et al., 2003; see Figure 7).

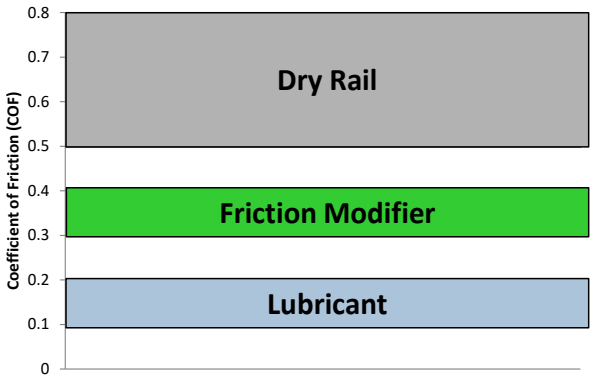

Figure 6. Coefficient of friction levels for different friction management products (Stock, et al., 2016)

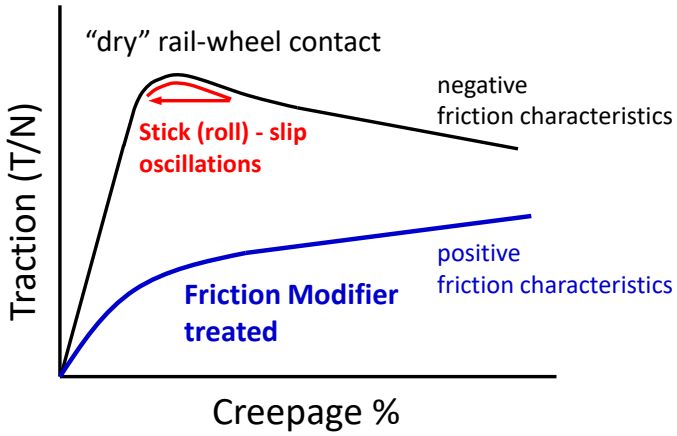

Figure 7. Creep force behavior in dry conditions and with a TOR product applied (Stock, et al., 2016)

2.2.2 Traction Enhancers and Lubricants

A traction enhancer increases friction from low-level conditions and a lubricant reduces the friction to a minimum (e.g., below a friction level of 0.2 at the gauge face). Figure 6 shows the friction levels associated with lubricants versus TOR-FMs. Traction enhancers are expected to bring low adhesion conditions (below 0.1) up to approaching dry conditions.

2.2.3 TOR Lubricants

Recently, new material concepts have been introduced (Stock, et al., 2016). These have significantly different friction mechanisms and cannot be classified as Friction Modifiers. They are generally classified as TOR lubricants:

- TOR-oil (oil-based TOR material)
- TOR-grease
- TOR-hybrid (oil and water-based material)

Field data from Davis (2015; Figure 8) show the performance of the drying, water-based TOR-FMs and the newer TOR lubricants. Application information for each product is in Table 2.

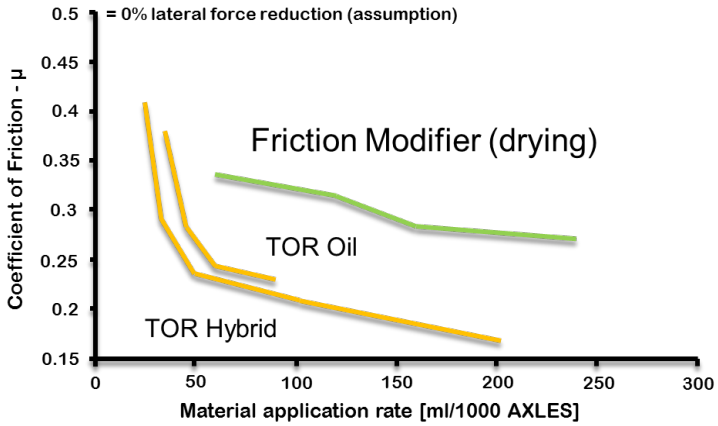

Figure 8. Performance of different TOR products from field measurements (Davis, 2015)

Table 2. Applications of the TOR products using a Protector IV application device

TOR Material Type	TOR-FM	TOR-Oil	TOR-Grease	TOR-Hybrid
Amount applied	0.2-0.6 L per 1000 axles	0.2-0.6 L per 1000 axles	90-360 g per 1000 axles	0.2-0.6 L per 1000 axles
Frequency of application (axle nos.)	Every 8 to 24 axles	Every 10 to 48 axles	Every 10 to 48 axles	Every 8 to 24 axles
Pump activation time (secs)	0.15-0.25	0.15-0.25	0.15-0.25	0.15-0.25
Actual amount per rail per activation	1-5 ml	1-5 ml	1-5 g	1-5 ml

Given the range of observed behaviors in terms of friction levels between the different products, the researchers decided that all product types should be assessed: TOR-FM, TOR-oil, TOR-grease, and a TOR-hybrid product. The team sourced these via project partners and stakeholders.

2.3 Modeling Strategy

From the interactions with stakeholders and FRA, the research team determined that the creep force model to be developed in this project needed to describe the effects of TOR products on creep forces, including temporal and spatial transient effects caused by subsequent load cycles (axle passes). In addition, the model needed to be computationally efficient (i.e., have short calculation times) to be suitable for integration into VTI software. The team reviewed several models to identify a suitable approach.

2.3.1 Review of Modeling Approaches

Creep Force Modeling

A creep force model describes the relationship between frictional forces in rolling contacts and the relative movement of surfaces, the normal contact force, and the contact geometry. Buckley-Johnstone, et al. (2015) and Trummer, et al. (2017) have reviewed various creep force models regarding their ability to account for the effect of water on the adhesion level. These models are either built on the theory of boundary lubrication or on the theory of hydrodynamic lubrication.

Examples of creep force models based on boundary lubrication theory are: CONTACT (Kalker, 1967; Vollebregt, 2014) and FASTSIM (Kalker, 1982; Spiryagin, et al., 2013), the Polach model (Polach, 1999; Polach, 2005), and the ECF model (Meierhofer, 2015; Six, et al., 2015). Creep force models such as the Chen model (Chen, et al., 2002; Chen, et al., 2005), the Popovici model

(Popovici, 2010), the Tomberger model (Tomberger, 2009; Tomberger, et al., 2011), and the Zhu model (Zhu, et al., 2013) use boundary lubrication theory for the contact between surface asperities and hydrodynamic lubrication theory to describe the behavior of the fluid layer.

The Polach model (Polach, 1999; Polach, 2005) is considered the most promising creep force model in this project. It is used as a fast alternative to the FASTSIM model in VTI software. The model can describe changes in the initial slope of the traction curve, which are attributed to the influence of surface roughness and third-body layers in the contact. It predicts a decrease of the coefficient of friction with increasing slip velocity, which is attributed to frictional heating in the contact. The model has been calibrated for dry and wet contact conditions, and it should also be possible to calibrate the model to conditions involving friction modifiers.

The widely used FASTSIM model (Kalker, 1982) has recently been extended by Spiryagin, et al. (2013), similarly to the Polach model. This extension allows for a reduction of the slope of the creep force curve at low creepage and allows for a reduction of the coefficient of friction with increasing slip velocity at high creepage. The FASTSIM model is considered computationally more demanding compared to the Polach model because the contact area is described by discrete elements.

The ECF model (Meierhofer, 2015; Six, et al., 2015) extends the FASTSIM model by a temperature- and normal stress-dependent, elasto-plastic, third-body layer model that addresses the effects of large creepage and solid interfacial layers (e.g., sand, wear debris, friction modifiers) on the traction characteristics. The effects of TOR friction modifier materials have not been incorporated so far. The model and its source code are not publicly available; thus, the model cannot be used as the basis for further model development in this project.

Modeling of Transients Contaminated in the Wheel/Rail Contacts

Two kinds of transient effects are of interest for wayside application of TOR products: the carry-on of product originating from the application site and the removal/degeneration of product from the surface of the rail by repeated wheel/rail contacts.

No model has been found in the literature addressing the carry-on behavior of TOR products in railway operations. However, Hibbert (2017) qualitatively studied the carry-on of a TOR-FM (drying, water-based product) in the laboratory using a modified band saw. Results show that most of the liquid component of the TOR-FM is squeezed out of the contact during a wheel pass so that only traces of friction modifier remain in the contact area. The TOR-FM is carried forward by the edges of the contact and is transferred from the wheel to the rail in several subsequent wheel/rail interactions. A dry layer of TOR-FM transfers from the wheel to the rail and vice versa, but it is not squeezed out of the contact area.

The removal of contaminants from the wheel/rail interface has been modeled in the literature in the past. The model of Allotta, et al. (2014) focuses on degraded adhesion conditions and adhesion recovery based on the frictional work in the contact area. The Polach model includes models for both the creep force curve for degraded adhesion conditions and the creep force curve for recovered adhesion conditions. While rolling without traction, the degraded adhesion condition persists in the model. Adhesion recovery is caused by rolling with creepage. The transition between degraded and recovered adhesion conditions is modeled by an exponential

relationship based on the (instantaneous) value of the specific frictional work per unit of rolling distance.

Voltr and Lata (2015) investigated changes of the adhesion level with varying longitudinal creepage for oil-contaminated conditions on a tram wheel test rig. A typical recording of a creep force curve starts with slowly increasing the driving torque on the wheel from zero. During large sliding between wheel and rail, the torque on the wheel is reduced to zero. The large sliding events typically last several seconds. The (transient) adhesion characteristic is reconstructed from the measured time histories of creepage and tangential frictional force. In the model the transition from contaminated condition to dry (clean) condition is modeled proportionally to the specific dissipated work over a time interval. In addition, the increase/decrease of the coefficient of friction is modeled proportionally to the time derivative of the creep velocity (hysteresis effect). Relating the specific dissipated work over a time interval to the adhesion change causes a time lag in the system response.

2.3.2 Proposed Modeling Approach

The proposed modeling approach in this project can be divided into a creep force model and a TOR product model. The latter is sub-divided into a TOR product consumption model and a TOR product carry-on model. Figure 9 shows the proposed modeling approach.

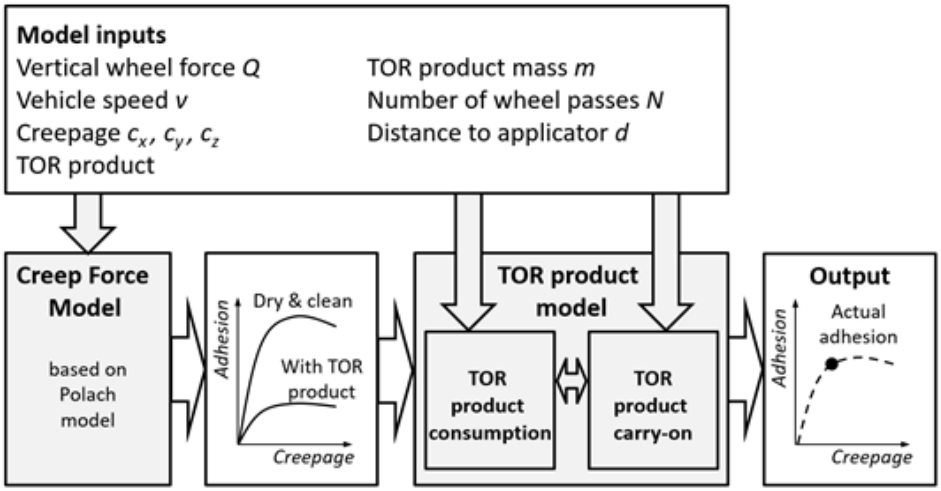

Figure 9. Flow chart of model structure

The creep force model to be used in the project needs to provide information about the adhesion (ratio of the resulting tangential frictional contact force to the normal contact force) as a function of creepage (creep force curves) under various conditions. In this project the Polach model (Polach, 1999; Polach, 2005) will be used, but other creep force models could be used, as well.

The TOR product consumption model addresses the removal/degradation of TOR product with the number of wheel passes on the rail. It uses the creep force curves of the creep force model as an input. Similarly to the work of Allotta, et al. (2014) and Voltr and Lata (2015; see Section

2.3.1), this project's researchers propose that the TOR product consumption model is based on the dissipated frictional work in the contact.

The TOR product carry-on model describes the pick-up of friction modifier from the rail by the wheel and the re-depositing of friction modifier along the track. It is based on the principle of mass conservation. The TOR product model (with its sub-models TOR product consumption and TOR product carry-on) will use the representative (steady-state) creep force curves provided by the creep force model and modify them accordingly as a function of the number of axle passes and the distance to the applicator. The main output of the modeling approach will be the value of adhesion (in form of a working point) along the track.

The minimum set of required input parameters for this modeling approach is listed in Table 3.

Table 3. Minimum set of input parameters for modeling approach

Input parameter	Comments
Vertical wheel force Q	Representative but fixed values will be chosen for the rail head radius, the wheel radius, and the material parameters (steel) to fully specify the Hertzian contact problem.
Vehicle speed v	-
Creepage c_x, c_y, c_z	The relative motion between wheel and rail are given by longitudinal creepage c_x, lateral creepage c_y, and spin creepage c_z
TOR product	Material types considered will include TOR friction modifier, TOR oil, TOR grease and TOR hybrid.
TOR product mass m	Mass of TOR product deposited at the application site
Number of wheel passes N	-
Distance to applicator d	-

2.4 Experimental Approach

After making decisions on the modeling strategy, the researchers selected experimental approaches to assess TOR product performance and determine model inputs and validation data. It was important in the testing to be able to:

- Test across a number of scales to enable model parameterization at a small-scale and comparison with full-scale predictions for model validation.
- Generate appropriate model inputs (thus, friction levels and consumption information were critical).
- Test across a range of creepages and contact stresses.
- Assess pick-up, carry-on, and friction behavior.

After consideration of a range of potential test approaches, in consultation with FRA, the team decided to use a twin-disc approach for small-scale testing for consumption and friction levels and then a scaled wheel rig and full-scale rig to assess pick-up and carry-on, with the full-scale rig also allowing friction measurement. Full details of all the rigs used are shown in Section 3.2.

3. Work Package 2: Tribological Testing

Work package 2 focused on studying the essential behaviors of TOR products (pick-up, carry-on, and consumption) and how these affect the friction levels achieved in the wheel/rail interface.

After the TOR product is applied onto a rail from a wayside applicator, the pick-up and carry-on phenomena determine how much product stays on the wheel and how much product can be carried along the rail. Pick-up is defined as the TOR product being transferred from the rail to the wheel, while carry-on is the TOR product being transferred from the wheel to the rail. The study of product consumption is vital because it shows how long the product could stay on both wheel and rail before a re-application of TOR product is needed. The test rigs selected to study TOR product behavior and their purposes are summarized in Table 4.

Table 4. Allocation of test rigs to study various behaviors of TOR product

Test Rig	Pick-up Behavior	Carry-on Behavior	Consumption Behavior	Friction
Scaled wheel	X	X		
Full-scale	X	X	X	X
SUROS twin-disc			X	X

3.1 Types of TOR Product

A list of TOR products, product types (using definitions from Stock, et al., 2016), and respective test labels are shown in Table 5. This study examines five TOR products: two friction modifier products, two lubricant products, and one hybrid product. Respective test labels are used throughout this study.

Table 5. TOR product types and respective TOR product

TOR Product Type	Test Label
Friction Modifier	FM-A
Friction Modifier	FM-B
Lubricant	TOR-oil
Lubricant	TOR-grease
Hybrid	TOR-hybrid

3.2 Experimental Approaches

The following sections contain details of the test rigs proposed to study the effect of TOR products on wheel/rail interactions. Although each test rig has its advantages and disadvantages, the test rigs have given sufficient data to fully understand the role of TOR products in wheel/rail interaction.

3.2.1 Scaled Wheel Rig

The scaled wheel rig (SWR) is comprised of a scaled wheel (1/5 diameter, full-size profile) and a standard-size rail, as shown in Figure 10. The SWR is manually powered and easy to operate. It provides a quick visualization of how a third-body layer or TOR product interacts with the wheel and rail at contact, such as when studying how TOR products are distributed to the wheel and rail after each wheel pass through a puddle of TOR product or how a wheel carries TOR product

down the rail. However, it does not have load cells or speed sensors to measure the wheel contact force (which is only the weight of the wheel and is relatively low) or the wheel speed.

Figure 10. Scaled wheel rig

3.2.2 Full-Scale Rig

The full-scale rig (FSR; see Figure 11) is a linear device in which the rail is pulled under the wheel as it rotates. It can apply realistic wheel loads via a vertical actuator. Two linear actuators are incorporated, one to pull the rail under the wheel (which stays in a fixed position) and one to pull the wheel (via a chain attached to the wheel) to give the wheel a slightly different speed to achieve controlled creepage at the wheel/rail interface. Normal force, friction force, and creepage are measured during a test. From this information, friction coefficients can be obtained. It is the most representative of the real-world condition among the rigs used. The only limitation is the speed of operation, which is limited to 1 m/s. The rail on the FSR had a removable "pocket" to make taking measurements of the surface easier.

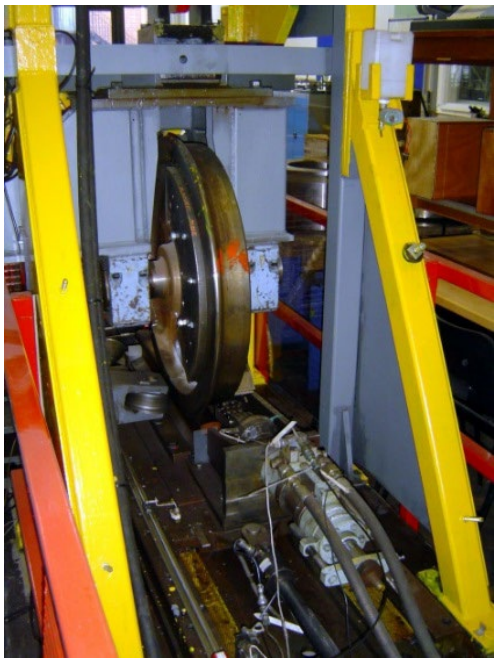

Figure 11. Full-scale rig

3.2.3 SUROS Twin-Disc Rig

The SUROS twin-disc rig, as shown in Figure 12, is used to study the build-up or consumption of TOR products between two rail and wheel discs and to measure friction levels. Normal pressure, creepage, and the amount of product added per application can be varied to investigate how they affect the twin-disc interaction.

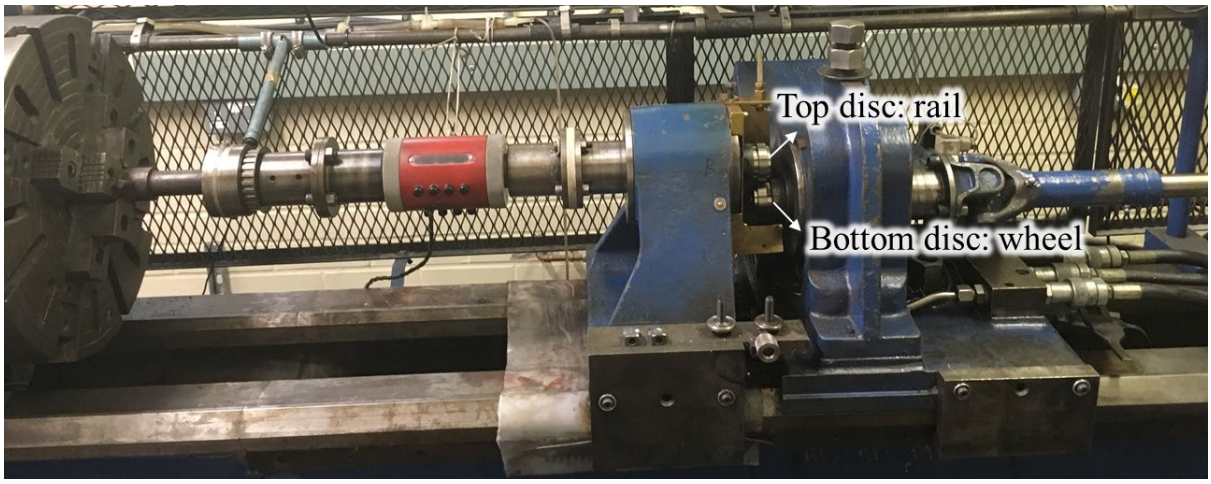

Figure 12. SUROS twin-disc rig

3.3 Pick-Up Behavior

Pick-up behavior is defined as the amount of TOR product being transferred to the wheel from the rail when each untreated wheel passes through a puddle of TOR product, as shown in Figure 13. The research team measured the amount of TOR being picked up each time a clean wheel

passed through the puddle of TOR product on the rail by using an SWR and an FSR. Pick-up tests were performed only on TOR-FMs.

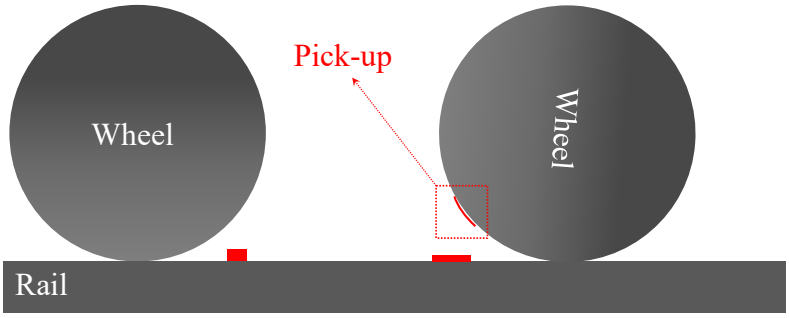

Figure 13. Concept of pick-up phenomenon

3.3.1 Scaled wheel Rig

The team performed pick-up tests using the SWR by rolling the scaled wheel across a puddle of TOR product on the rail, as shown in Figure 14. Then, they lifted the scaled wheel off the rail and returned it to its starting position. They rolled the scaled wheel across the puddle and returned it to its original position two more times. The patches of TOR-FM, labelled region 1 to region 4, were removed using a cleaning cloth after the test. The weight of TOR was calculated by subtracting the weight of the cleaning cloth before and after removing the TOR product.

In these tests, the team investigated the amount of TOR-FM product applied. To evaluate the performance of the TOR products in the amounts of 0.1 ml, 0.2 ml, 0.3 ml, 0.4 ml, 0.5 ml, and 0.6 ml to capture a wide range. The TOR product was measured and applied using a syringe. The pick-up test was repeated twice for each volume. In addition to volume, the weight of the TOR product in each application was measured to minimize the error.

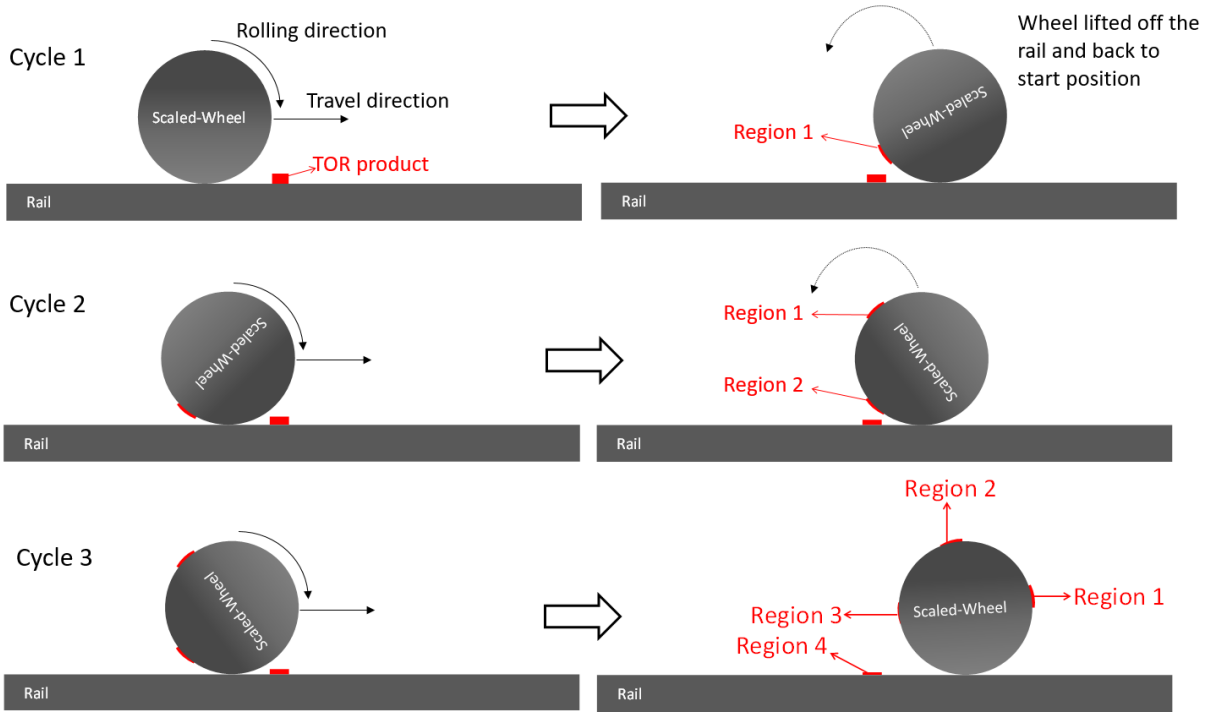

Figure 14. Pick-up test using the SWR

3.3.2 Full-Scale Rig

In the FSR pick-up test, the research team rolled the wheel against the rail while the rail was moving linearly after the initial product application, as shown in Figure 15. After the cycle was finished, they lifted the wheel up and spun it while the rail returned to its original position. They lowered the wheel after both the wheel and rail had returned to their original positions. The TOR patch on the wheel was then removed using a clean cloth (weighed previously) and weighed to measure the amount of TOR removed. Then, the wheel was cleaned using acetone before repeating the test for another two cycles, as shown in Figure 15. The amount of TOR product in region 1, region 2, and region 3 in the figure represents the amount of TOR product picked up by three different wheel cycles. The amount of TOR product in region 4 is what was left on the rail after three cycles.

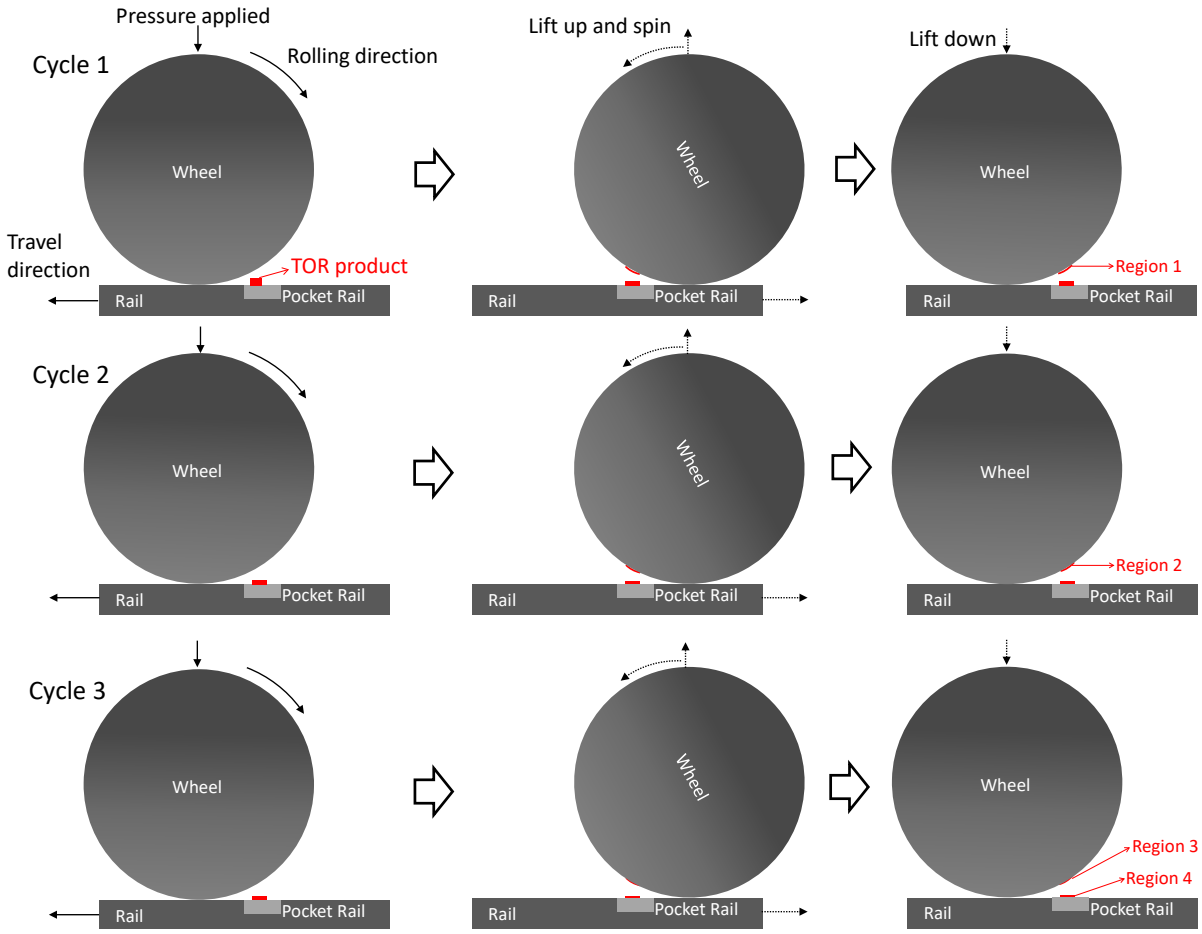

Figure 15. Illustration of pick-up test using FSR

The pick-up tests on TOR-FMs were performed with six amounts: 0.1 ml, 0.2 ml, 0.3 ml, 0.4 ml, 0.5 ml, and 0.6 ml. The test conditions of the FSR pick-up tests were 80 kN normal load, a speed of 100 mm/s, and a creepage of 5 percent.

Additional FSR pick-up tests were carried out without measuring the amount of TOR-FM in each cycle. These tests were performed more than three cycles until the traction force reached a steady dry state without a significant drop due to the lubricating effect of the TOR-FM. The amounts of TOR-FM investigated were 0.1 ml, 0.3 ml, and 0.6 ml. These tests were not repeated.

3.4 Carry-On Behavior

Carry-on behavior is defined as the TOR product being transferred to the rail from the wheel as the wheel carries the TOR product forward to untreated rail, as shown in Figure 16. Only TOR-FMs were investigated in carry-on tests.

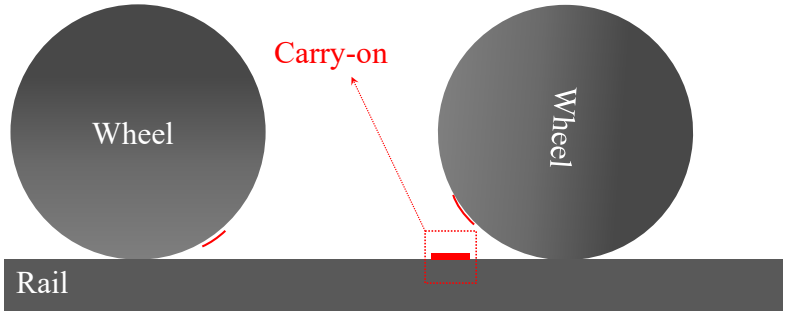

Figure 16. Concept of carry-on phenomenon

3.4.1 Scaled wheel Rig

In the SWR carry-on tests, the TOR-FM with a set volume was applied on the contact band on the rail. Next, the research team rolled the scaled wheel across a puddle of TOR product on the rail, as shown in Figure 17. Then, they spun the scaled wheel locally so the TOR-FM patch that had been picked up on the wheel surface was close to the rail. Then, they rolled the wheel along the clean rail, and some TOR-FM was deposited on the rail. The test stopped after 3 cycles of wheel/rail interaction. The patches with TOR product labelled as region 1 to region 4, as shown in the figure, were removed using a clean cloth and weighed.

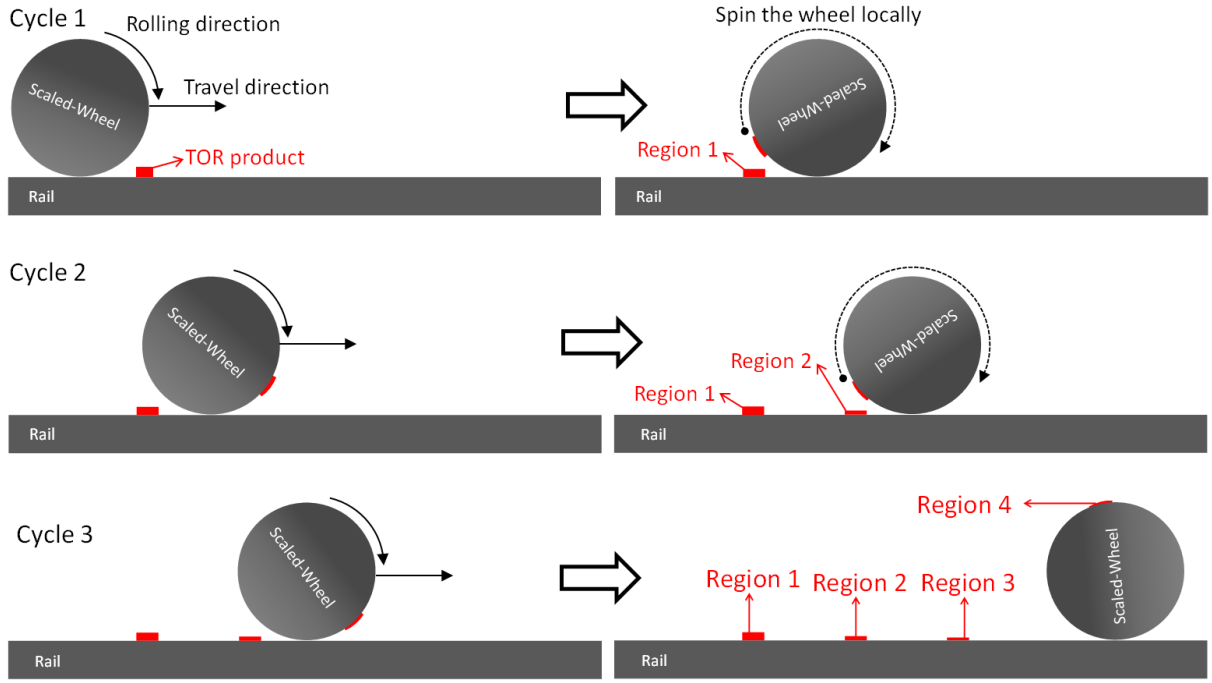

Figure 17. Carry-on test using SWR

Based on the carry-on phenomenon, TOR-FM in region 2 and region 3 were the TOR-FM carried on by the wheel, and the amount of TOR-FM in region 4 was the FM left after two consecutive carry-on cycles. As TOR products must be applied on the rail, the TOR-FM in region 1 was the amount of FM after the FM was picked up by the wheel.

The set volume of TOR-FM was varied: 0.1 ml, 0.2 ml, 0.3 ml, 0.4 ml, 0.5 ml, and 0.6 ml. The weight of the amount applied was also measured. Each carry-on test with set volume was repeated two times.

3.4.2 Full-Scale Rig

In a FSR carry-on test, the wheel was rolled against the rail while it was moving linearly after the initial application of TOR-FM, as shown in Figure 18. After the pick-up of TOR-FM was finished, the wheel was lifted up and spun, while the rail returned to its original position. The wheel was lowered after both the wheel and rail had returned to their original positions. The TOR patch on the rail was then removed using a clean cloth (weighed previously) and weighed to measure the amount of TOR removed. The rail was then cleaned with acetone before repeating the test for another two cycles, as shown in Figure 18. The amount of TOR product in region 2 and region 3 in the figure represent the amount of TOR product carried on. On the other hand, the amount of TOR product in region 4 resembled the product amount left on the wheel after three cycles.

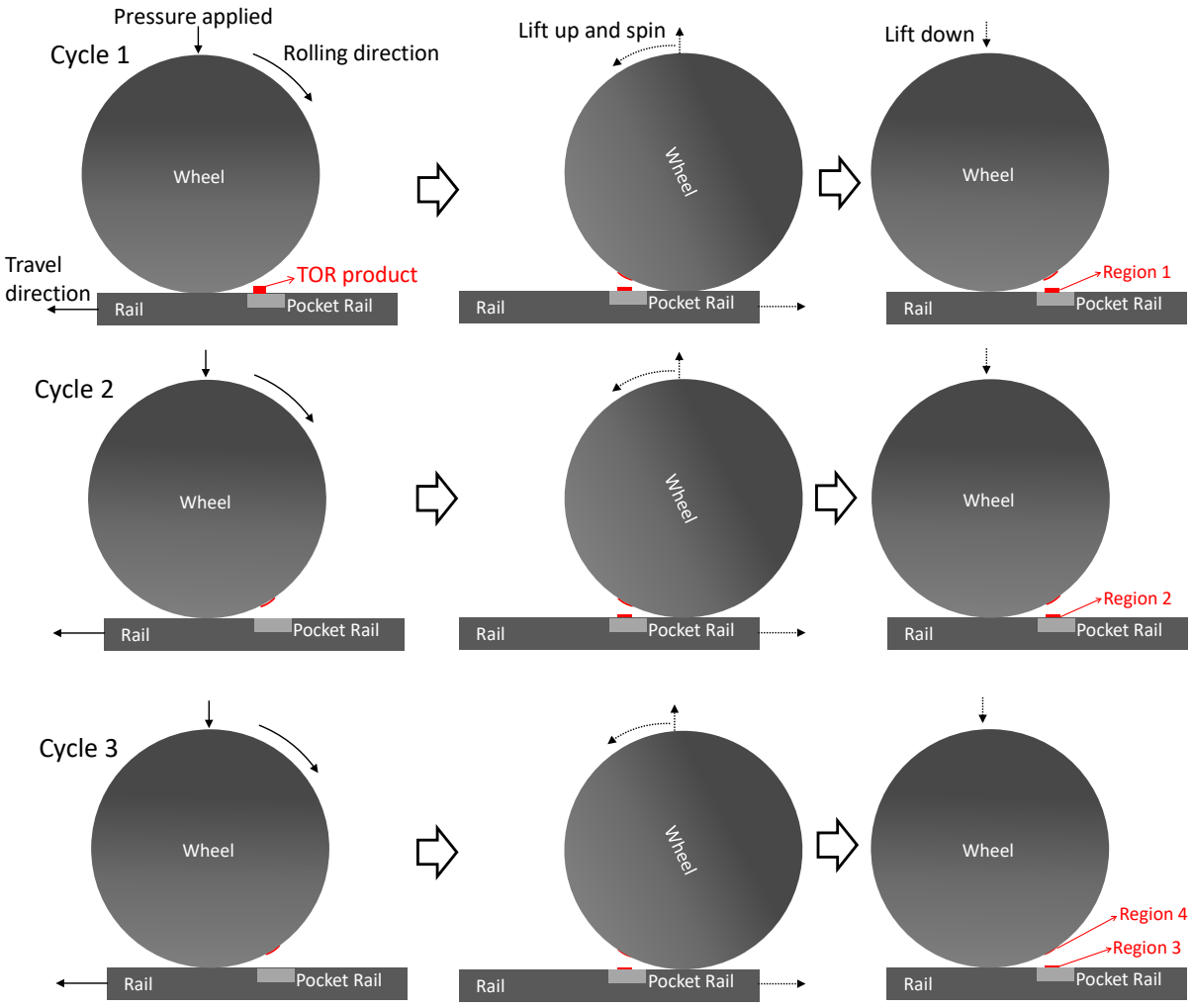

Figure 18. Carry-on test using FSR

The carry-on tests were performed on TOR-FMs for six set volume applications: 0.1 ml, 0.2 ml, 0.3 ml, 0.4 ml, 0.5 ml, and 0.6 ml. The test conditions of the FSR pick-up tests were 80 kN applied normal load, a speed of 100 mm/s, and creepage of 5 percent. Additional FSR carry-on tests were conducted without measuring the amount of TOR-FM in each cycle. These tests were performed for more than three cycles until the traction force reached a steady dry state without a significant drop due to the lubricating effect of TOR-FM. The amount of TOR-FM investigated was 0.1 ml, 0.3 ml, and 0.6 ml. These tests were not repeated.

3.5 Consumption Behavior

Consumption behavior refers to the continuing diminishment of the effects of TOR products to a point when the TOR product is completely spent in a wheel/rail interaction.

3.5.1 SUROS Twin-Disc Rig

Using the SUROS rig with an E8 wheel disc and a R260 rail disc, the research team performed a control test, labelled test (1). They performed the test under conditions of 1,500 MPa, rotational speed of 400 rpm, and 1 percent creepage. Initially, the twin discs ran under dry conditions for 1,000 cycles. Then, the team applied TOR product (weight set at 0.05 g) using a syringe—first, every 3,000 cycles, up to 5 times, next, every 500 cycles 5 times, then, 2 times every 1,500 cycles. The team performed a final application and left the twin-discs running until the product was completely spent. They determined the product was spent when the traction between the discs achieved a steady and stabilized region at an approximately dry coefficient of traction (CoT; 0.45).

The research team performed a second test, labelled test (2), with a decreased applied pressure (900 MPa), while the remaining conditions were kept the same as test (1). A third test, labelled test (3), had decreased creepage (0.5 percent). A fourth test, labelled test (4), had the same conditions as the control test, while the amount of product applied was doubled per application ($\approx$ 0.10 g).

The team performed the above test method on TOR-FMs and a TOR-hybrid. However, the amount of TOR-oil and TOR-grease applied in the control test was less than 0.05 g due to the high lubricity of these products. The same amount (0.05 g) of TOR-oil or -grease would require many more cycles to consume the products. In some cases, these products did not seem to be consumed. The changes in test conditions are summarized as below.

TOR-Oil

The team aimed to apply less than 0.02 g. They increased pressure to 1,800 MPa in test (2), increased the creepage to 5 percent in test (3), and aimed to apply less than 0.005 g in test (4).

TOR-Grease

The research team aimed to apply approximately 0.001 g. As with the main test plan, they decreased pressure to 900 MPa in test (2), decreased creepage to 0.5 percent in test (3), and increased the amount applied in test (4). The test conditions used for TOR-oil tests were not performed on TOR-grease because the increased pressure and increased slip test conditions caused high vibrations on the SUROS twin-disc rig.

For FM-A, FM-B, TOR-oil, and TOR-hybrid, the researchers applied the product with a syringe. For TOR-grease, they used a cotton swab (discarded after each application) instead, which made

it more difficult to achieve a consistent amount of applied TOR-grease. The weight of the applied product was determined by deducting the weight of syringe/cotton swab after application from its weight before application.

3.5.2 Full-Scale Rig

The research team conducted the FSR consumption test to further the study of consumption behavior of TOR-products in a more realistic scenario. Unlike the pick-up and carry-on tests, they did not remove TOR products from the wheel or the rail surface after each cycle. They performed the consumption tests on all TOR-FMs, and the TOR-oil and three pre-set volume applications were investigated: 0.1 ml, 0.3 ml, and 0.6 ml. The following test conditions were set during each consumption test: normal force of 80 kN; creepage of 5 percent, and speed of 100 mm/s. The rail and wheel were sanded and cleaned with acetone before each test. The TOR product was applied at a pre-set volume on the pocket rail before starting the consumption test.

3.6 Results: Pick-Up Behavior

The research team measured how much product had been picked up and how this would affect the frictional behavior during wheel/rail interactions during the investigation of pick-up behavior of TOR-FMs.

3.6.1 Product Distribution

Figure 19(a) and Figure 19(b) show that the FM-A had a fairly even distribution in the first two cycles of wheel/rail interaction. From the third cycle, the product distribution changed. The amount picked up significantly decreased due to the product being consumed and squeezed out of the running band. However, the amount of product picked up in the SWR test was quite low, as shown in Figure 19(a), due to the narrow running band in the SWR testing.

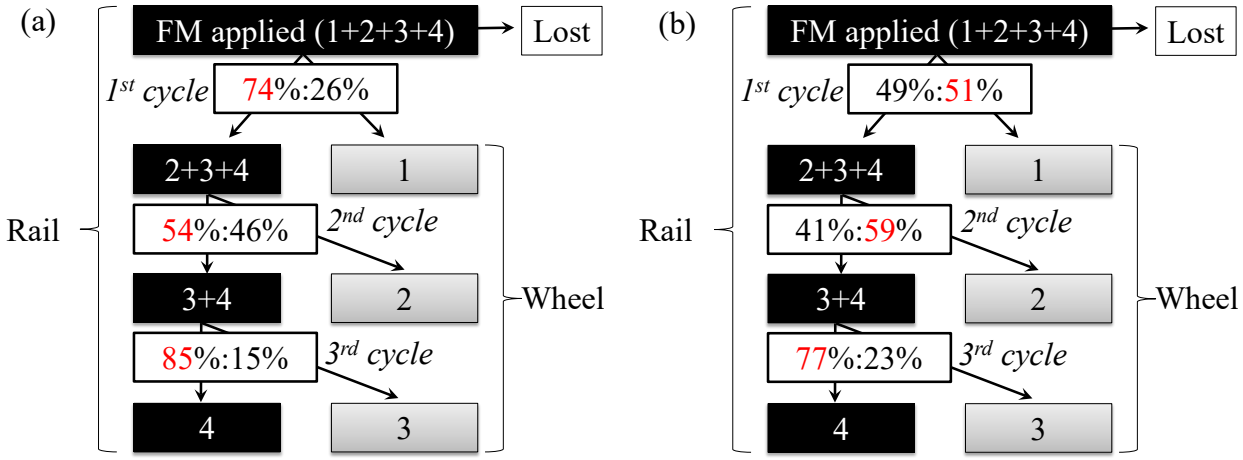

Figure 19. Amount distribution of FM-A in pick-up tests using (a) SWR and (b) FSR

Figure 20(a) and Figure 20(b) show a very consistent pick-up behavior of FM-B in both SWR and FSR tests. FM-B was evenly distributed in the first cycle. From the second cycle, the

percentage amount being picked up swiftly decreased as the FM-B had been pushed out from the running band during wheel/rail interaction.

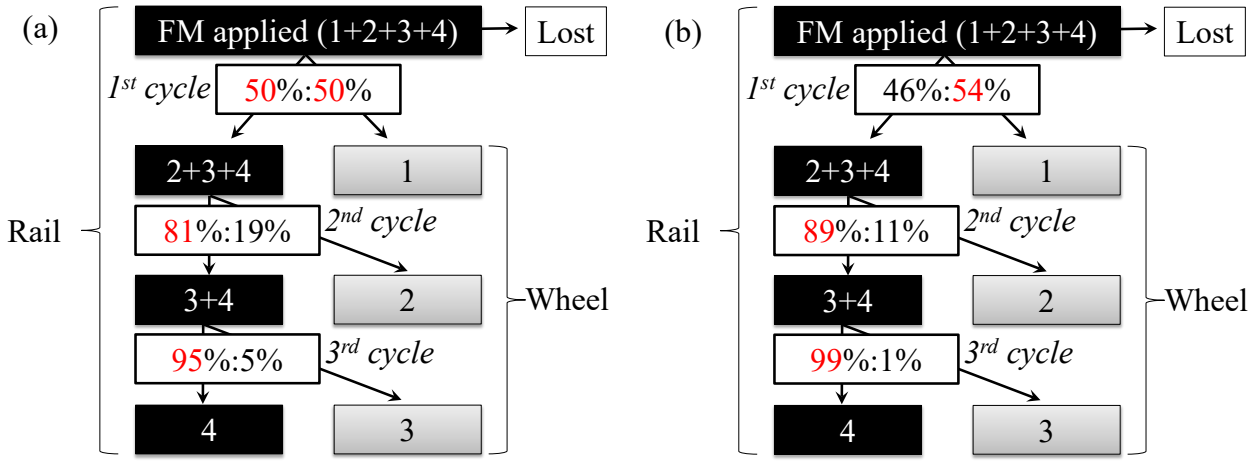

Figure 20. Amount distribution of FM-B in pick-up tests using (a) SWR and (b) FSR

3.6.2 Friction Behavior

Figure 21(a) shows a typical frictional behavior graph of wheel/rail interaction at various cycles with the effect of TOR products. Initially, the traction steadily increased and reached a stable dry value. Then, the traction dropped when the wheel contacted the rail as the TOR product was applied. The low traction maintained a certain distance as the wheel traveled further along the rail. The traction then increased steadily to the dry region as the TOR product was consumed. The overall dry value increased throughout the wheel/rail cycles due to the accumulation of wear debris that could not be cleaned from previous wheel/rail interactions.

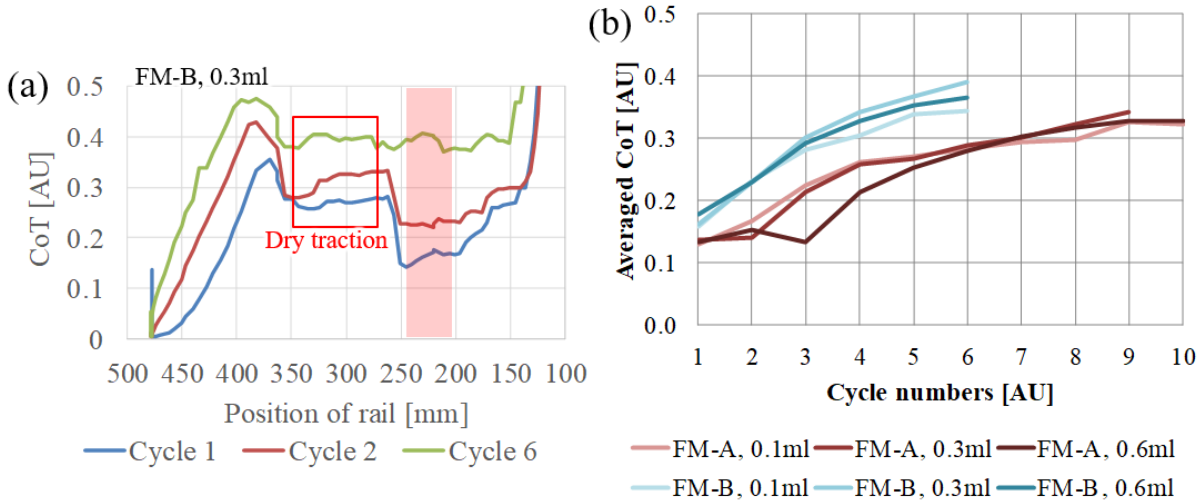

Figure 21. (a) The typical CoT at each position point of the rail and (b) the averaged CoT of different TOR-FMs from each cycle of wheel/rail interaction in FSR pick-up tests

The team averaged and plotted the CoT values in the highlighted red region in Figure 21(a) against the respective wheel/rail interaction cycle, as shown in Figure 21(b). A low amount of FM-A led to a swift increase in coefficient of traction from the third cycle because most of the

FM-A had been picked up in the initial cycles. However, when 0.6ml of FM-A was applied, the coefficient of traction only started to increase from the fourth cycle. This shows that the amount applied plays a role in the retentivity of FM-A. On the other hand, the amount applied of FM-B had little influence on the retentivity of FM-B because the CoT steadily increased from the initial cycles.

3.7 Results: Carry-On Behavior

In the carry-on tests, the carry-on phenomenon occurred from the second wheel/rail interaction cycle onwards, as the wheel had to pick-up the TOR products in the first cycle.

3.7.1 Product Distribution

Figure 22(a) and Figure 22(b) show that the wheel could carry-on a significant percentage of FM-A in the second cycle and a decreased amount in the third cycle. Note that the amount distribution of FM-A in the first cycle of the carry-on tests is in good agreement to that of pick-up tests in SWR and FSR settings, respectively, in Figure 19(a) and Figure 19(b).

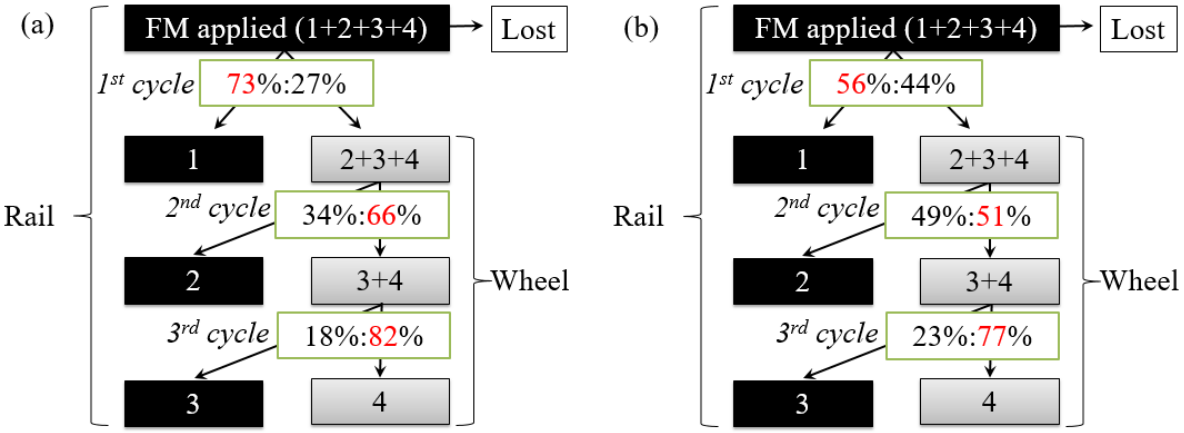

Figure 22. Amount distribution of FM-A in carry-on tests using (a) SWR and (b) FSR

Figure 23(a) and Figure 23(b) show that a significant amount of FM-B was picked up by the wheel. However, only small percentage of FM-B was carried-on further along the rail.

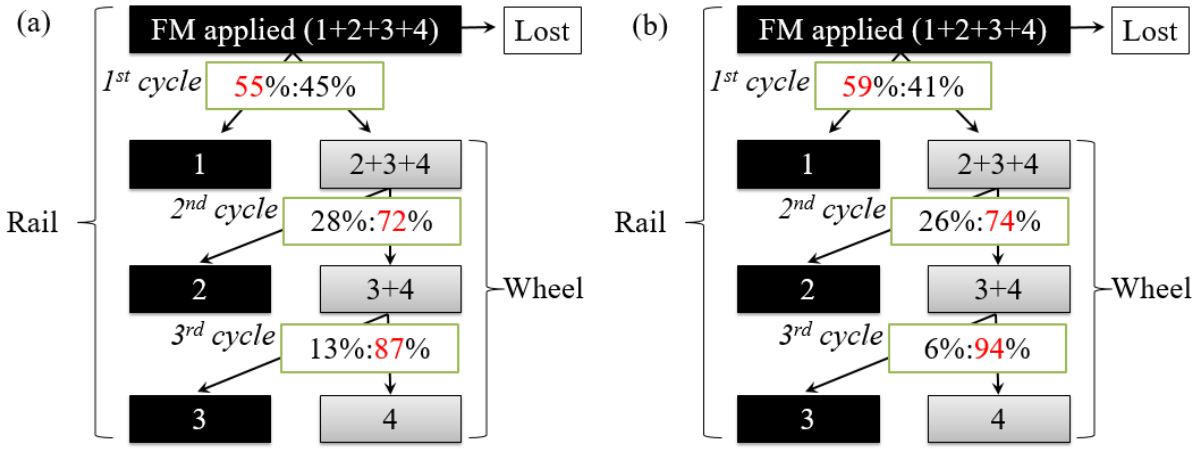

Figure 23. Amount distribution of FM-B in carry-on tests using (a) SWR and (b) FSR

3.7.2 *Frictional Behavior*

Figure 24 shows the traction level of each wheel/rail interaction in the carry-on tests. The CoT of the contact region treated with TOR friction modifiers was lower compared to dry traction. This difference was minimized as the cycle number increased. The number of cycles required to reach dry traction CoT could represent the effective length of the carry-on of the TOR product along the rails.

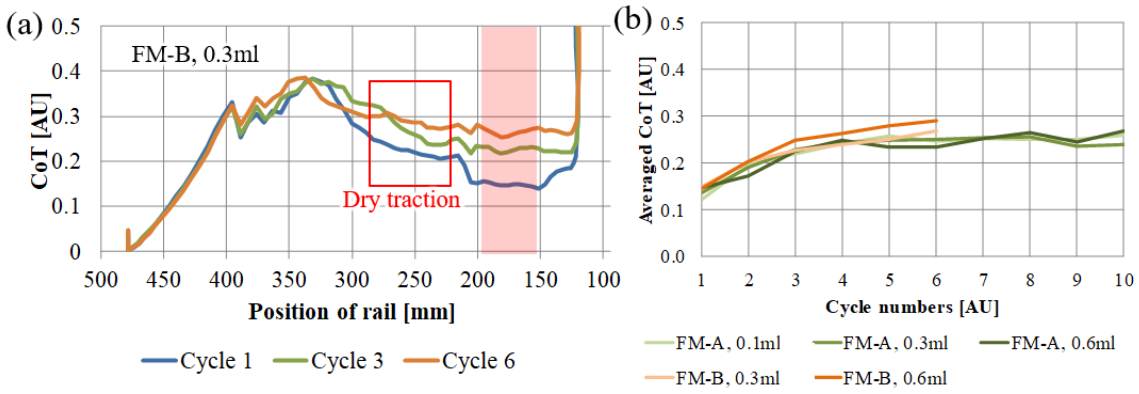

Figure 24. (a) The typical CoT at each position point of the rail in a carry-on test and (b) the averaged CoT of different TOR-FMs from each cycle of wheel/rail interaction in FSR carry-on tests

3.8 Results: Consumption Behavior

3.8.1 *SUROS Twin-Disc Rig*

In the control test, the research team applied FM-A every 3,000 cycles. Figure 25 shows that FM-A was consumed swiftly after each application. When the applications became more frequent, the peak CoT decreased steadily before subsequent application because FM-A accumulated on the disc surfaces. The peak CoT returned to a stable value after the final application, when FM-A was fully consumed. When the normal pressure was decreased in test (2), the peak Cot before subsequent application continuously decreased due to the increase in FM-A accumulation on the disc surfaces. The discs also took more cycles (~27,000 cycles) to fully consume FM-A. The overall CoT value was reduced significantly in test (3) due to the decreased traction from the slip reduction. Nevertheless, the consumption rate seemed similar to that of control test. In addition, the consumption rate in test (4) was very similar to the control test, especially in the latter half of the test.

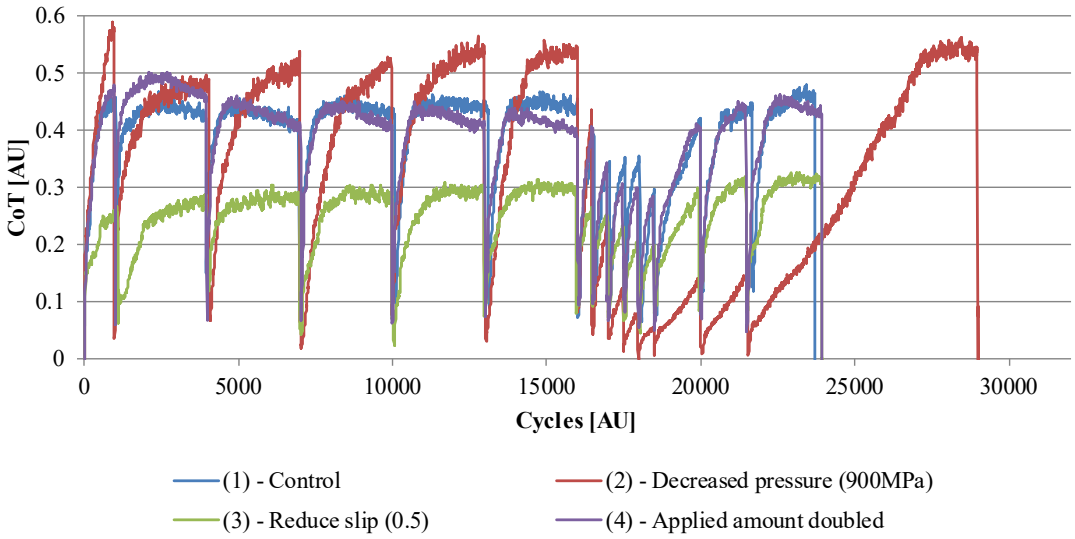

Figure 25. Consumption behavior of FM-A on SUROS

Figure 26 shows the FM-B was also consumed swiftly before subsequent applications throughout the control test. Unlike FM-A, FM-B was not able to accumulate on the disc surfaces despite frequent applications. However, the peak CoT steadily decreased in the region of frequent applications when lower pressure was applied. Nevertheless, the CoT of the discs returned to a dry value shortly after the final application. When the slip was decreased to 0.5 percent, the peak CoT slightly decreased in the region of frequent applications. However, the consumption rate was considered fast. In test (4), the amount applied was doubled, and the overall CoT of the test was lower in comparison to the control test.

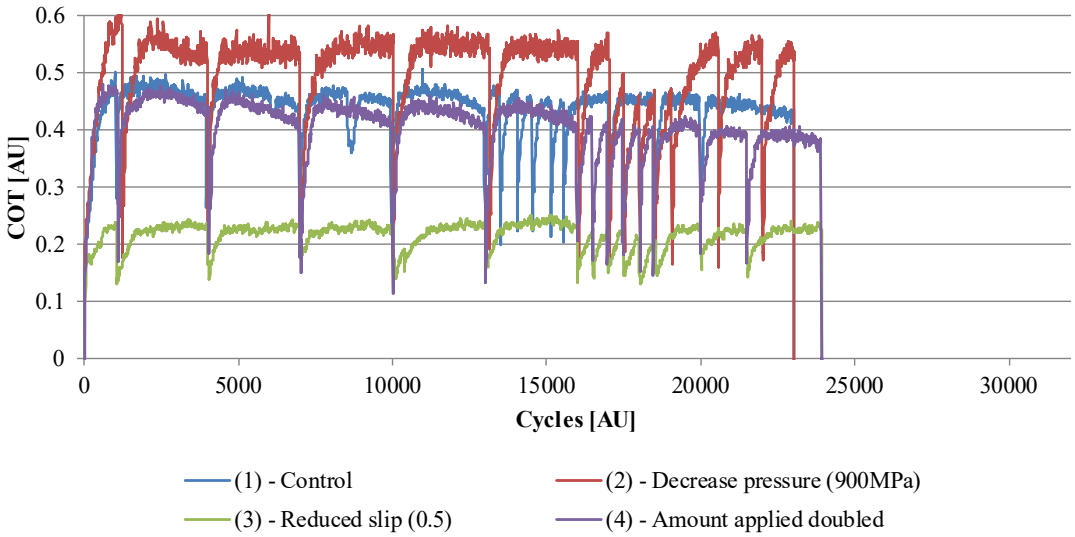

Figure 26. Consumption behavior of FM-B on SUROS

Figure 27 shows that the consumption behavior of TOR-oil was different. The amount applied in the control test was 0.0014±0.007 g. Although this was much lower than the 0.05 g applied previously, the twin-discs still had a low consumption rate of TOR-oil and had difficulty consuming the products in a timely manner under low pressure conditions. As such, the pressure

was increased to 1,800 MPa in test (2) to increase the product consumption rate. The applied amount in test (2) was 0.009±0.002 g. Next, the slip percentage was increased to 5 percent in test (3) for the same purpose. The respective amount applied was average at 0.017±0.005 g. Figure 27 shows the consumption rate was high in the first 16,000 cycles. However, frequent applications caused the subsequent peak CoT to rapidly decrease with each application. The traction steadily returned to dry conditions after the final application. Next, the amount applied in test (4) was further decreased to 0.002±0.002 g. Similar to test (3), the consumption rate of TOR-oil was high in the initial 16,000 cycles. Then, the frequent applications effect reduced the peak CoT before subsequent applications, as film of TOR-oil was being accumulated. The discs then spent a period of cycles to return to the dry state.

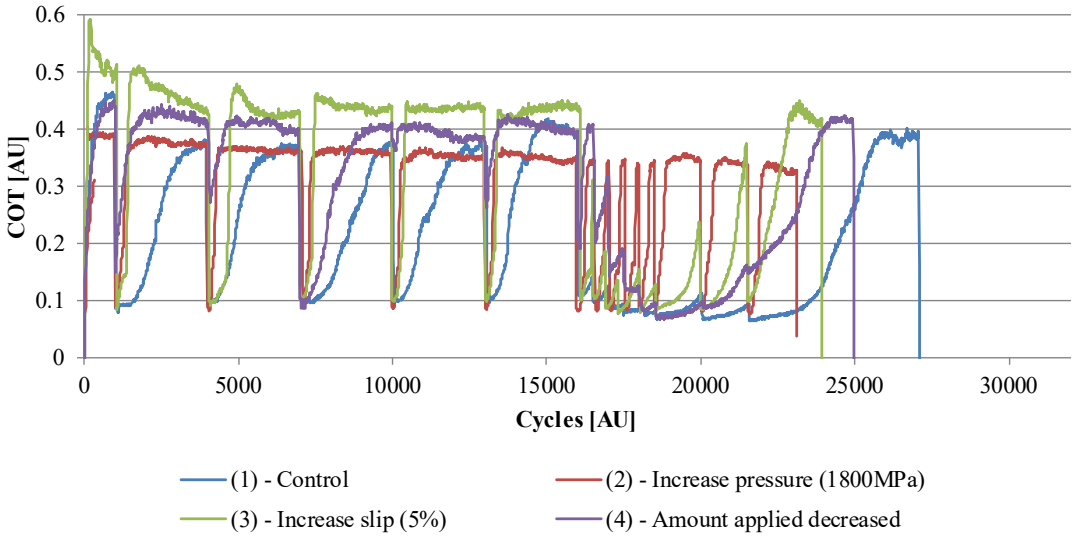

Figure 27. Consumption behavior of TOR-oil on SUROS

The test method used in TOR-oil consumption tests was not repeated in the grease consumption tests due to the potential damaging effects of extreme test conditions. Instead, the research team opted to use the main test method but further reduce the amount of grease applied. The amount applied in test (1), (2), and (3) was 0.0011±0.0006 g, while in test (4) the amount applied was increased to 0.013±0.0087 g. Figure 28 shows that the twin-discs consumed most of the applied grease in the first 16,000 cycles in tests (1), (3), and (4). Test (4) had the lowest consumption rate in this stage. Then, the peak CoT before subsequent applications rapidly decreased to a stable value (~0.05) during the stage of frequent applications for all consumption tests. The tests then allowed the remaining grease to be fully consumed. Test (2) required the greatest number of cycles (~45,000) to fully consume the remaining grease. Test (2) differed from the other tests at the initial consumption stage (first 16,000 cycles) because the peak CoT seemed to be stabilized at approximately 0.3. However, the CoT value of twin-discs was approximately 0.5 at the dry state or when grease was fully consumed under the test conditions of test (2). The conditions of test (2) may have formed a thin film on the disc surfaces that required a high number of cycles to be fully consumed.

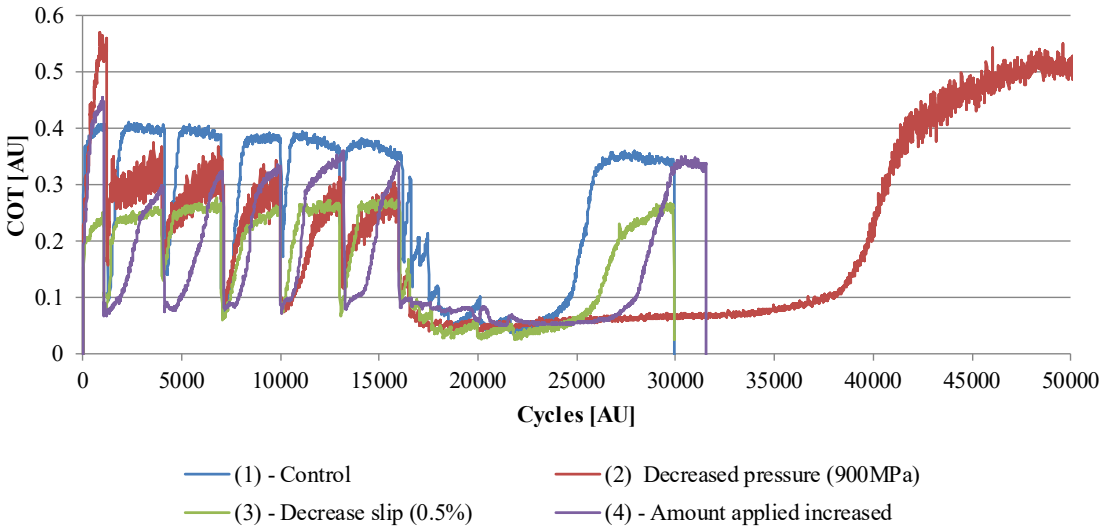

Figure 28. Consumption behavior of TOR-grease on SUROS

Figure 29 shows the consumption behavior of TOR-hybrid. All the twin-disc tests were initially able to consume the TOR-hybrid in a timely manner. Then, the frequent applications reduced the peak CoT significantly. However, TOR-hybrid was steadily consumed after the final application. Test (2) required the greatest number of cycles to fully consume TOR-hybrid. In addition, the peak CoT before subsequent application in the first 16,000 cycles did not stabilize at the expected dry state CoT value. The consumption rate was very similar among all the tests in the first 16,000 cycles. The differences in consumption rate were made obvious only after the final application.

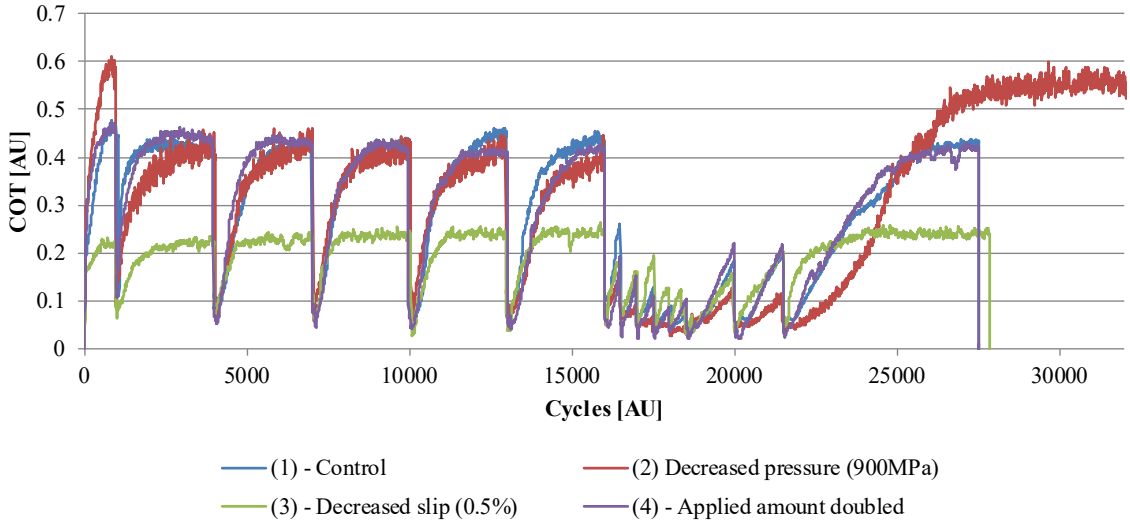

Figure 29. Consumption behavior of TOR-hybrid on SUROS

3.8.2 Full-Scale Rig

Figure 30 shows the consumption behavior of TOR-FMs under a more realistic wheel/rail interaction. Both TOR-FMs had a higher consumption rate when the application amount was

smaller. As the amount applied increased, the consumption rate also became slower. However, the consumption behavior did not experience significant changes after an amount threshold was achieved. When the TOR-FM products are fully consumed, the CoT should be approximately 0.6.

The TOR-oil had a much slower consumption rate overall compared to other TOR products when applied similarly. However, the CoT behavior was seemingly distinctive because it reached and maintained a stable (low) traction level for approximately 300 cycles before steadily increasing to the dry CoT value of 0.6.

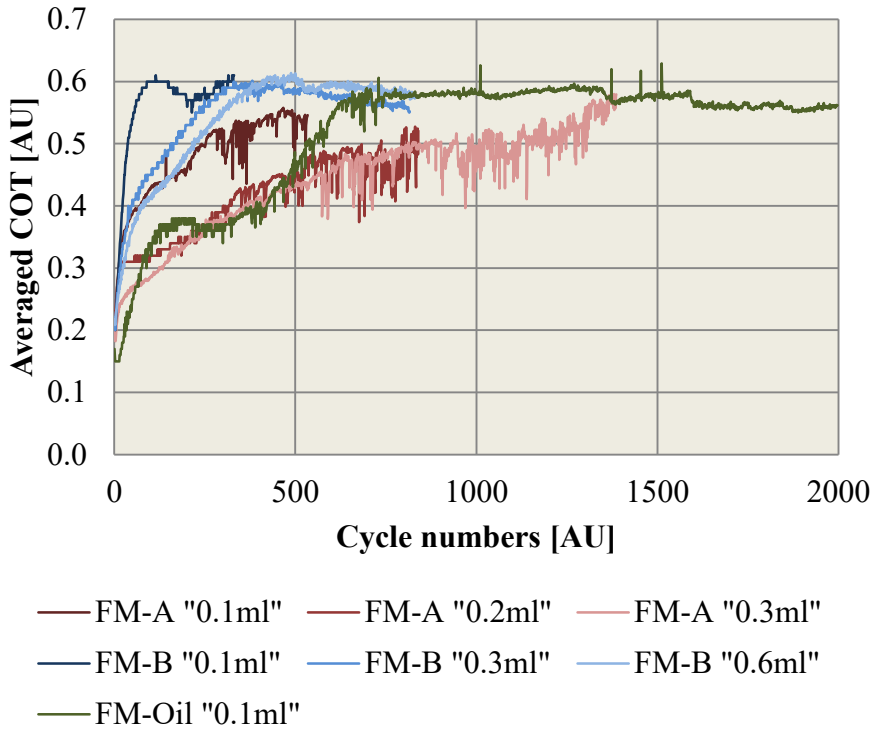

Figure 30. CoT of consumption behavior of various products on FSR

3.9 Discussion

3.9.1 Pick-Up Behavior

Studying pick-up behavior helps researchers understand the transfer mechanism of TOR products from the rail to the wheel. The pick-up phenomenon could occur at any point of the rail if the TOR product lies on the running band of wheel/rail interaction. The pick-up phenomenon where the TOR product is first applied was of particular interest in this study.

Results show that approximately half of a TOR-FM was picked up in the first cycle after the TOR-FM was applied. The amount of TOR-FM picked up then decreased in later cycles until the TOR-FM on the running band was thinned enough not to be picked up. This state is when there is 0 percent product being picked up by the wheel or 100 percent product remaining. The number of cycles required to reach this state could be dependent on the material properties of the TOR-FMs, such as viscosity, tackiness, etc. Due to the tackiness of FM-A, some strings of FM-A

(formed during the separation of wheel/rail) could fall on the running band where they would be picked up by the subsequent wheel. Alternatively, the subsequent wheel would have difficulties picking-up FM-B after the first cycle because FM-B has less viscosity and tackiness. As such, FM-B is less likely to return to the running band after being squeezed out of the contact. Secondly, the amount applied may affect the cycles amount required to reach the "0 percent picked up" state in the case of FM-A, as shown in Figure 21(b). CoT of FM-A stayed at approximately 0.15 for 3 cycles from the initial application. In the case of FM-B, the required number of cycles to reach "0 percent picked up" was not affected by the amount applied.

This study investigated the pick-up and carry-on behavior in a laboratory controlled environment, where the wheel was always in contact with the TOR product at the same lateral point on the rail head. However, in the real world, the wheels may contact the TOR products at different lateral positions; this would affect the overall pick-up and carry-on behavior and the consumption rate.

3.9.2 Carry-On Behavior

Contrary to pick-up behavior, the purpose of studying carry-on behavior is to understand the transfer mechanism of TOR products from the wheel to the rail. Due to the application method of TOR products, the wheel must first pick-up the TOR products and transfer them further along the rail.

The tests in this study focused on how the first wheel carried on the TOR product after it was picked up. In the case of FM-A, the wheel could transfer about half of the TOR-FM it was carrying to the rail. However, only about 27 percent of FM-B was carried on by the wheel. The main reason is the difference in material properties, such as viscosity and tackiness. FM-A adhered more easily to the wheel or rail surfaces due to its tackiness. However, the carried-on FM-A did not seem to affect the frictional behavior of wheel and rail during carry-on tests. This could be due to the product falling outside the running band of the wheel after pick-up. Therefore, the thin layer of product started to be consumed instead of being transferred.

3.9.3 Consumption Behavior

The research team studied the consumption behavior of all TOR products extensively because doing so could highlight the most fundamental differences between the TOR products.

Based on the SUROS twin-disc results, three distinct consumption behaviors could be categorized according to the product type (FM, lubricant, and hybrid). First, under the test conditions used, FMs generally had the fastest consumption rate among TOR products regardless of the application frequency. The consumption rate was influenced by the difference in material properties of the FM. In the case of FM-A, the consumption rate declined significantly at high application rates under lower normal pressure test conditions.

Second, TOR-lubricant products would be required in much smaller amounts to be consumed within the main test method time frame. The next distinct characteristic of TOR-lubricants was the reduction of the peak CoT and consumption rate during high application rates. This was due to the accumulation of such products and their high adhesion to the disc surfaces. In addition, extreme test conditions (1,800MPa and 5 percent slip) were used on TOR-oil to study the relative changes in consumption behavior with a similar low amount. Researchers found that the

consumption rate increased significantly, provided the products had been consumed before re-application.

Third, the TOR-hybrid product had mixed characteristics from both TOR-FM and TOR-lubricants. TOR-hybrid had a similar consumption rate as TOR-FMs under the condition that re-application was completed after the product deposited from previous application was fully consumed. In addition, the peak CoT and consumption rate declined significantly when the application rate was increased. However, the peak CoT was not as low as TOR-lubricants. These characteristics were based on the assumption that TOR-hybrid was thoroughly mixed before application. These distinct consumption behavior characteristics of TOR-FM, lubricant, and hybrid are useful in various scenarios of railway transports.

The team also studied consumption behavior of TOR products using the full-scale rig, which simulated the actual contact conditions between a wheel and a rail, such as the contact shape, contact area, and load distribution. Preliminary results showed that the application amount affected the consumption rate of respective TOR-FMs, although the increased amount in a SUROS setting had little influence on consumption behavior. This could be because the pre-set amount used in SUROS twin-disc consumption tests had already achieved the amount threshold. Therefore, an additional amount would not contribute to the improvement/changes in the consumption rate of the products.

4. Work Package 3: Development of Parameterized Friction Modifier Model

The modeling approach in this project is divided into a creep force model and a TOR product model. The latter is sub-divided into a TOR product consumption model and a TOR product carry-on model. The TOR product model uses the representative (steady-state) creep force curves provided by the creep force model and modifies them accordingly as a function of the number of axle passes and the distance to the applicator. The main output of the modeling approach will be the value of adhesion (in form of a working point) along the track. The model development, structure, and input parameters are outlined in Section 2.3.

4.1.1 Discretization of Track

The friction condition is calculated at discrete points x_i along the rail (see Figure 31). These points are spaced by distance *dx*. This distance is chosen as the mean circumference of the wheels that pass over the track, which means that the evolution of the contact conditions of one point on the wheel surface is followed in the simulation.

$$dx = D \cdot \pi \qquad Equation\ 1$$

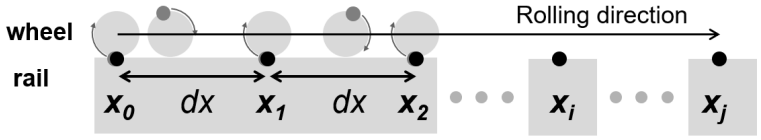

Figure 31. Discretization of track

In rail operation, the characteristic distance *dx* is not a constant; wheels with different diameter *D* roll on the track, the effective rolling radius changes with the lateral position of the wheel, and longitudinal creep occurs in case of traction and braking. The model describes the average friction conditions in the contact area on the rail head and neglects effects that arise from varying lateral contact positions of the wheels on the rail head.

4.1.2 Creep Force Model

To describe the relationship between the relative movement of surfaces in rolling contact and the coefficient of adhesion (ratio of the tangential contact force to the normal contact force) the research team chose Polach's model (Polach, 1999; Polach, 2005). This model is widely used in multibody simulations of railway vehicles. For an overview of these considerations, see Section 2.3.1.

Applying the Polach model to a twin-disc contact situation requires specifying an equivalent contact ellipse that approximates the line contact of the twin-disc experiment. Because the characteristic quantities of the line contact are the contact length (in the rolling direction of the discs) and the contact area, the researchers decided to prescribe these quantities as boundary conditions for the equivalent contact ellipse.

Figure 32 shows the creep force curves for clean, uncontaminated surface condition and for two TOR-FMs determined by twin-disc experiments from Gutsulyak, et al. (2018). The coefficients of friction have been adjusted individually for each creep force curve calculated by the Polach

model. In Figure 32, experimental twin-disc results have been taken from Gutsulyak, et al. (2018) and compared to Polach model results (Q = 2750 N, a = 6.37 mm, b = 0.194 mm, $k_A = k_S$ = 0.6, $A = B$ = 1). The coefficient of friction was chosen individually for each curve (μ_{clean} = 0.60, $\mu_{TOR\text{-}FM\ A}$ = 0.47, $\mu_{TOR\text{-}FM\ B}$ = 0.25). The results show that the friction modifier not only changes the coefficient of friction but also the initial slope of the creep force curve.

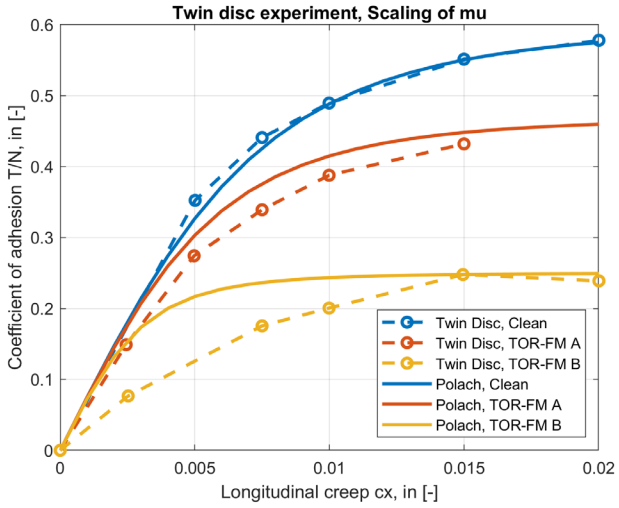

Figure 32. Creep force curves for clean, dry baseline and for two TOR-FMs

The research team obtained a better fit of the experimental data with TOR-FMs by using the clean, dry baseline curve as a reference and scaling the entire creep force curve according to the following equation:

$$\left(\frac{T}{N}\right)_{TORprod.} = \left(\frac{T}{N}\right)_{clean} \cdot \frac{\mu_{TORprod.}}{\mu_{clean}} \qquad Equation\ 2$$

This approach changes both the adhesion level and the initial slope of the creep force curves so that they match the experimental results, as shown in Figure 33. In this figure, the Polach curves for TOR-FM A and TOR-FM B have been scaled according to Equation 2.

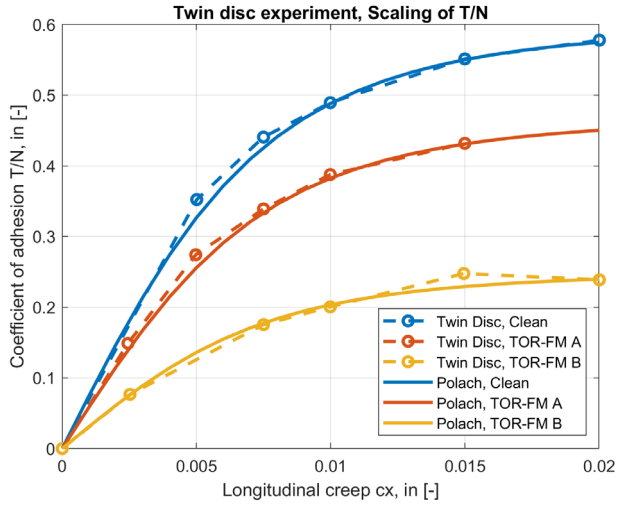

Figure 33. Creep force curves for clean, dry baseline and for two TOR-FMs with scaled creep force

This approach (scaling the entire creep force curve based on the clean, dry baseline curve) has been implemented in the friction modifier model developed in this project.

4.1.3 Consumption Model

TOR product consumption is modeled as TOR product mass loss per load cycle $dm_{TORprod.}/dN$. Based on experimental results from SUROS and FSR experiments, the following form has been chosen:

$$\frac{dm_{TORprod.}}{dN} = k_0 + k_{m1} \cdot \left(1 - exp\left(-\frac{m_{TORprod.}}{m_0 \cdot k_{m2}}\right)\right) \cdot f_p(p_m) \cdot f_c(c_x) \cdot f_i \qquad Equation\ 3$$

This approach causes a constant rate of TOR product mass loss per load cycle for $m_{TORprod.} \gg (m_0 \cdot k_{m2})$ and an exponential decrease for $m_{TORprod.} \approx (m_0 \cdot k_{m2})$. This is visualized in Figure 34.

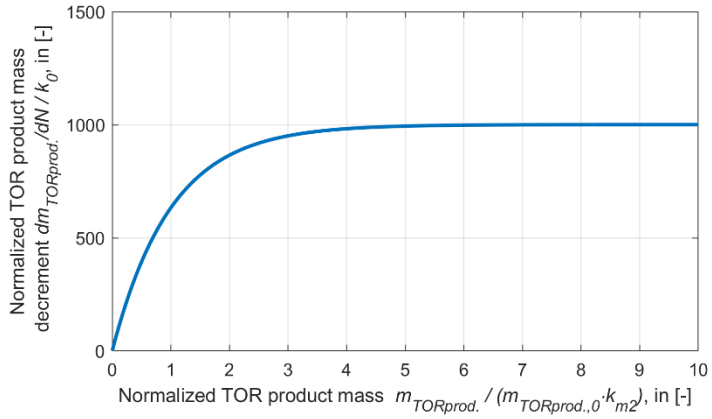

Figure 34. Normalized TOR product mass decrement per cycle $(dm_{TORprod.}/dN)/k_0$ as a function of normalized TOR product mass $(m_{TORprod.})/(m_0 \cdot k_{m2})$ for k_{m1}/k_0 =1000

Experimental data from SUROS and FSR experiments suggest that the contamination condition saturates when large amounts of TOR product are applied. This means that a further increase of TOR product in the contact area does not change the friction characteristic anymore, presumably because excess TOR product does not enter the contact area. This is addressed in the model by limiting the maximum mass of TOR product in the contact area to the value k_x as:

$$m_{TORprod.} = min\left(m_{TORprod.}, k_x\right) \qquad Equation\ 4$$

Likewise, the value of m_0 is limited to a maximum value by $m_0 = \min(m_0, k_{x0})$.

The influence of (mean) normal pressure p_m and creepage c_x on TOR product consumption is considered by factors f_p and f_c, while f_i addresses the change in TOR product consumption in case of TOR-grease and TOR-hybrid.

To account for the change in TOR product consumption in the SUROS experiments as a function of normal pressure the following linear expression for f_p in Equation 3 is used to reproduce the experimental results:

$$f_p = 1 + k_p \cdot \left(\frac{p_m}{1178\ \mathrm{MPa}} - 1\right) \qquad Equation\ 5$$

Test condition 1 of the SUROS experiments with a mean contact pressure of p_m = 1,178 MPa serves as the reference. k_p in Equation 5 was chosen to fit experimental SUROS data at p_0 = 900 MPa for TOR-FM-A, TOR-FM-B, TOR-grease, and TOR-hybrid and at p_0 = 1,800 MPa for TOR-oil.

The team observed a change in the TOR product consumption when the creepage changed in the SUROS experiments. A linear expression for f_c in Equation 3 (similar to Equation 5) is used to account for this influence:

$$f_c = 1 + k_c \cdot \left(\frac{\sqrt{c_x^2 + c_y^2)}}{0.01} - 1 \right) \qquad \textit{Equation 6}$$

Test condition 1 of the SUROS experiments at creepage c_x = 1 percent (and lateral creepage c_y = 0 percent) served as a reference case. k_c was chosen to fit experimental SUROS data at c_x = 0.5 percent for TOR-FM-A, TOR-FM-B, TOR-grease, and TOR-hybrid, and at c_x = 5 percent for TOR-oil.

Spin creepage c_z was not included in the above expression and thus did not change the value of f_c. The form of expressions f_p and f_c (Equation 5 and Equation 6) must be treated with caution, as they were derived based on two levels of normal pressure and creepage in the twin-disc experiment. If additional experiments at different levels and combinations of normal pressure and creepage are available, this may require a modification of these expressions.

Expression f_i in Equation 3 addresses the decreased TOR product consumption in the case of little TOR product on the surface. This behavior was only observed for TOR-grease and for TOR-hybrid in the SUROS experiments. For other TOR products, this factor was set to f_i = 1. A simple way to account for this effect is by introducing a step function to change the TOR product mass decrement per load cycle based on the TOR product mass in the contact:

$$f_i = 1 - k_{i1} \cdot \frac{1 + \mathrm{sgn}\left(k_{i2} - m_{TORprod.}\right)}{2} \qquad \textit{Equation 7}$$

k_{i1} and k_{i2} are model constants that were fitted to experimental results; sgn is the signum function. The effect of f_i on the normalized TOR product mass decrement is illustrated in Figure 35. This figure shows the normalized TOR product mass decrement per cycle $(dm_{TORprod.}/dN)/k_0$ as a function of normalized TOR product mass $(m_{TORprod.})/(m_0 \cdot k_{m2})$ for k_{m1}/k_0 =1000. For the dashed line, the influence of f_i is switched off; for the solid line the TOR product mass decrement was reduced by 70 percent for $(dm_{TORprod.}/dN)/k_0 < 3$.

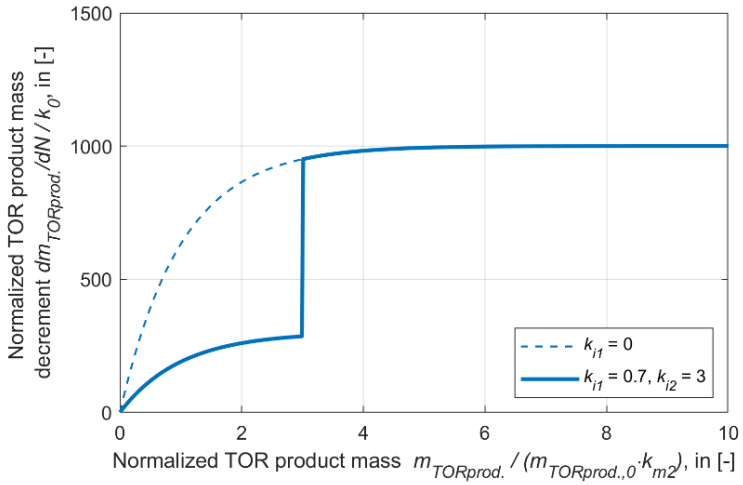

Figure 35. Normalized TOR product mass decrement per cycle (as a function of normalized TOR product mass

4.1.4 TOR Product Amount: Coefficient of Friction Relation

For the prediction of the friction condition, the TOR product mass in the contact must be linked to the coefficient of friction μ. This is done in the model by the following equation:

$$\mu = \mu_{TORprod.} + (\mu_{clean} - \mu_{TORprod.}) \cdot \exp\left(-\frac{m_{TORprod.}}{k_m}\right) \qquad Equation\ 8$$

μ_{clean} is the coefficient of friction in clean, uncontaminated conditions; $\mu_{TORprod.}$ is the corresponding value in the limiting case of a large amount of TOR product in the contact area. The constant k_m determines the exponential decay behavior as a function of the TOR product mass $m_{TORprod.}$ in the contact. The change of μ as a function of TOR product mass $m_{TORprod.}$ is visualized in Figure 36.

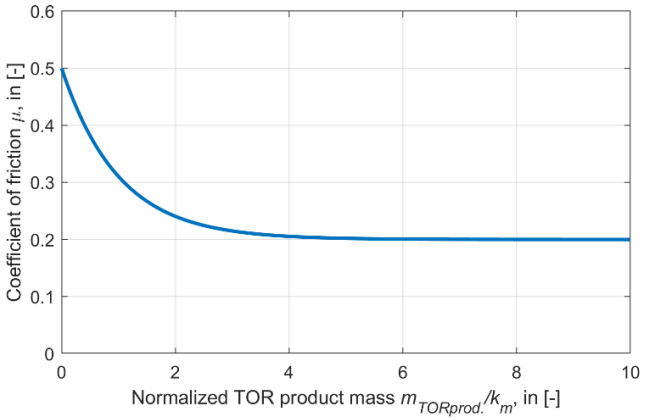

Figure 36. Change of coefficient of friction μ as a function of normalized TOR product mass $m_{TORprod.}/k_m$ for μ_{clean} = 0.5 and $\mu_{TORprod.}$ = 0.2

The combination of Equation 3 for the TOR product mass decrement per load cycle with Equation 8 for the TOR product mass-friction relation allowed the team to reproduce typical S-shaped curves observed for the evolution of the coefficient of friction as a function of number of

load cycles N. This is visualized in Figure 37 and Figure 38 for different masses $m_{TORprod.,0}$ of applied TOR product. Note that in Figure 37 increasing the TOR product mass not only shifts the curves towards higher load cycle numbers, but also decreases the friction recovery rate. Figure 38 is based on TOR product masses $m_{TORprod.,0}$ applied; $\mu_{TORprod.} = 0.2$, $\mu_{clean} = 0.5$, $k_0 = 0$, $k_{m1} = 1$, $k_{m2} = 3$, $k_m = 0.5$, $f_p = f_c = f_i = 1$ used in Equation 8.

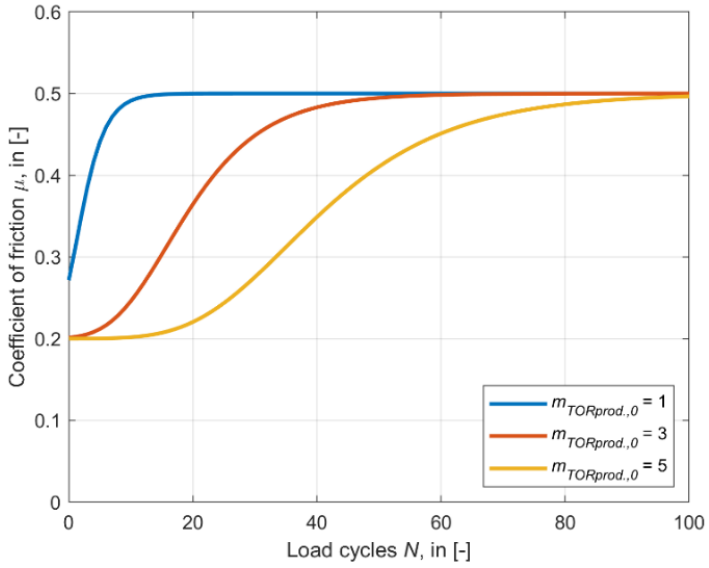

Figure 37. Change of coefficient of friction μ with number of load cycles N for different TOR product masses

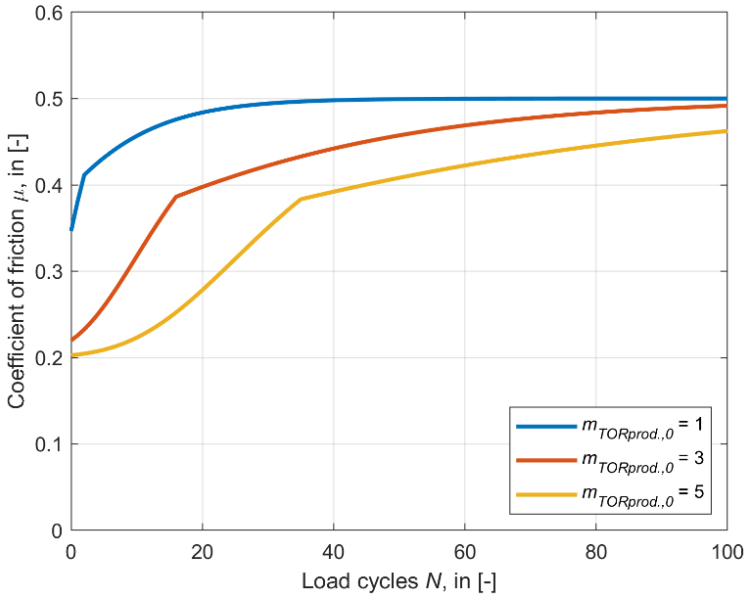

Figure 38. Change of coefficient of friction μ with number of load cycles N for different reduced TOR product masses

In Figure 38, the TOR product mass decrement is reduced by 70 percent for $m_{TORprod.} < 0.5$, which results in a delayed recovery of the coefficient of friction towards the value for the uncontaminated surface. In Figure 38, the parameters were changed to $k_{i1} = 0.7$, $k_{i2} = 0.5$, $k_m = 3$, $f_p = f_c = f_i = 1$.

4.1.5 Carry-On Model

The carry-on model addresses the pick-up and redistribution of TOR product between wheel and rail and as such describes the spreading of the TOR product along the rail. The modeling is based on the TOR product mass $m_{TORprod.}$ On the wheel and rail surfaces. Figure 39 outlines the individual TOR product masses entering and leaving the contact patch at an arbitrary position x_i along the track.

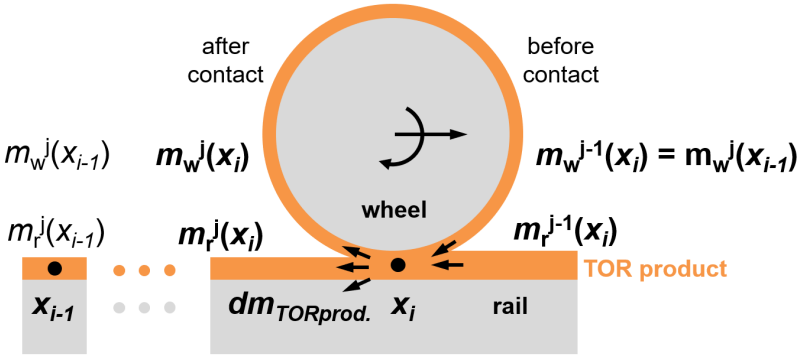

Figure 39. Relevant TOR product masses on rail m_r and wheel m_w at track position I for wheel/rail interaction j

At track position i for wheel/rail interaction j, a certain TOR product mass enters the contact patch on the rail side (denoted as $m_r^{j-1}(x_i)$ and on the wheel side (denoted as $m_w^{j-1}(x_i)$). Due to the wheel/rail interaction TOR product mass $dm_{TORprod.}$ is removed from the contact. At the trailing edge of the contact patch, TOR product remains on the rail side (denoted as $m_r^j(x_i)$) and on the wheel side (denoted as $m_w^j(x_i)$). Thus, the mass balance reads as follows:

$$m_w^j(x_i) + m_r^j(x_i) + dm_{TORprod.} = m_w^{j-1}(x_i) + m_r^{j-1}(x_i) \qquad \textit{Equation 9}$$

Note that the mass of TOR product on the wheel that enters the contact $m_w^{j-1}(x_i)$ is the mass of TOR product that adhered to the wheel surface in the preceding wheel/rail interaction $m_w^j(x_{i-1})$). The TOR product mass $dm_{TORprod.}$ that is removed from the surface during each wheel/rail interaction represents the consumption part of the model. The mass of removed TOR product $dm_{TORprod.}$ is assigned to the rail and the wheel in proportion to the mass of TOR product sticking to the rail surface m_r and to the wheel surface m_w.

When the TOR product leaves the contact patch, the product is redistributed according to an experimentally determined function k. This function k represents the ratio of TOR product mass that sticks to the original surface as determined in the pick-up and carry-on experiments in Section 3. For low TOR product mass, as well as high number of load cycles, hardly any transfer of TOR product between the surface takes place, so that this ratio approaches 1. To ensure the TOR product mass is equally distributed between wheel and rail in the limiting case of an infinite number of wheel/rail interactions, only the difference of TOR product mass between rail and wheel $m_r - m_w$ is redistributed.

4.2 Model Variants: Track vs. Twin-Disc

With small modifications, the TOR product model can also be used to model twin-disc and full-scale laboratory experiments, in which the same parts of two surfaces are in repeated contact.

These experiments provide information about the TOR product consumption as a function of the number of load cycles. Because TOR product mass that leaves the contact patch re-enters the contact patch again after one revolution of the disc in the twin-disc experiment (see Figure 40), the next load cycle in the full-scale experiment (the carry-on part of the model) is obsolete. Only the TOR product consumption model changes the mass of TOR product in the system. Thus, Equation 9 simplifies to the following form:

$$m^j + dm_{TORprod.} = m^{j-1} + m_a^j \qquad Equation\ 10$$

In the equation above, m is the mass of TOR product in the contact, $dm_{TORprod.}$ is the mass of TOR product consumed at one point of the wheel disc during one interaction, and m_a is the mass of TOR product that is applied at interaction j.

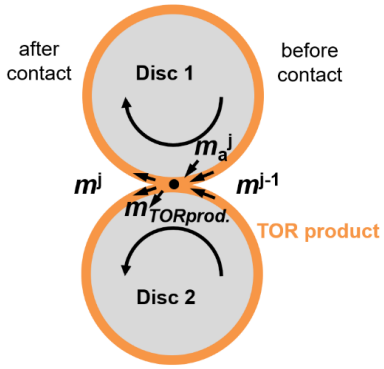

Figure 40. Relevant TOR product masses for wheel/rail interaction *j* in a twin-disc experiment

4.3 Model Parameterization

4.3.1 Parameterization of the Consumption Model

The research team investigated four different experimental conditions at the SUROS test rig for each TOR product. The details of the experimental conditions are listed in Table 6. Condition 1 is the reference condition; it is identical for all TOR products. Conditions 2 to 4 for TOR-oil deviate from those of the other TOR products.

Table 6. Overview of SUROS testing conditions

Condition	Description
1	Reference condition, p_0 = 1500 MPa, c_x = 1%
2	Variation of maximum normal pressure Decrease to p_0 = 900 MPa for TOR-FM A, TOR-FM B, TOR-hybrid, TOR-grease Increase to p_0 = 1,800 MPa for TOR-oil
3	Variation of creepage Decrease to c_x = 0.5% for TOR-FM A, TOR-FM B, TOR-hybrid, TOR-grease Increase to c_x = 5% for TOR-oil
4	Variation of applied TOR product mass Increase in applied TOR product mass for TOR-FM A, TOR-FM B, TOR-hybrid, TOR-grease Decrease in applied TOR product mass for TOR-oil

For each TOR product, the team derived one set of model parameters that describes the frictional behavior observed in SUROS experiments in conditions 1 to 4. For TOR-FM A, TOR-FM B, and

TOR-oil consumption, experiments carried out at the full-scale test rig have also been used for the model parameterization.

Table 7 lists the model parameters for the different types of TOR product.

Table 7. Model parameter for different types of TOR product

Parameter	Unit	TOR-FM A	TOR-FM B	TOR-Oil	TOR-Grease	TOR-Hybrid
k_0	in [kg]	1.0449e-09	1.2410e-08	2.3016e-09	9.6262e-13	6.3067e-11
k_{m1}	in [kg]	1.1617e-06	3.6770e-06	1.7334e-06	7.1333e-08	9.5581e-07
k_{m2}	in [-]	0.5300	0.6551	9.1751	0.1783	0.1113
k_p	in [-]	1.8400	1.0232	-1.4322	2.3383	2.3508
k_c	in [-]	0.5700	0.2778	0.3365	0.8729	0.6434
k_{i1}	in [-]	--	--	--	0.88739	9.20e-01
k_{i2}	in [kg]	--	--	--	2.2009e-06	7.81e-06
$\mu_{TORprod.}$	in [-]	0.15	0.15	0.15	0.12	0.05
k_m	in [kg]	1.6290e-04	1.4198e-04	2.1523e-05	2.2039e-06	6.0430e-06
k_x	in [kg]	2.00e-04	2.00e-04	2.00e-04	5.38e-05	4.00e-05
k_{x0}	in [kg]	4.82e-04	5.89e-04	1	1	1

For the model parameterization, the coefficient of adhesion was set to $\mu_{clean} = 0.58$. The reduction factors k_A and k_B in the Polach creep force model were set to 0.85. The team did not consider a decrease of adhesion with increasing rolling speed in the parameterization process by setting $A = B = 1$ in the Polach creep force model.

As an example, the parameterization results for TOR-FM A are shown in Figure 41 and Figure 42. The first five applications of TOR product in the experiment were used for the parameterization. In the figures, the experimentally measured adhesion as a function of disc revolutions (shown as symbols) is compared to the predicted values of the model (shown as lines). The scatter in the predicted adhesion values results from the use of the experimentally measured creepage data as input for the model prediction. This approach ensures that changes of the creepage in the experiment immediately after application of the TOR product due to sudden decrease of the tangential loading are taken into account in the parameterization process. The complete set of parameterization results can be found in Appendix E.

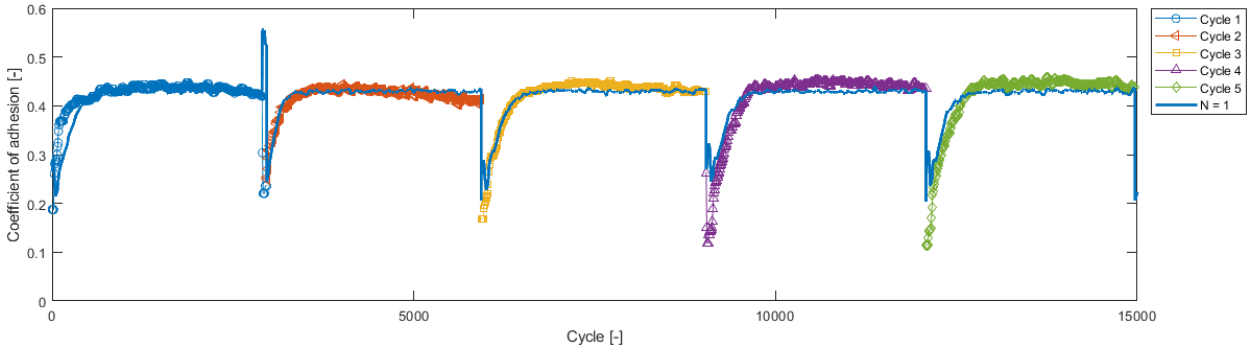

Figure 41. TOR-FM A, Experimental SUROS twin-disc data and model comparison for for 5 applications (for p_0 = 1500 MPa, c_x = 1% Condition 1)

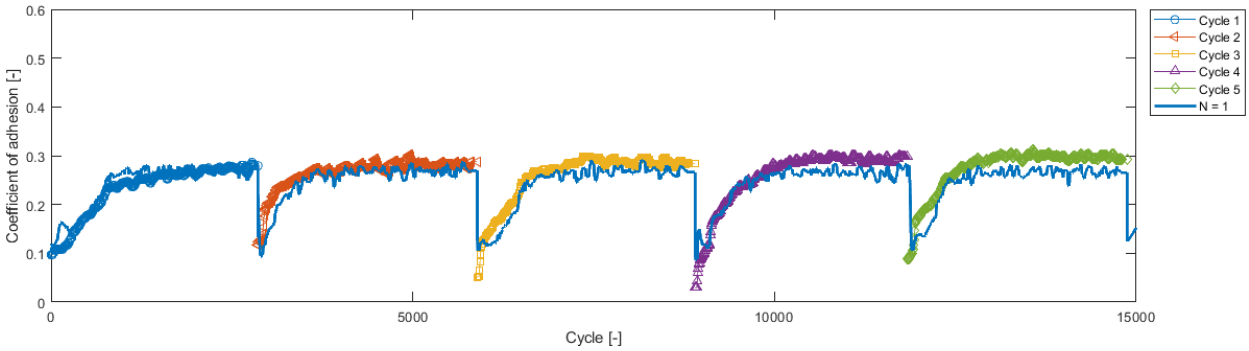

Figure 42. TOR-FM A, Experimental SUROS twin-disc data and model comparison for 5 applications (p_0 = 1500 MPa, c_x = 0.5% Condition 3)

To describe the change of adhesion in both the small-scale twin-disc experiment and full-scale test rig experiment with the same set of model parameters, the applied TOR product mass in the twin-disc experiment needed to be increased by a factor of five. The exact reasons for this are unclear and have not been investigated in detail. It may have been caused by different aspect ratios of the contact patch (high aspect ratio in line contact of the twin-disc experiment versus low aspect ratio of the point contact in the full-scale experiment), different surface conditions with respect to surface roughness, and differences associated with the different contact patch sizes.

Figure 43 compares the data recorded at the full-scale rig to the results of the model prediction to check the parameterization process at 80 kN Wheel load and creepage c_x = 5% for 0.1-, 0.3-, and 0.6-ml applied TOR.

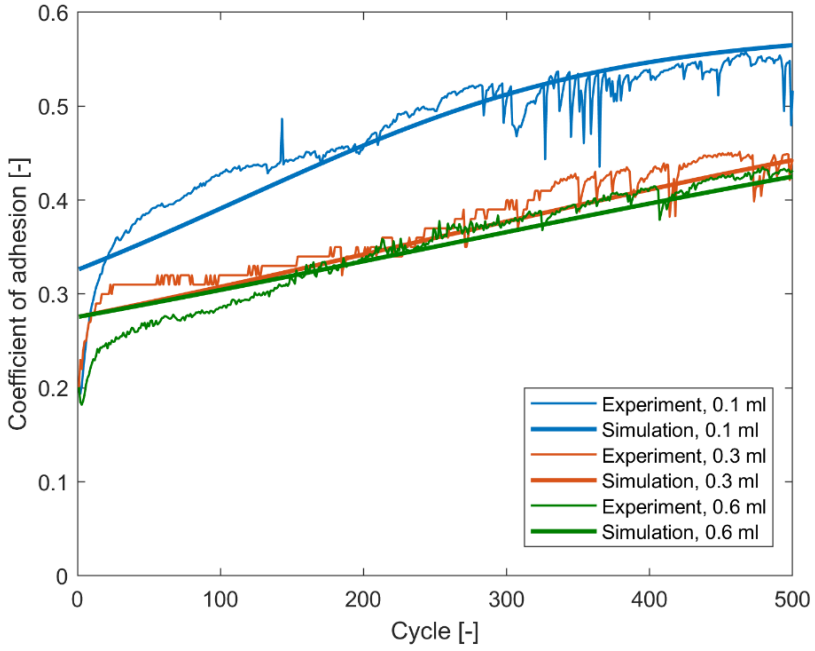

Figure 43. Experimental Full Scale Rig data and model predictions for applied TORs

Parameterization of TOR-oil, TOR-grease, and TOR-hybrid were challenging due the small amounts of friction modifier masses applied in the SUROS experiments. This increased the relative uncertainty of the mass measurements, which led in turn to an increase in scatter in the

time evolution of the adhesion. Differences in the limiting value of adhesion for uncontaminated conditions between the experiment and the model prediction occurred because only one creep force curve was used for uncontaminated surface conditions in the parameterization process. In some of the experimental data (e.g., TOR-oil) the recorded adhesion data needed to be increased to match the coefficient of adhesion of uncontaminated condition.

4.3.2 Parameterization of the Carry-On Model

When a wheel rolls over the rail, part of the TOR product is transferred to the wheel surface. In subsequent wheel/rail interactions TOR product is also transferred back to the rail surface. The (re)distribution behavior of TOR product is important for the carry-on characteristics of the TOR product.

The research team investigated the ratio of TOR product on the surface after the wheel/rail interaction to the mass of TOR product before the wheel/rail interaction by pick-up and carry-on experiments on the scaled wheel test rig and on the full-scale test rig (see Section 3). Experimental data from the pick-up experiment at the full-scale test rig are shown in Figure 44 for TOR-FM A and in Figure 45 for TOR-FM B. The surfaces in the figures are approximations of the experimental data that is used for the distribution function k in the TOR product model.

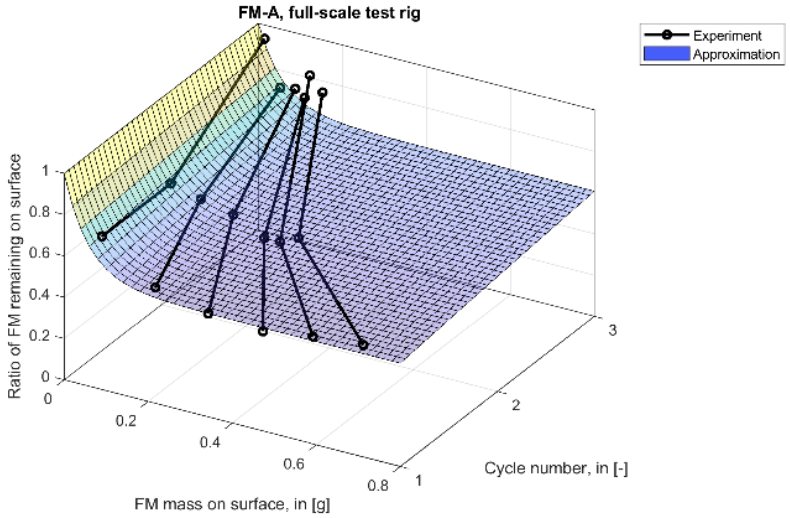

Figure 44. Ratio of TOR product mass k remaining on the surface as a function of TOR product mass $m_{TORprod.}$ and number of load cycles N for TOR-FM A

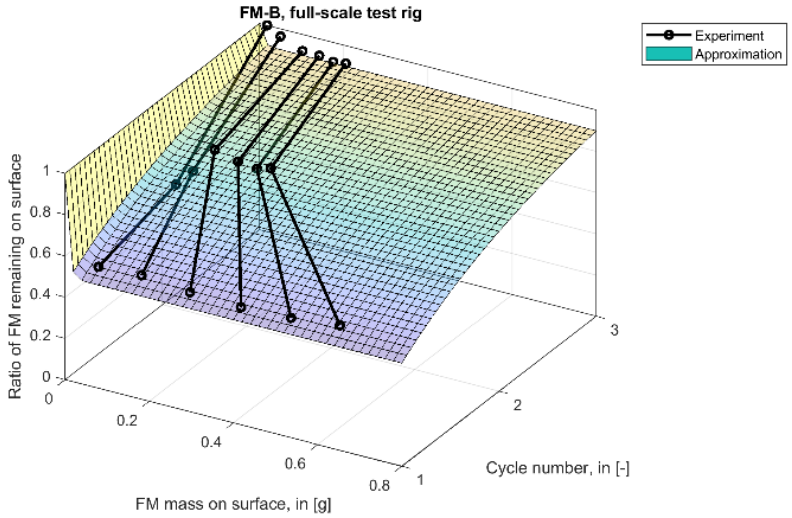

Figure 45. Ratio of TOR product mass *k* remaining on the surface as a function of TOR product mass $m_{TORprod.}$ and number of load cycles *N* for TOR-FM B

The team chose the function describing the ratio of TOR product *k* that remains on the surface to be a function of the mass of TOR product on the surface $m_{TORprod.}$ and the number of load cycles *N*. For TOR product masses approaching 0, the ratio approaches 1. Likewise, for large number of cycles, the function also approaches the value 1. Table 8 gives the functions used in the friction modifier model for the different types of TOR product.

Table 8. Functions *k* describing the ratio of TOR product mass that remains on the respective surface after the load cycle

TOR product	Ratio of FM remaining on surface
TOR-FM A	$k(m, N) = 0.5000 + 0.5000*\exp(-m/0.0582) + 0.5000*(1-\exp(-(N-1)/8.3684)) - 0.5000*\exp(-m/0.0582)*(1-\exp(-(N-1)/8.3684))$
TOR-FM B	$k(m, N) = 0.5000 + 0.5000*\exp(-m/0.0074) + 0.5000*(1-\exp(-(N-1)/1.2523)) - 0.5000*\exp(-m/0.0074)*(1-\exp(-(N-1)/1.2523))$

4.4 Field Simulations

As part of the model development, the team created a graphical user interface (GUI) that allows easy use of the TOR product model and provides access to the main model variables. Figure 46 shows a screenshot of the GUI.

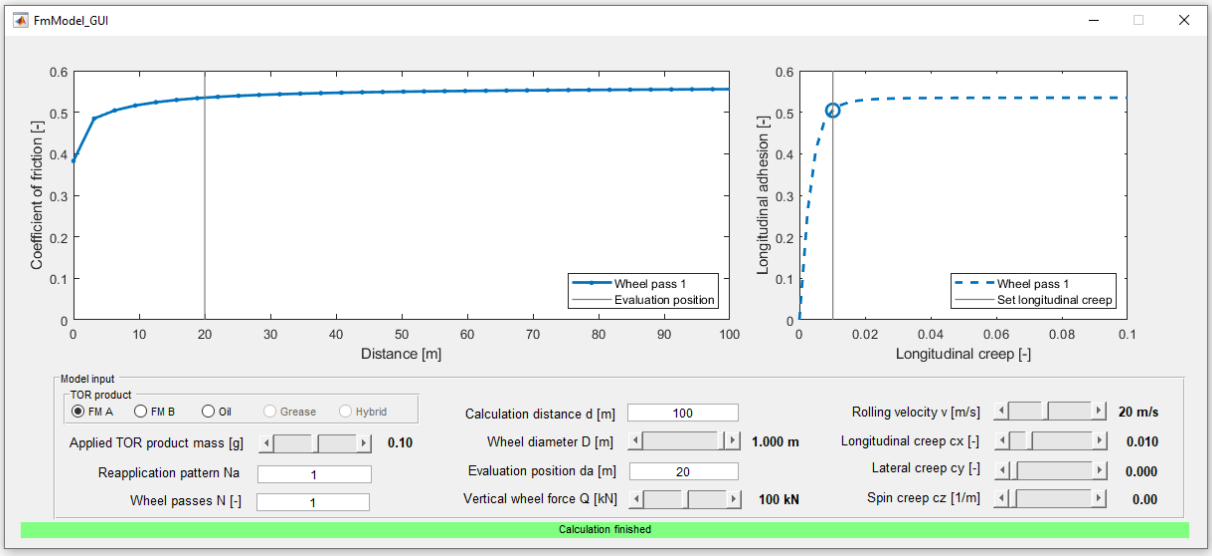

Figure 46. Model GUI

The GUI can be used to explore the model behavior with respect to field operation in a variety of ways. However, the model predictions are extrapolations that are made based on laboratory experiments from small-scale twin tests and full-scale wheel-rail rig tests.

The evolution of the friction conditions along the rail in the model predictions for the field are determined by two main processes: the pick-up of TOR product at the application site followed by a steady redistribution of TOR product between wheel and rail, and the consumption behavior of the TOR product as a result of the wheel/rail interaction. These two processes are visualized in Figure 47.

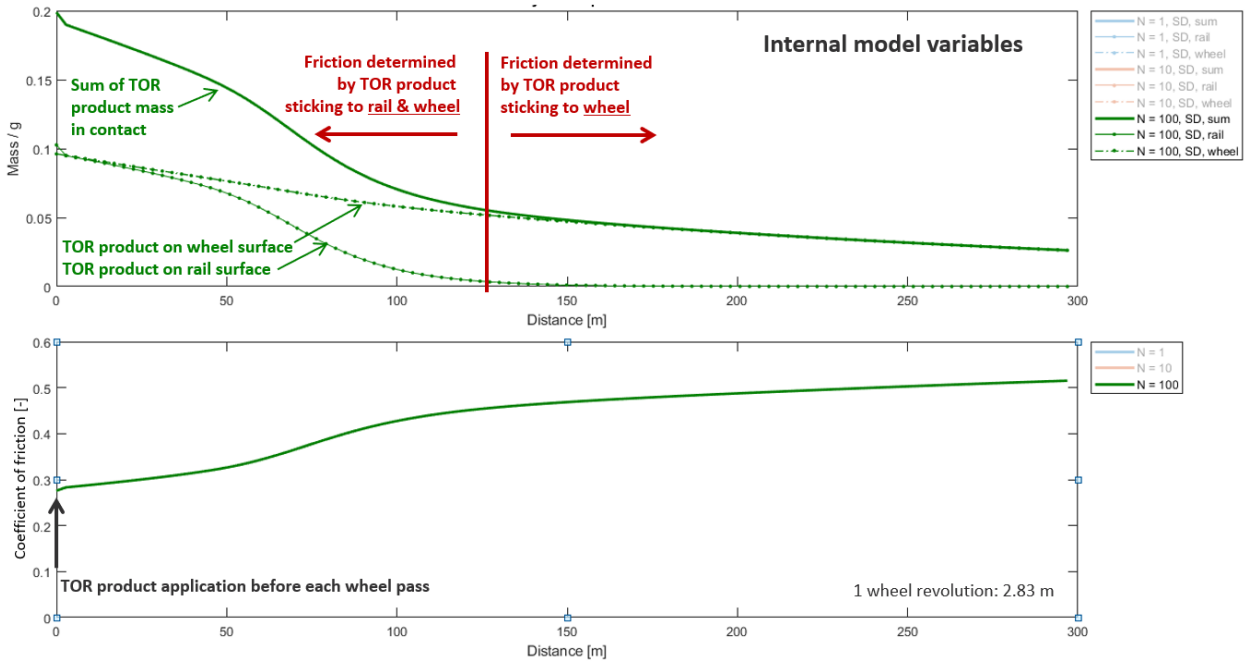

Figure 47. a) Distribution of internal model variable "TOR product mass" on the surfaces of wheel and rail, b) corresponding coefficient of friction with 5 percent creepage

The figure shows the distribution of internal model variable “TOR product mass” on a wheel and rail after 100 wheel passes, for which TOR product was applied before every wheel pass. The bottom figure shows the predicted friction condition along the track. At distance 0, TOR product was applied to the rail and picked up by the wheel. In the track section following the application site, TOR product was transferred from the wheel back to the rail surface. In this part, the friction was determined by the mass of TOR product on both the wheel and the rail surface. After some distance (approximately at 125 m from the application site in the example), transfer of TOR product from wheel to rail ceased due to the small amount of TOR product on the wheel surface and the high number of wheel/rail interactions as specified in the distribution function k. Friction was determined by the TOR product sticking to the wheel. TOR product mass on the wheel surface decreased with increasing distance to the application site due to TOR product consumption during each wheel rail interaction. This caused a gradual increase of the friction toward the limiting value for uncontaminated surface condition.

Figure 48 compares the friction condition for wheels rolling over the track with a creepage of 1 percent to the case with 5 percent for 100 wheel passes after 0.2 g of TOR application before each wheel pass. One percent creepage was at the onset of full sliding condition. Increasing the creepage increased TOR product consumption in the model, which can be seen as an increase in the friction value. However, the general shape of the friction as a function of distance along the track was similar in both cases. This was due to the fact that the shape was mainly determined by the pick up and carry-on behavior of the TOR product.

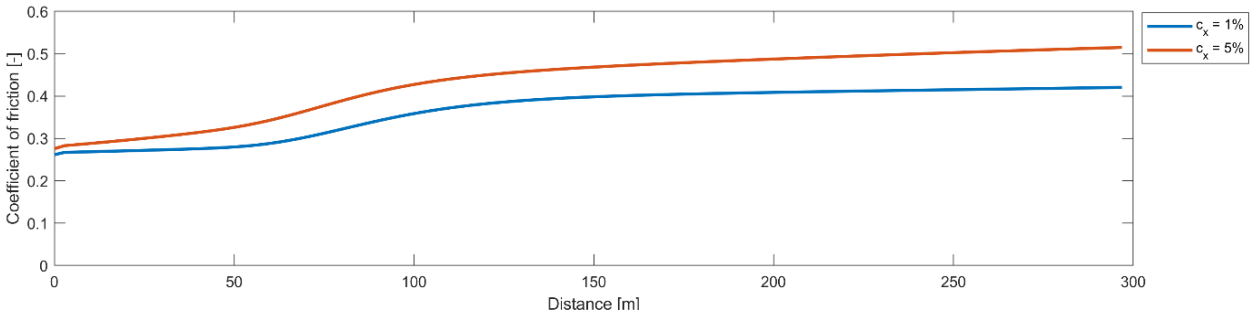

Figure 48. TOR-FM A, predicted friction along the track for wheel pass for 1 percent and 5 percent creepage

There are two extreme scenarios that must be addressed with respect to TOR product pick-up at the application site. In the first, there was enough TOR product at the application site so that every wheel picked up the maximum amount of TOR product (i.e., the wheels passing through a reservoir of TOR product; Figure 49). Although there was a sufficient supply of TOR product at the application site, the maximum carry-on distance eventually reached a limit. This was due to the characteristics of the TOR product transfer between wheel and rail in combination with TOR product consumption.

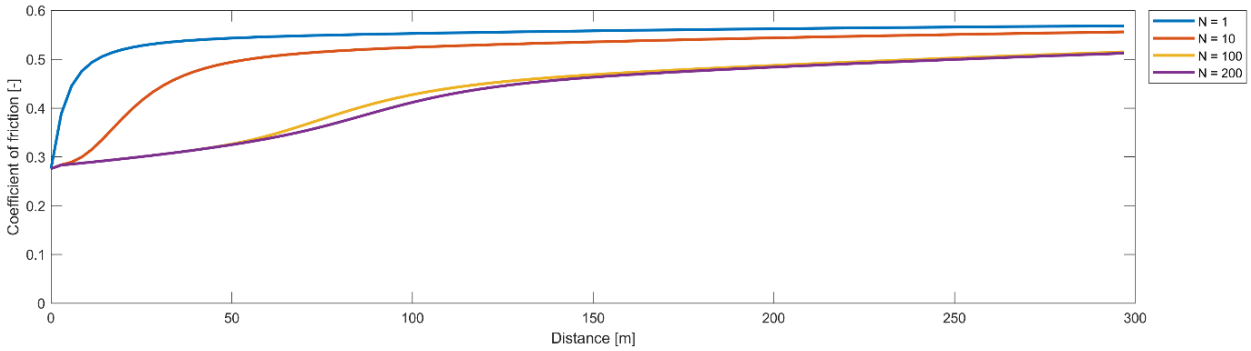

Figure 49. TOR-FM A, Predicted evolution of friction condition along the track for several wheel passes for 0.20 g TOR product at distance 0 before every wheel pass

The other extreme was that only the first wheel was able to pick up TOR product after application of a large amount of TOR product at the application site. Subsequent wheels may contact the same exact part of the railhead that has been cleared of TOR product by the first wheel (Figure 50). The amount of TOR product mass that affected friction was greatly reduced in this case, thus a reduction in friction was already minimal for the tenth wheel pass.

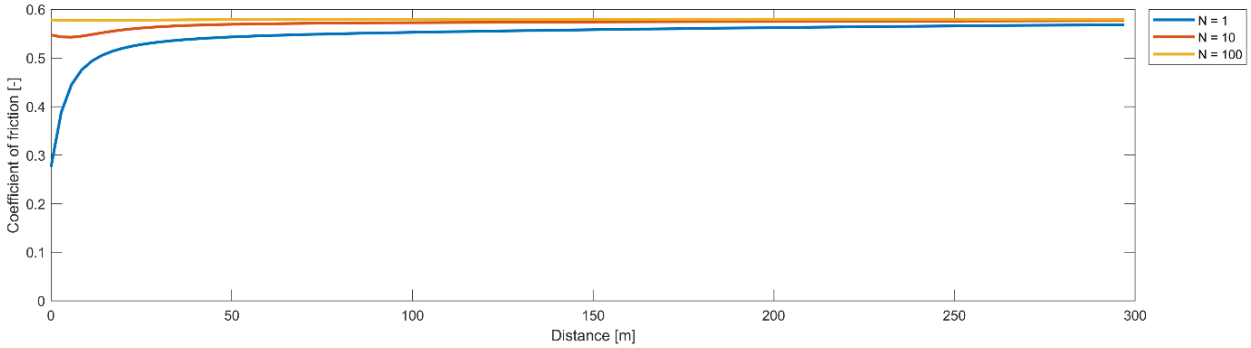

Figure 50. TOR-FM A, Predicted evolution of friction condition along the track for several wheel passes for 0.20 g TOR product at distance 0 only before wheel pass 1

In railway operation, conditions will fall somewhere between these extreme cases because the lateral contact position at the application site will be different, e.g., for wheels on leading and trailing axles and because of different wheel profile geometries. This shows that the pick-up efficiency at the application site is also a crucial factor in predicting the evolution of the friction along the track.

Figure 51 compares different types of TOR product for the first wheel pass (N=1) after application of 0.2 g TOR. Friction values were distinctively lower for TOR-oil. The same TOR product mass was applied in the simulation, which may represent an over-application of TOR-oil. The applied TOR product masses in the twin-disc experiments to study the consumption behavior of TOR-oil were five times lower than those for TOR-FM A and TOR-FM B.

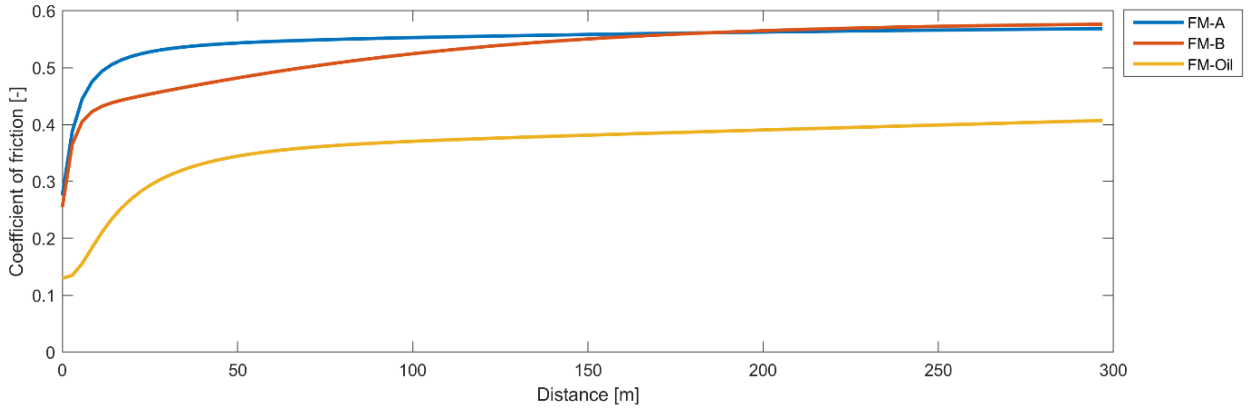

Figure 51. Comparison of friction as a function of distance from the application site for TOR-FM A, TOR-FM B and TOR-Oil

Finally, the model also allows the study of different application patterns of TOR product. This is illustrated in Figure 52. Before each wheel pass, 0.05 g of TOR-FM A was applied in case A (blue line). In case B, 0.20 g TOR-FM A was applied before every fourth wheel pass. The results show that the friction varied right after the application site in case B, depending on whether TOR product application had occurred just before the wheel pass (compare wheel pass N=100 to N=101 in Figure 52). But more interestingly, friction further away from the application site was slightly lower for case B, although the same amount of TOR product had been applied at the application site in both cases. The model predictions suggest that it is advantageous to apply larger amounts of TOR product less frequently to achieve larger carry-on distances.

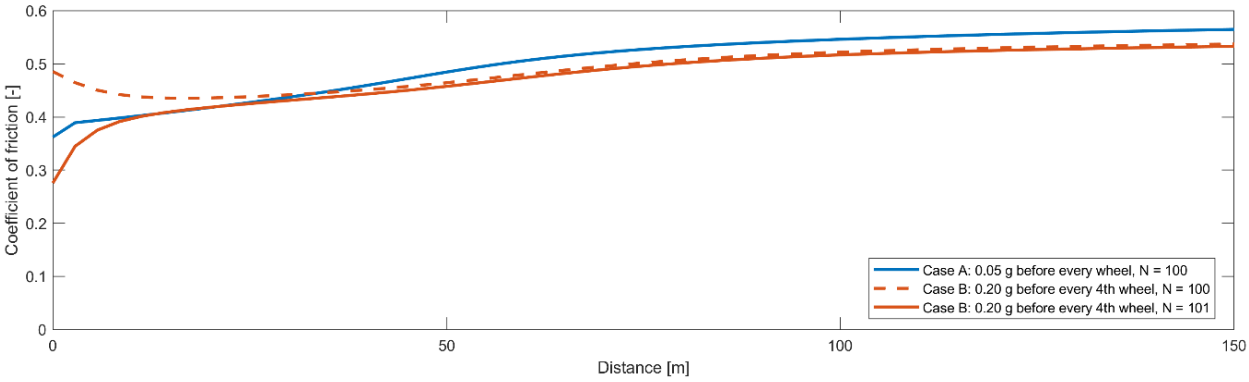

Figure 52. Influence of application pattern on friction along the track for different applications of TOR

5. Conclusion

The research team conducted experimental assessment of different types of TOR product (TOR-FMs [water-based drying products] and two TOR lubricants [TOR-oil and TOR grease] and a hybrid product (TOR-hybrid) to assess the pick-up, carry-on, and friction performance of each. They conducted the tests across several scales using a twin-disc simulation of the wheel/rail interface, a scaled wheel rig, and a full-scale rig. Below are the conclusions from this testing.

Pick-up performance:

- Both FM-A and FM-B had the same pick-up behavior in the first wheel/rail interaction. Approximately half of the initial amount applied was picked up by the first wheel, assuming all the product applied was in contact with the wheel and the rail.
- FM-A was continuously picked up by consecutive wheels because some of the product fell on the running band when breaking up from the first wheel, leaving the pool of FM-A. This was a result of the material properties of the FM-A product, such as the viscosity and tackiness.
- FM-B was less likely to be picked up by consecutive wheels at the same lateral position because the product was easily squeezed out of the contact.

Carry-on performance:

- More FM-A was carried further along the rail than the FM-B because FM-A could stay within the running band longer than FM-B. This was due to the viscosity and tackiness of the TOR product.

Friction performance:

- TOR friction modifiers had a higher traction level (assuming the same amount of product was applied at the contact), reaching the “intermediate level” of traction required from TOR products. TOR lubricants achieved traction levels that would be associated with lubricants.
- If more TOR product was applied, traction level decreased. Based on the full-scale tests, however, the traction level of the TOR friction modifiers did not decrease further when a threshold application amount was reached.

Consumption performance:

- TOR friction modifier products generally had the fastest consumption rate among TOR products.
- TOR lubricants had the slowest consumption rate. The product consumption could be very slow for an extended number of cycles if a sufficient layer was built up.
- TOR lubricants also required a much smaller application amount to be consumed within the set time frame of the SUROS twin-disc tests.
- The TOR hybrid had mixed consumption behavior characteristics from both TOR friction modifiers and TOR lubricants.

Rig Comparison:

- The scaled wheel rig could easily assess the TOR product distribution during a wheel/rail interaction.
- The SUROS twin-disc rig, as a small-scale test, could provide a quick overview of the tribological performance of TOR products.
- The full-scale rig was able to generate traction data that represented real life wheel-rail interactions.

The tests themselves can be used to assess new product performance and benchmark them against the products trialed in this project. However, this study investigated the pick-up and carry-on behavior under a laboratory-controlled environment, where the wheel was always in contact with the TOR product at the same lateral point on the railhead. In the real world, the wheels may contact the TOR products at different lateral positions, thus affecting the overall pick-up and carry-on behavior and the consumption rate.

The team used the data from the tests to inform the development of models for TOR product pick-up and consumption. As part of the model development, they created a GUI that allows easy use of the TOR product model and provides access to the main model variables. The GUI can be used to explore the model behavior with respect to field operation in a variety of ways. However, model predictions are extrapolations based on laboratory experiments from small-scale twin tests and full-scale wheel-rail rig tests.

The evolution of the friction conditions along the rail in the model predictions for the field were determined by two main processes: the pick-up of TOR product at the application site followed by a steady redistribution of TOR product between wheel and rail, and the consumption behavior of the TOR product as a result of the wheel/rail interaction.

The model code can be integrated into other models, such as multi-body dynamics simulations, to facilitate assessment of TOR products on vehicle dynamic performance. The code can be obtained from FRA. University of Sheffield/Virtual Vehicle Research Center engineers can provide training in the model used for this project.

6. Next Steps

As shown in Figure 53, at the beginning of the project several future activities were planned as work packages 4 through 8. The first step would be to expand the model to take account of the changing lateral position of the wheel; currently, the model only works for a fixed position. The next step would be to integrate the model into a MBD simulation to assess different operating scenarios, e.g., curving. This would be coupled with field measurements using a vehicle with an instrumented wheelset to validate the model. Finally, the model would be used to assess the impact of TOR product use on vehicle dynamic performance and integrated with damage models (for wear and RCF) to study the impact on these on TOR product use.

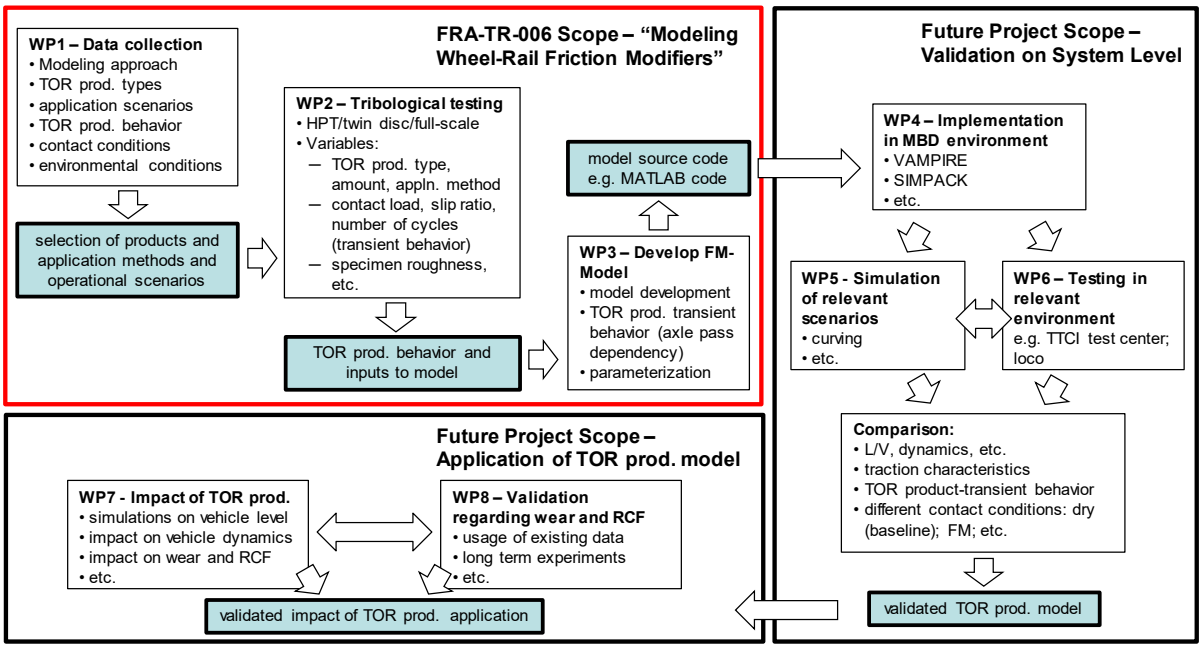

Figure 53. Project plan and future activities

7. References

Allotta, B., Meli, E., Ridolfi, A., & Rindi, A. (2014). Development of an innovative wheel-rail contact model for the analysis of degraded adhesion in railway systems. *Tribology International, 69*, 128-140. doi:http://dx.doi.org/10.1016/j.triboint.2013.09.013

Buckley-Johnstone, L., Lewis, R., Six, K., & Trummer, G. (2015). *Modelling and quantifying the influence of water on wheel/rail adhesion levels, Phase 1 report.*

Chen, H., Ban, T., Ishida, M., & Nakahara, T. (2002). Adhesion between rail/wheel under water lubricated contact. *Wear, 253*, 75-81.

Chen, H., Ishida, M., & Nakahara, T. (2005). Analysis of adhesion under wet conditions for three-dimensional contact considering surface roughness. *Wear, 258*, 1209-1216.

Davis, D. (2015). Effectiveness of new friction control materials - vehicle track systems research. *Presentation at Annual AAR Research Review, March 31st - April 1st 2015.*

Evans, M. D. (2017). *Performance assessment of friction management products in the wheel/rail interface.* Ph.D. thesis, University of Sheffield, Mechanical Engineering, Sheffield, United Kingdom.

Gutsulyak, D. V., Stanlake, L. J., & Qi, H. (2018). Twin disc evaluation of third body materials in the wheel/rail interface. *Proceedings of the 11th International Conferenceon Contact Mechanics and Wear of Rail/Wheel Systems (CM2018).* Delft, The Netherlands.

Hibbert, M. J. (2017). *Understanding the wheel/rail transfer mechanism in liquid friction modifier carry-down.* Master thesis, The University of British Columbia, Mechanical Engineering, Vancouver, Canada.

Kalker, J. J. (1967). *On the rolling contact of two elastic bodies in the prescence of dry friction.* Ph.D. thesis, Delft University of Technology, Delft, The Netherlands.

Kalker, J. J. (1982). A fast algorithm for the simplified theory of rolling contact. *Vehicle System Dynamics, 11*, 1-13.

Lewis, S. R., Lewis, R., Goodwin, P., Fretwell-Smith, S., Fletcher, D., & Murray, K. (2016). Laser cladding of railway track to promote wear/RCF, bend fatigue and IBJ lipping resistance. *Proceedings of the Third International Conference on Railway Technology: Research, Development and Maintenance*.

Lewis, S. R., Lewis, R., Oloffson, U., Eadie, D. T., Cotter, J., & Lu, X. (2012). Effect of humidity, temperature and railhead contamination on the performance of friction modifiers: pin on disk study. *Proceedings of Institution of Mechanical Engineers. Part F: Journal of Rail and Rapid Transit, 227*(2), 115-127.

Lewis, S. R., Lewis, R., Richards, P., & Buckley-Johnstone, L. E. (2013). Investigation of the isolation and fricitonal properties of hydrophobic products on the rail head, when used to combat low adhesion. *Wear, 314*, 213-219.

Meierhofer, A. (2015). *A new wheel-rail creep force model based on elasto-plastic third body layers.* Ph.D. thesis, Graz University of Technology, Graz, Austria.

Polach, O. (1999). A fast wheel-rail forces calculation computer code. *Vehicle System Dynamics, 33*, 728-739.

Polach, O. (2005). Creep forces in simulations of traction vehicles running on adhesion limit. *Wear, 258*, 992-1000.

Popovici, R. (2010). *Friction in wheel-rail contacts.* PhD thesis, University of Twente, Enschede, The Netherlands.

Six, K., Mierhofer, A., Müller, D., & Dietmaier, P. (2015). Physical processes in wheel-rail contact and its implications on vehicle-track interaction. *Vehicle System Dynamics: International Journal of Vehicle Mechanics and Mobility, 53*, 635-650. doi:http://dx.doi.org/10.1080/00423114.2014.983675

Spiryagin, M., Polach, O., & Cole, C. (2013). Creep force modelling for rail traction vehicles based on the Fastsim algorithm. *Vehicle System Dynamics: International Journal of Vehicle Mechanics and Mobility, 51*, 1765-1783. doi:10.1080/00423114.2013.826370

Stock, R., Stanlake, L., Hardwick, C., Yu, M., Eadie, D., & Lewis, R. (2016). Material concepts for top of rail friction management - Classification, characterisation and application. *Wear, 366-367*, 225-232.

Suda, Y. (2003). The basic study on friction control between wheel and rail (experiments by test machine and scale model vehicle). *The 6th International Conference of Contact Mechanics and Wear of Rail/Wheel Systems (CM2003)*, (pp. 343-348). Gothenburg, Sweden.

Temple, P. D., Harmon, M., Lewis, R., Burstow, M. C., Temple, B., & Jones, D. (2017). Optimisation of grease application to railway track. *Proceesings of the Instituition of Mechanical Engineers. Part F: Journal of Rail and Rapid Transit*.

Tomberger, C. (2009). *Der Rad-Schiene Kraftschluss unter Berücksichtigung von Temperatur, fluiden Zwischenschichten und mikroskopischer Oberflächenrauheit.* Ph.D. thesis, Technische Universität Graz, Graz, Austria.

Tomberger, C., Dietmaier, P., Sextro, W., & Six, K. (2011). Friction in wheel-rail contact: A model comprising interfacial fluids, surface roughness and temperature. *Wear, 271*, 2-12. doi:10.1016/j.wear.2010.10.025

Trummer, G., Buckley-Johnstone, L. E., Voltr, P., Meierhofer, A., Lewis, R., & Six, K. (2017). Wheel-rail creep force model for predicting water induced low adhesion phenomena. *Tribology International, 109*, 409-415. doi:http://dx.doi.org/10.1016/j.triboint.2016.12.056

Vollebregt, E. A. (2014). Numerical modeling of measured railway creep versus creep-force curves with CONTACT. *Wear, 314*, 87-95. doi:http://dx.doi.org/10.1016/j.wear.2013.11.030

Voltr, P., & Lata, M. (2015). Transient wheel–rail adhesion characteristics under the cleaning effect of sliding. *Vehicle System Dynamics, 53*, 605-618. doi:10.1080/00423114.2014.961488

Zhu, Y., Olofsson, U., & Söderberg, A. (2013). Adhesion modeling in the wheel–rail contact under dry and lubricated conditions using measured 3D surfaces. *Tribology International, 61*, 1-10. doi:http://dx.doi.org/10.1016/j.triboint.2012.11.022

Appendix A. Questionnaire

The University Of Sheffield. virtual vehicle LBFoster

1 Background

A top of rail (TOR) product is commonly used in the rail industry to manage the friction between the wheel and rail. It is a material that moderates the friction to give an intermediate level to help address squealing noise, damage development and energy consumption while allowing for safe train operations [1][1]. The University of Sheffield is currently leading an FRA sponsored project with the Virtual Vehicle Research Center and L.B. Foster that aims to develop a wheel-rail creep force model that takes into account the effects of third-body layers resulting from the application of a range of Top of Rail (TOR) materials (such as TOR friction modifiers, TOR lubricants, etc. – see Figure 1 for details of their relative friction performance). The work will focus on wayside application devices. The model should be able to predict the creep force characteristic (over creepage) dependent on the distance from the applicator and the number of wheel passes since application (material consumption).

The work will help to provide a basis to assess and to utilize the full benefits of TOR materials regarding all aspects of Vehicle-Track-Interaction (VTI). The development will be based on the understanding of the main physical phenomena occurring in the wheel-rail interface (carry down effects, load dependency, material consumption due to energy dissipation in the wheel/rail contact, etc.). The project deliverable will be a MATLAB tool that can be integrated into any VTI software. The experimental work that will be carried out to derive inputs for the model will also provide a means to benchmark TOR materials prior to field application.

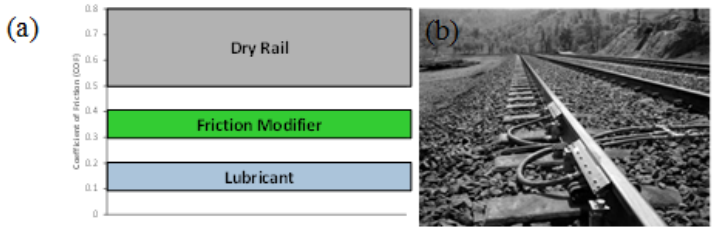

Figure 1. (a) Friction Modifier (FM) performance [1] and (b) a FM wayside applicator

[1] Stock et al., 2016, *Wear*, Vol. 366-367, 225-232.

2 Questionnaire Layout

This questionnaire has 5 sections; the first consists of general questions on the top of rail (TOR) products and also your expectations from the creep force model. Section 2 to 5 are more specific in terms of the product details and operating conditions that will be considered during experimental testing and might also serve as an input in the creep force model.

Note: This questionnaire is designed to cover both general and specific aspects of the project. Therefore, participants may not be able to answer all questions. Participant can leave some questions unanswered if they are unable to answer them.

3 Questions

Section 1: General

1) What does the company you work for do?

☐ Railway company ☐ TOR product supplier ☐ Rail manufacturers

☐ Rail maintenance company ☐ Research group ☐ Train manufacturer

☐ Other: _____

2) Do you think the application of friction modifiers is important? If you think it is not important then you can skip question 4.

☐ Important ☐ Marginal ☐ Not considered

3) What do friction modifier products influence from your point of view?
   a. Vehicle dynamics

      ☐ Important ☐ Marginal ☐ Not considered

   a. Braking performance

      ☐ Important ☐ Marginal ☐ Not considered

   b. Traction performance

      ☐ Important ☐ Marginal ☐ Not considered

   c. Wheel-rail damage (RCF, corrugation, etc.)

      ☐ Important ☐ Marginal ☐ Not considered

   d. Noise

      ☐ Important ☐ Marginal ☐ Not considered

e. Energy consumption

☐ Important ☐ Marginal ☐ Not considered

f. Others (please describe): _____

4) Is it important to use the laboratory experimental data to assess the performance of TOR products?

☐ Important ☐ Marginal ☐ Not considered

5) The importance of the interaction of friction modifier products with environmental conditions (temperature, humidity, precipitation, etc.)?

☐ Important ☐ Marginal ☐ Not considered

6) Where do you see possible applications of a model describing the behaviour of friction modifier products in your field of work?

a. Investigations regarding vehicle dynamics

☐ Important ☐ Marginal ☐ Not considered

b. Investigations regarding braking performance

☐ Important ☐ Marginal ☐ Not considered

c. Investigations regarding traction performance

☐ Important ☐ Marginal ☐ Not considered

d. Investigations regarding wheel-rail damage (RCF, corrugation, etc.)

☐ Important ☐ Marginal ☐ Not considered

e. Investigations regarding noise

☐ Important ☐ Marginal ☐ Not considered

f. Investigations regarding energy consumption

☐ Important ☐ Marginal ☐ Not considered

g. Others (please describe)

_____

7) Would you prefer the creep force model to be modelled specifically for wayside application or on-board application of TOR products?

☐ Wayside only ☐ On-board only ☐ Both ☐ Unsure

8) Would you like the creep force model be used as a standalone graphical user interface (GUI)? An example of a typical GUI interface is shown in 2.

☐ Yes ☐ No ☐ Unsure

9) Would you foresee the creep force model being implemented in multi-body-dynamics (MBD) software?

☐ Yes ☐ No ☐ Unsure

10) Would you like to use the creep force model as a standalone tool for selecting the right TOR product for a particular operating scenarios?

☐ Yes ☐ No ☐ Unsure

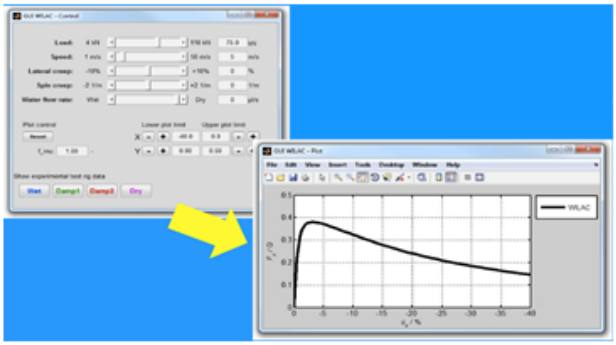

Figure 2. GUI interface of creep force prediction for water in contact[2]

[2] Trummer et al., 2017, *Tribology International*, Vol. 109, 409-415.

Section 2: Top of rail (TOR) product

TOR product and its application

This section will focus on which TOR product is used, how often it is used, where is it applied etc.

For example:

TOR material type	Friction Modifier/Oil/Grease/Hybrid
Product	Caltrek
Application device	Protector Type 2
Application amount	3L per 1000 axles
Frequency application (axle nos.)	Every 39 axles
Pump activation time	0.1 seconds
Applied location	Top of rail

Four columns are provided if more than one TOR product is used

TOR material type	_____	_____	_____	_____
Product	_____	_____	_____	_____
Application device[1]	_____	_____	_____	_____
Application amount	_____	_____	_____	_____
Frequency of application (axle nos.)	_____	_____	_____	_____
Pump activation time	_____	_____	_____	_____
Applied location	_____	_____	_____	_____

[1] Only wayside application being considered

Additional question(s)

1) Is it important to have contaminants/third body materials included in the experiments and model (e.g. oxides, water, etc.)?

☐ Yes ☐ No ☐ Unsure

Section 3: Operational conditions

1) Operating scenario

☐ Freight ☐ Passenger ☐ Light rail ☐ Other (please describe) _____

2) Average speed of train (if known) /Range of train speed (if known)

_____

3) Axle loads (if known)

_____

Section 4: Rail & Wheel conditions

1) Material of wheel (if known)

_____

2) Material of rail (if known)

_____

3) Is it important to measure surface roughness of wheel and/or rail?

☐ Important ☐ Marginal ☐ Not considered

4) Do you have surface roughness data for the wheel and/or rail you can share?

☐ Yes (Both Rail and Wheel) ☐ Yes (Rail only) ☐ Yes (Wheel only) ☐ No

Section 5: Environmental conditions

1) Temperature range (if known)

_____

2) Humidity range (if known)

_____

3) Typical precipitation range (if known)

_____

4) Confidence rating on completing the questionnaire?

☐ Low confidence ☐ Somewhat confident ☐ Confident ☐ Very confident

Appendix B.
Questionnaire Responses

Section 1: General

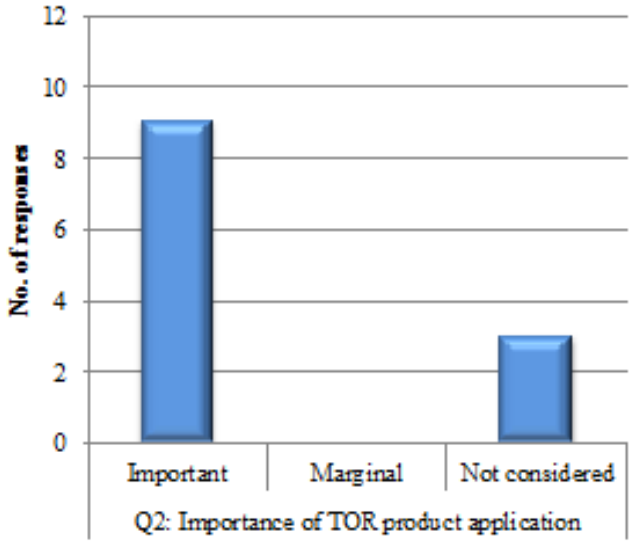

Q2: Importance of TOR product application

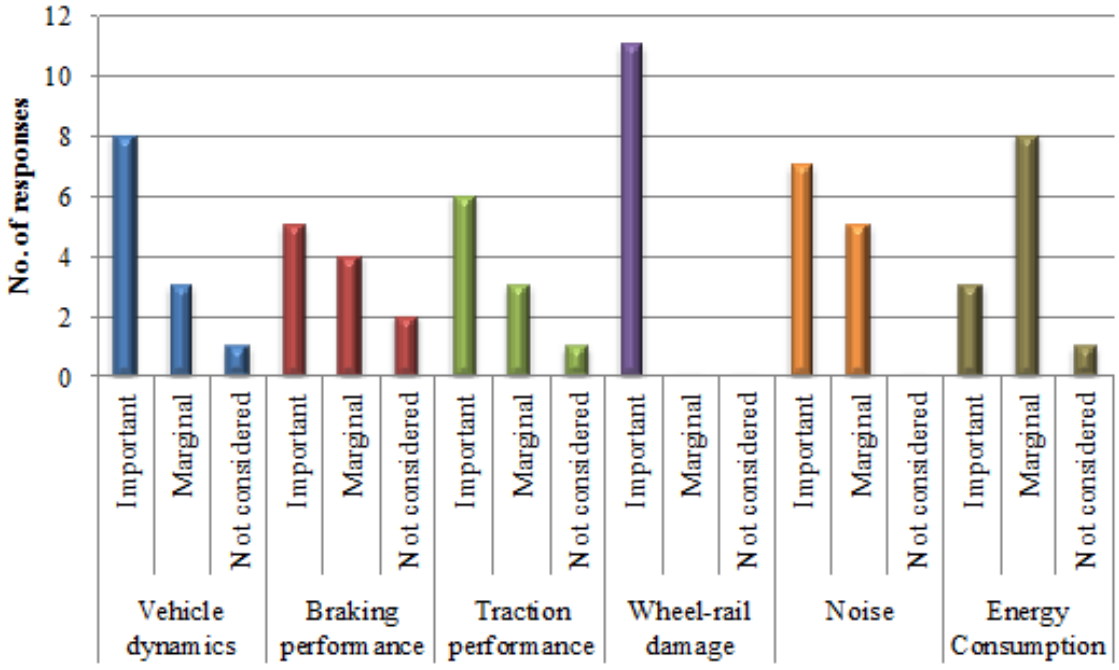

Q3: Area where TOR product application is important

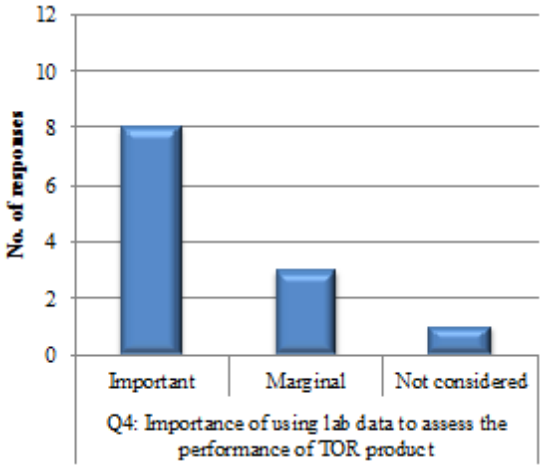

Q4: Importance of using lab data to assess the performance of TOR product

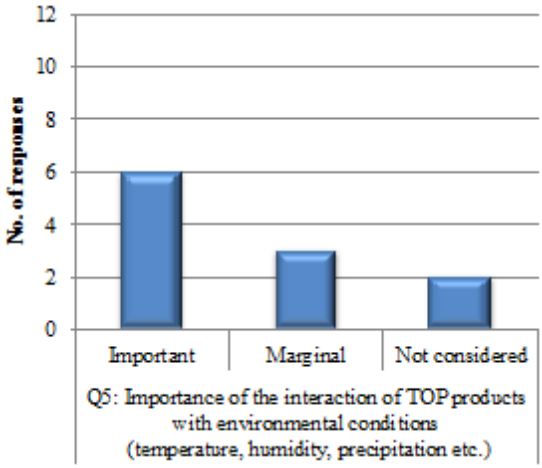

Q5: Importance of the interaction of TOP products with environmental conditions (temperature, humidity, precipitation etc.)

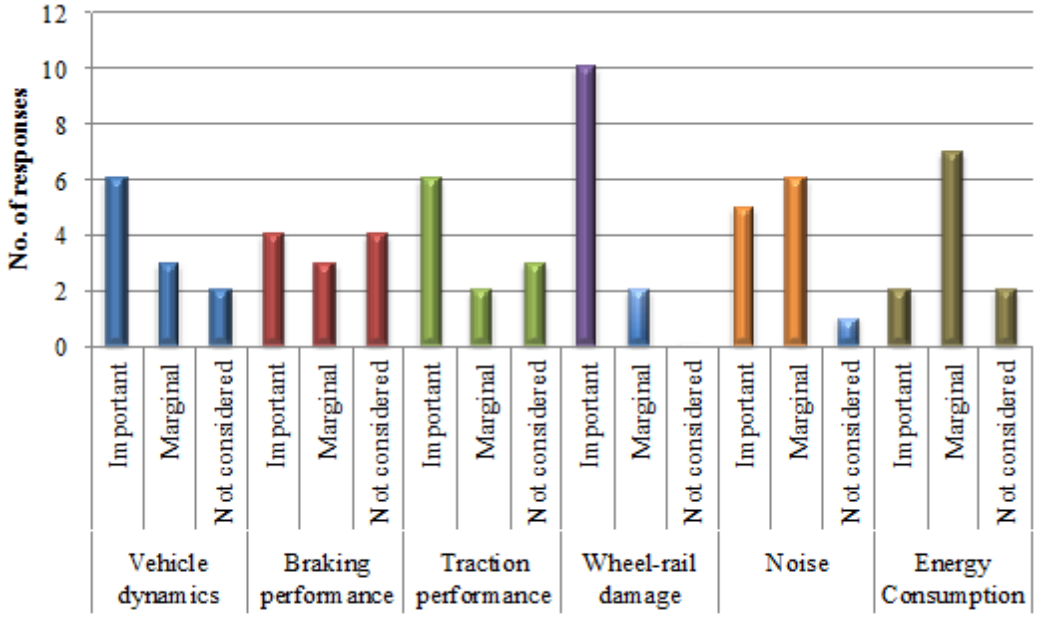

Q6: Area where creep force model of TOR product is feasible

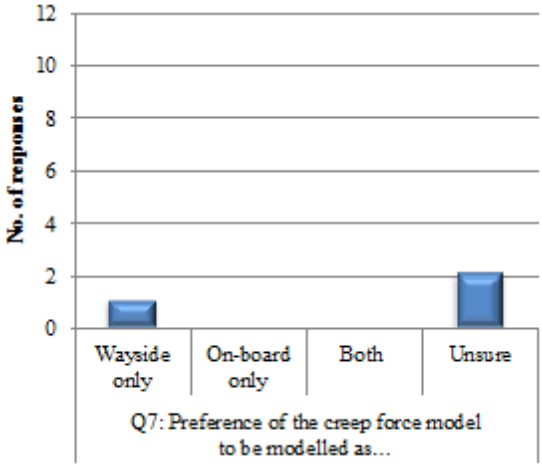

Q7: Preference of the creep force model to be modelled as…

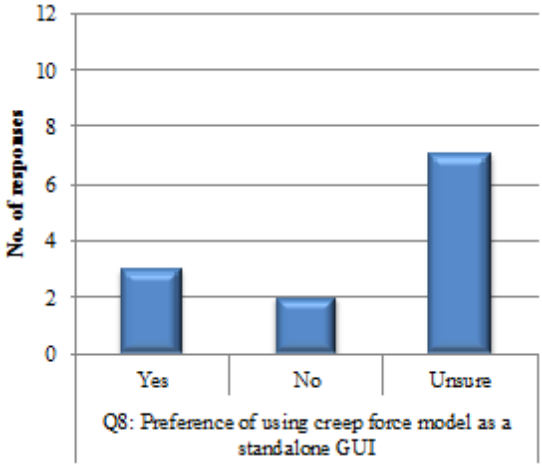

Q8: Preference of using creep force model as a standalone GUI

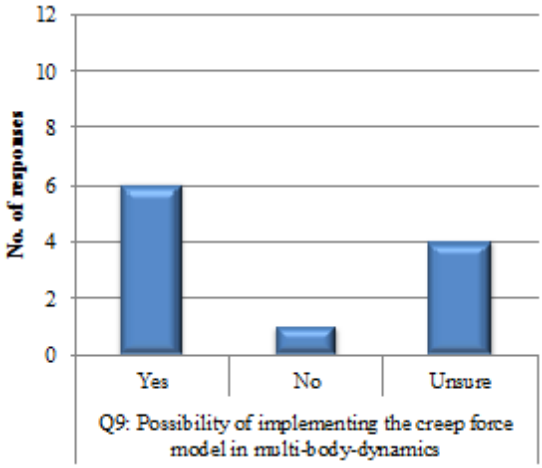

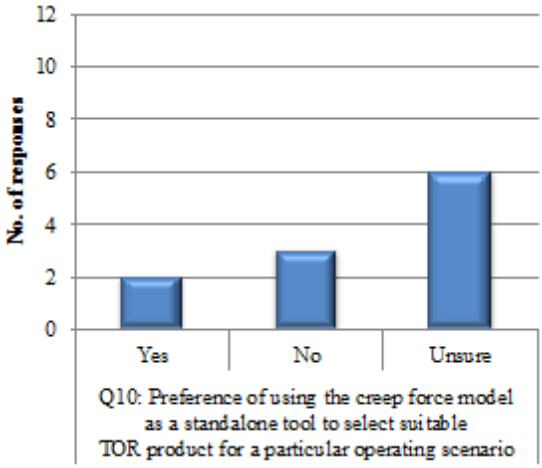

Section 2: Top-of-rail (TOR) product

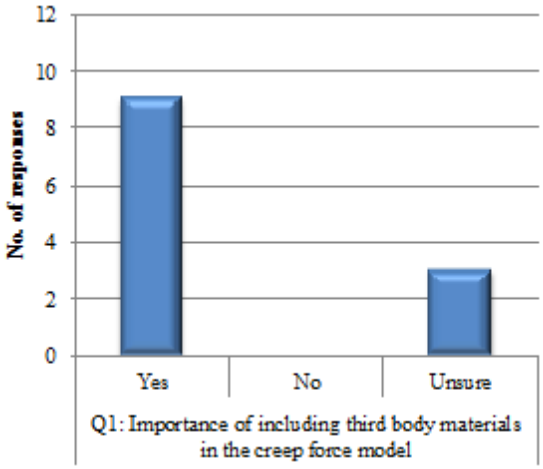

Section 3: Operational conditions

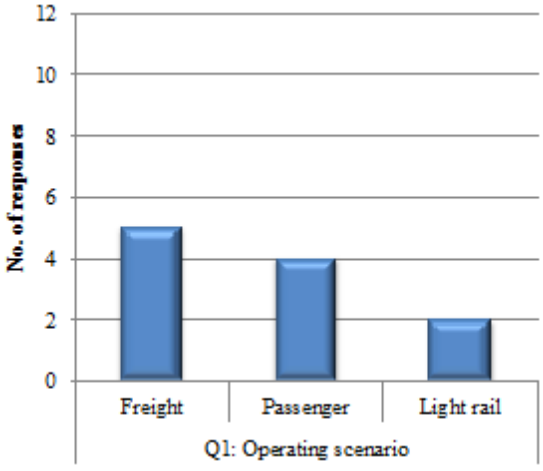

Section 4: Rail and wheel conditions

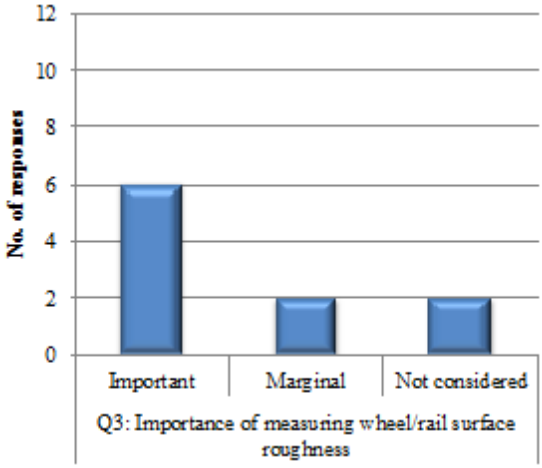

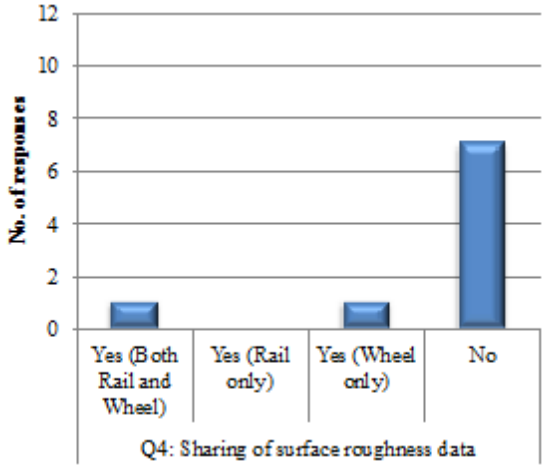

Section 5: Environmental conditions

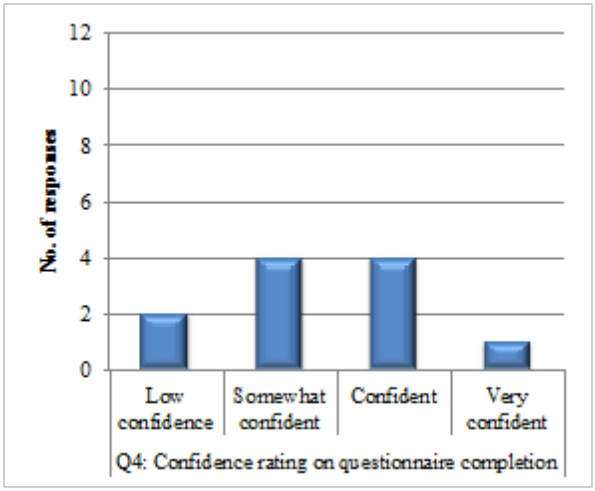

Appendix C.
Pick-Up Behavior: Raw Data

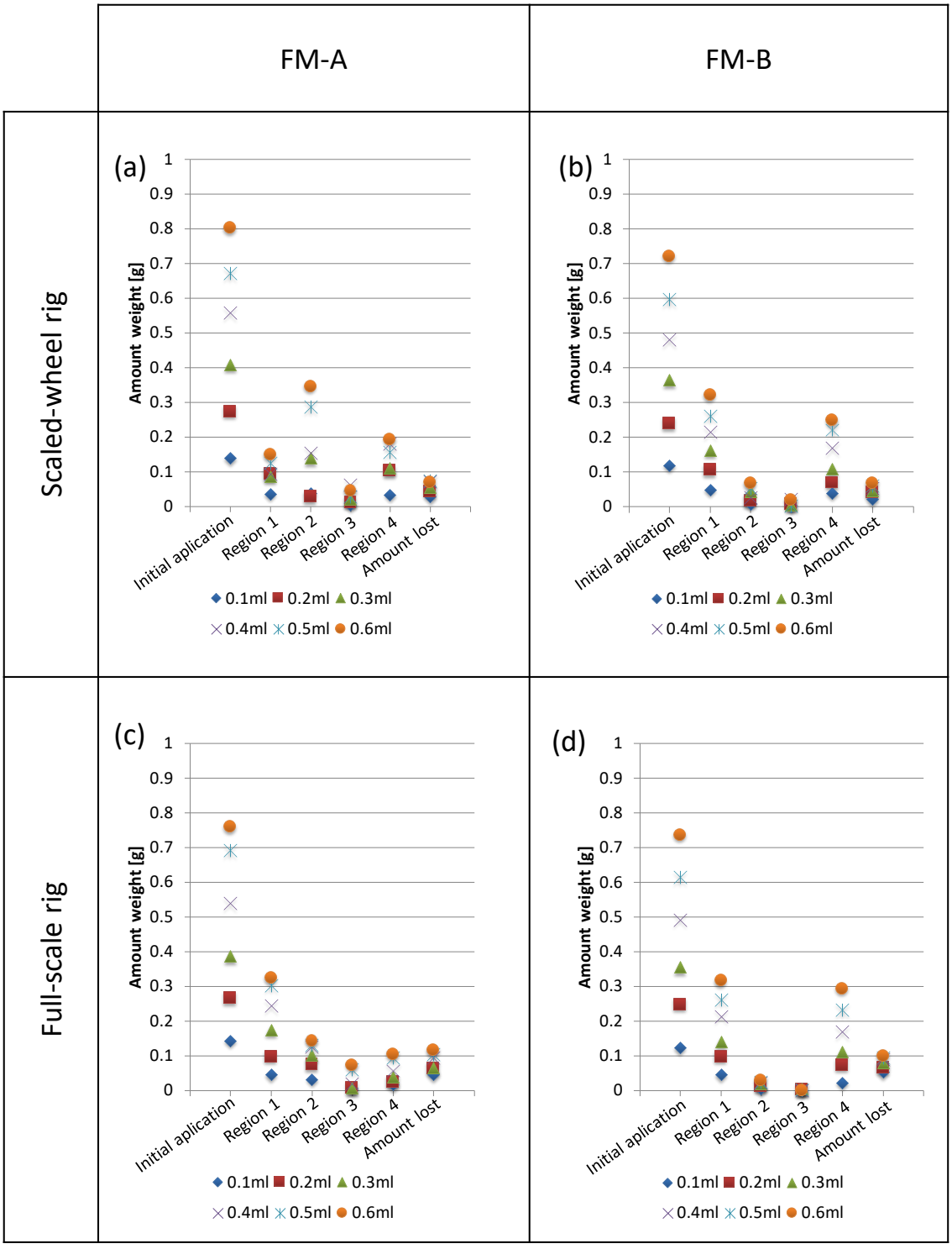

Figure 54. Amount distribution of TOR-FM A during pick-up tests using (a) scaled wheel rig, (c) full-scale rig and TOR-FM B using (b) scaled wheel rig and (d) full-scale rig

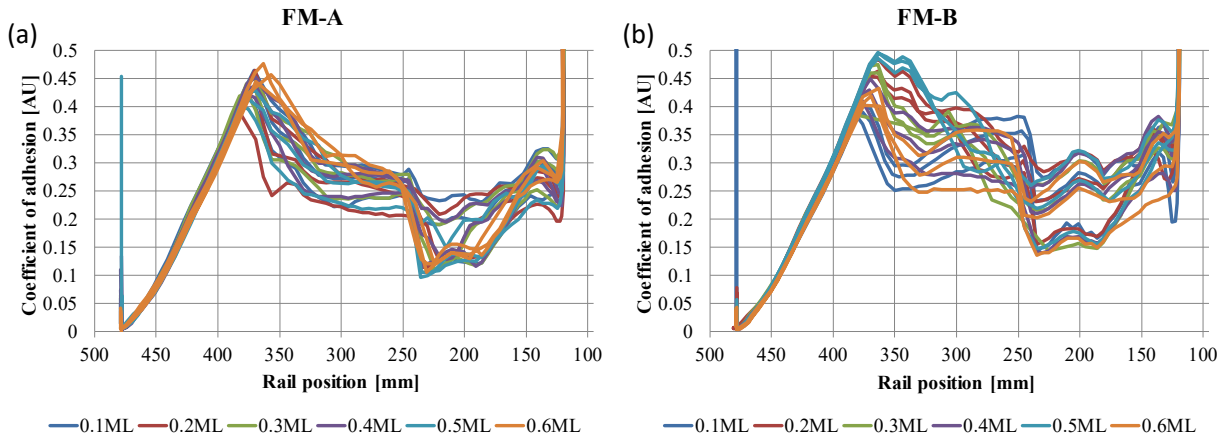

Figure 55. Frictional behavior of wheel-rail interaction during pick-up tests using full-scale rig with the application of (a) TOR-FM A and (b) TOR-FM B at a specific region along the rail

Appendix D.
Carry-On Behavior: Raw Data

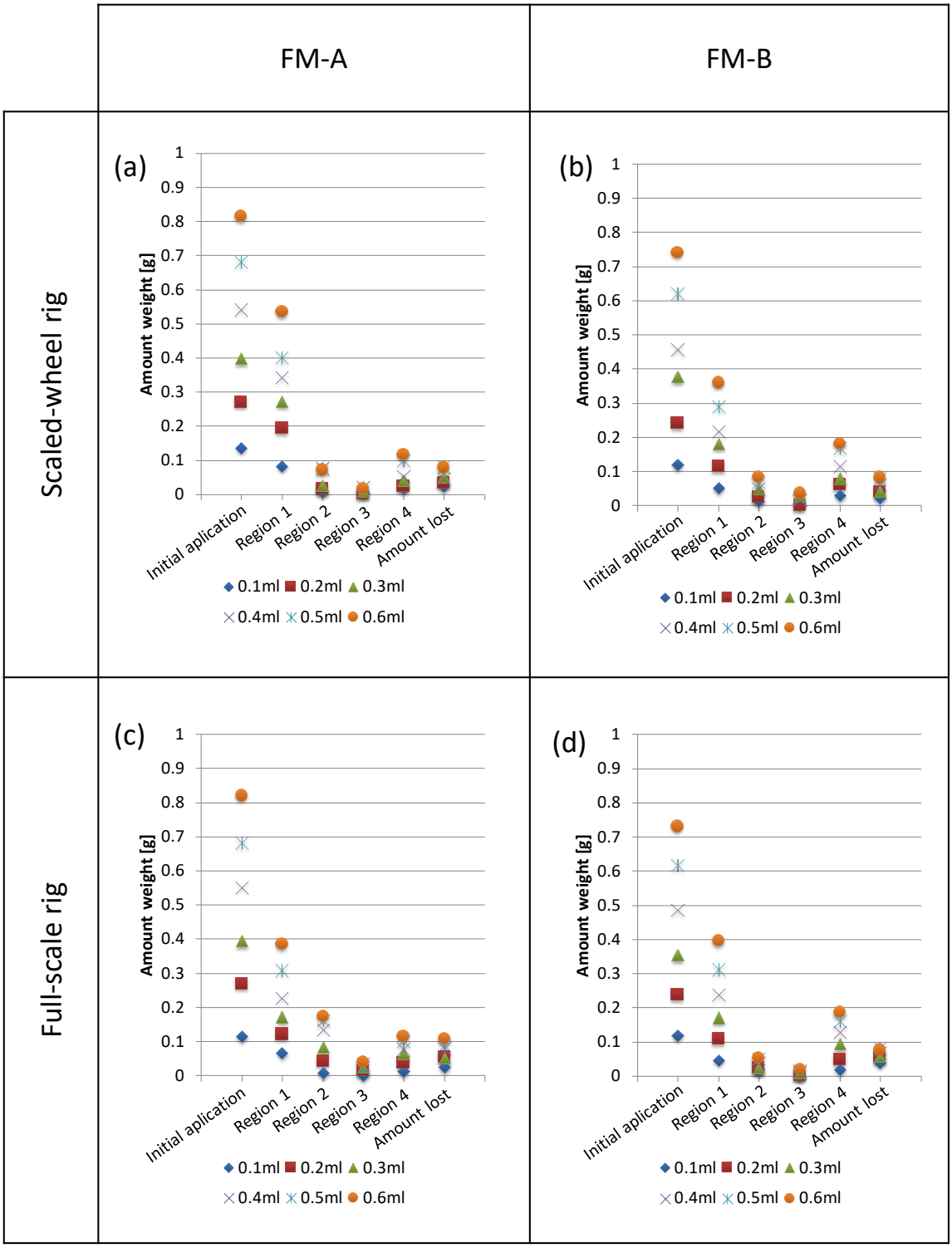

Figure 56. Amount distribution of TOR-FM A during carry-on tests using (a) scaled wheel rig, (c) full-scale rig and TOR-FM B using (b) scaled wheel rig and (d) full-scale rig

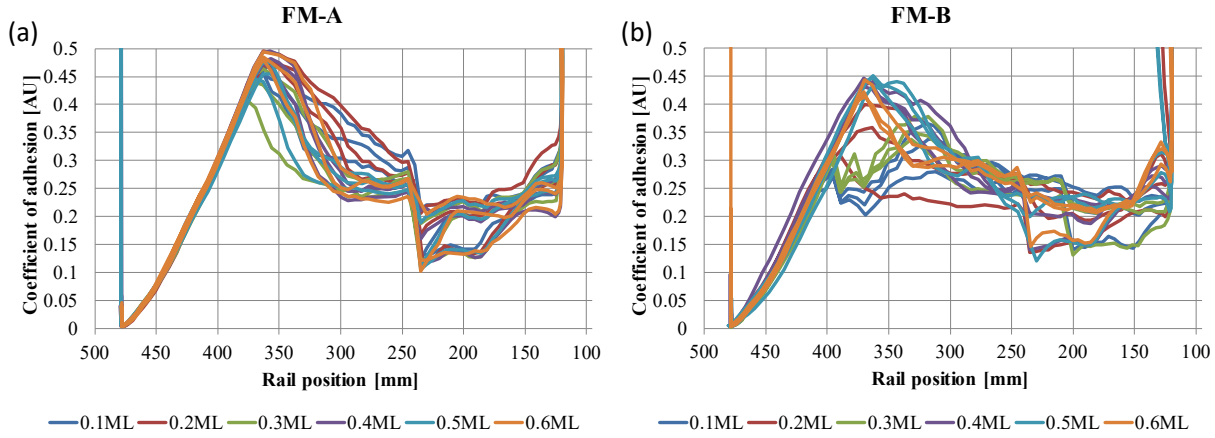

Figure 57. Frictional behavior of wheel-rail interaction during carry-on tests using full-scale rig with the application of (a) TOR-FM A and (b) TOR-FM B at a specific region along the rail

Appendix E.
Model Parameterization: Twin-Disc Experiments

For some conditions, the model fit seems to be sub-optimal. Note, however, that in the parameterization process the sum of error over conditions 1 to 4 was minimized and the curves were not fitted individually to the experimental data of the different experimental conditions.

(a) FM-A

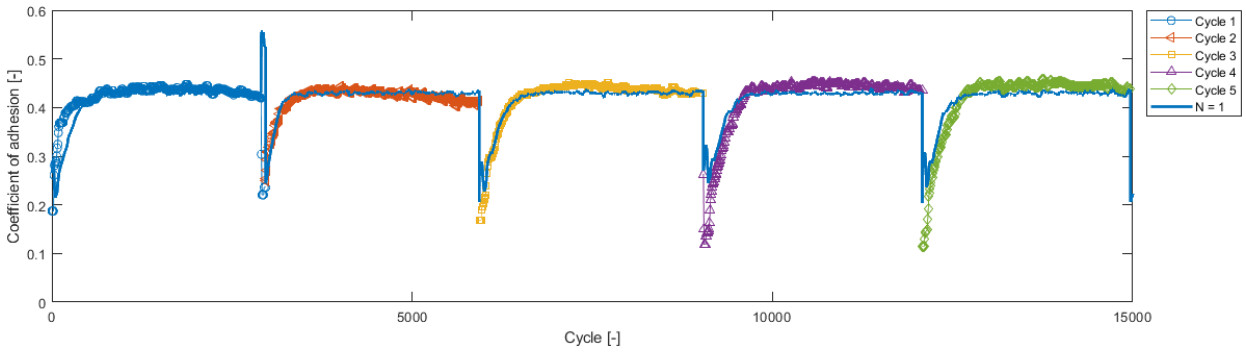

Figure 58. TOR-FM A, condition 1; symbols: SUROS experiment, application 1 to 5; line: TOR product model result

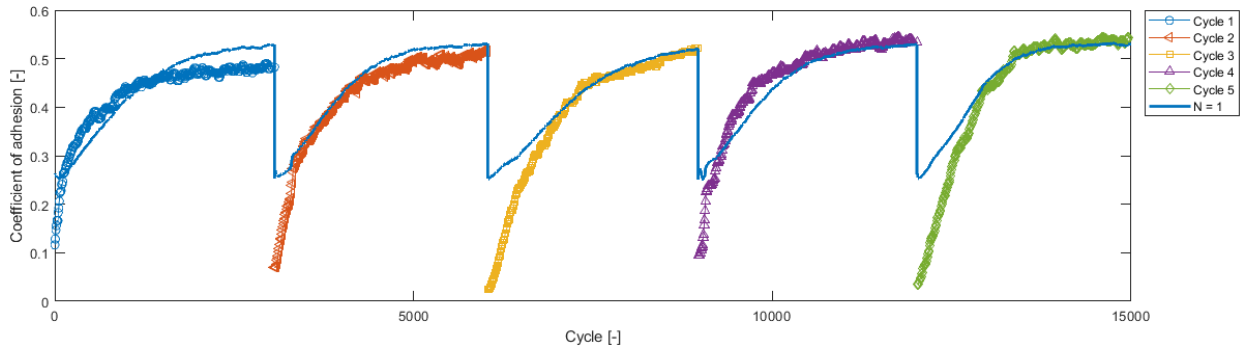

Figure 59. TOR-FM A, condition 2; symbols: SUROS experiment, application 1 to 5; line: TOR product model result

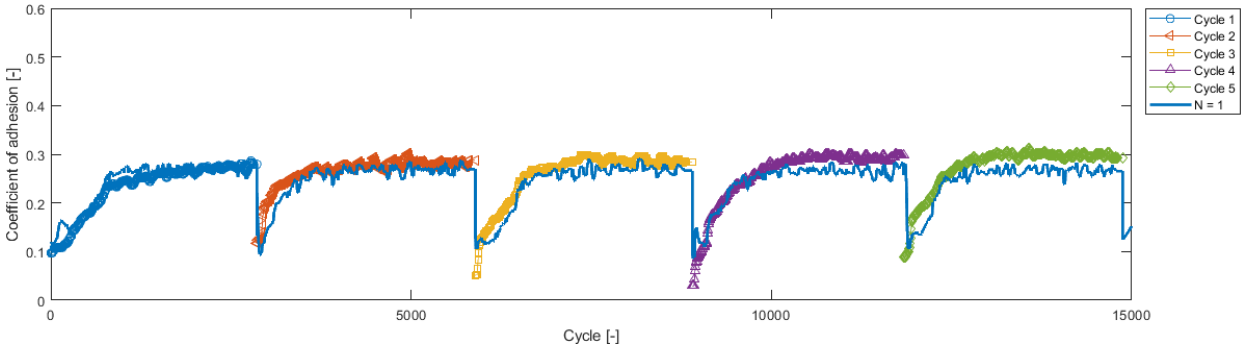

Figure 60. TOR-FM A, condition 3; symbols: SUROS experiment, application 1 to 5; line: TOR product model result

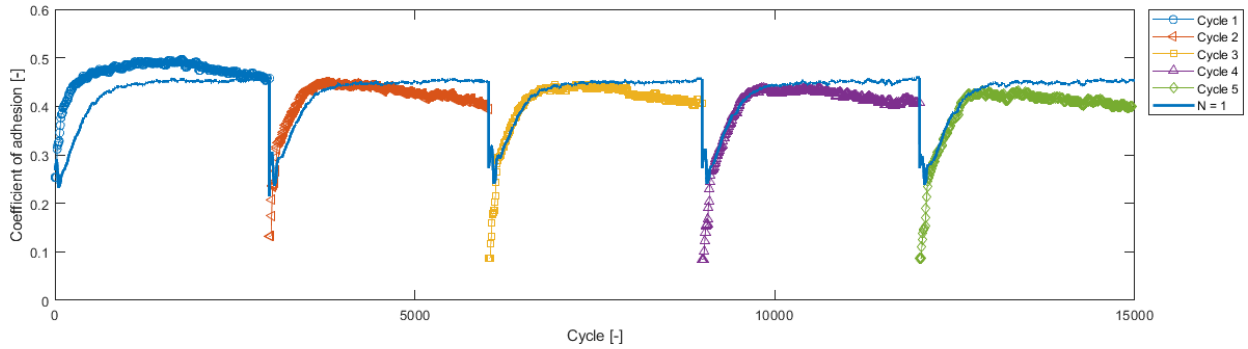

Figure 61. TOR-FM A, condition 4; symbols: SUROS experiment, application 1 to 5; line: TOR product model result

(b) FM-B

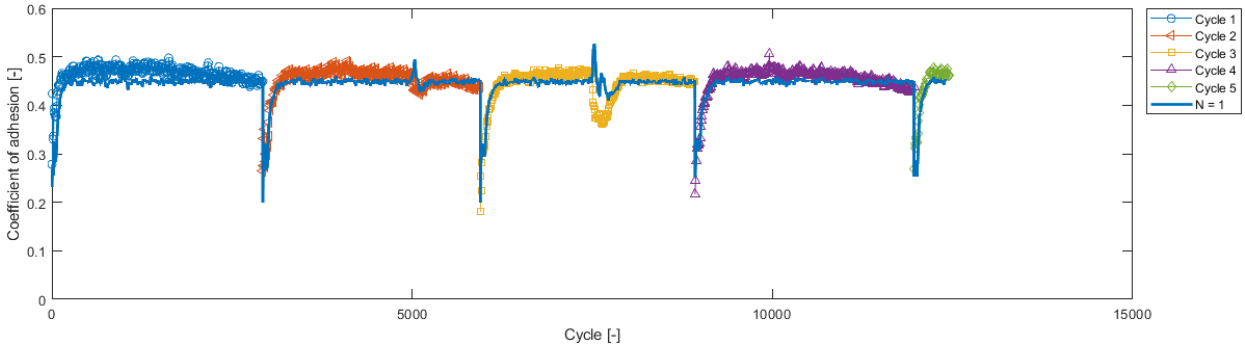

Figure 62. TOR-FM B, condition 1; symbols: SUROS experiment, application 1 to 5; line: TOR product model result

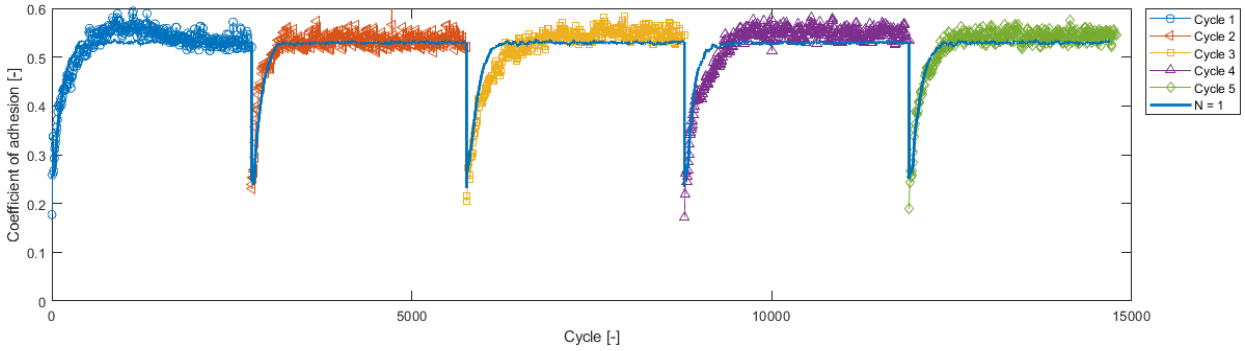

Figure 63. TOR-FM B, condition 2; symbols: SUROS experiment, application 1 to 5; line: TOR product model result

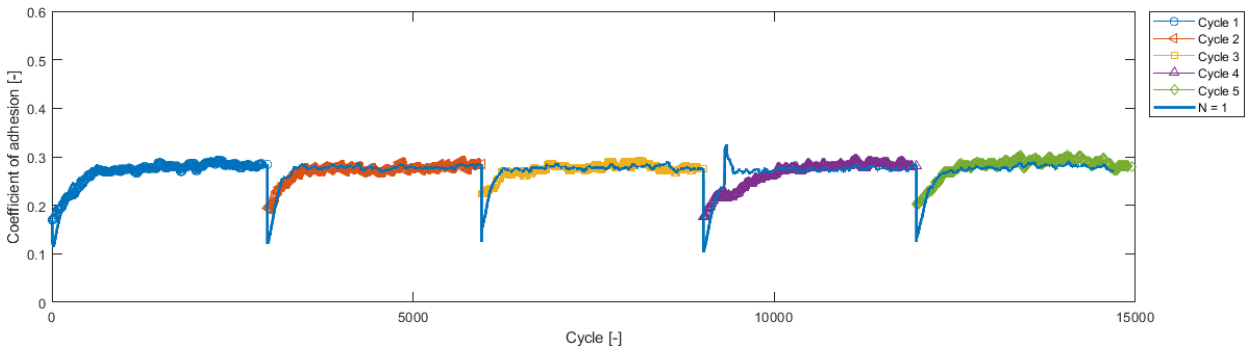

Figure 64. TOR-FM B, condition 3; symbols: SUROS experiment, application 1 to 5; line: TOR product model result

Note: Experimental adhesion data were increased by 22 percent to match the coefficient of adhesion of uncontaminated conditions.

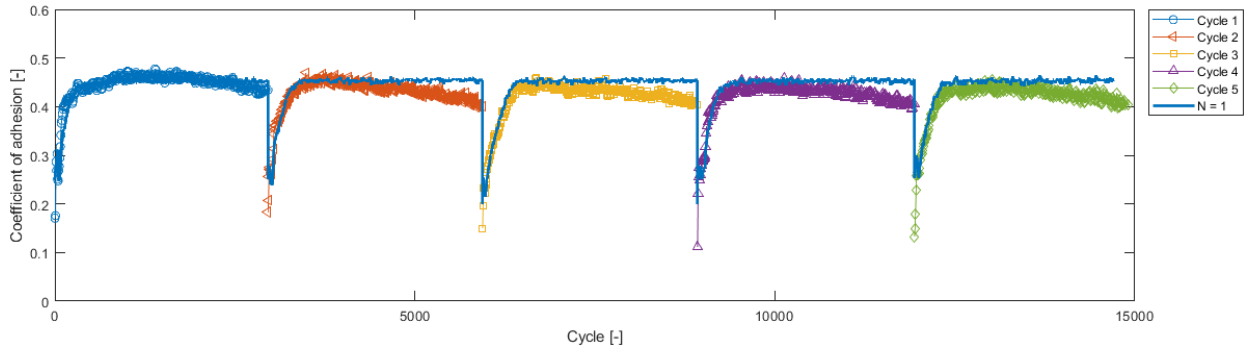

Figure 65. TOR-FM B, condition 4; symbols: SUROS experiment, application 1 to 5; line: TOR product model result

(c) FM-Oil

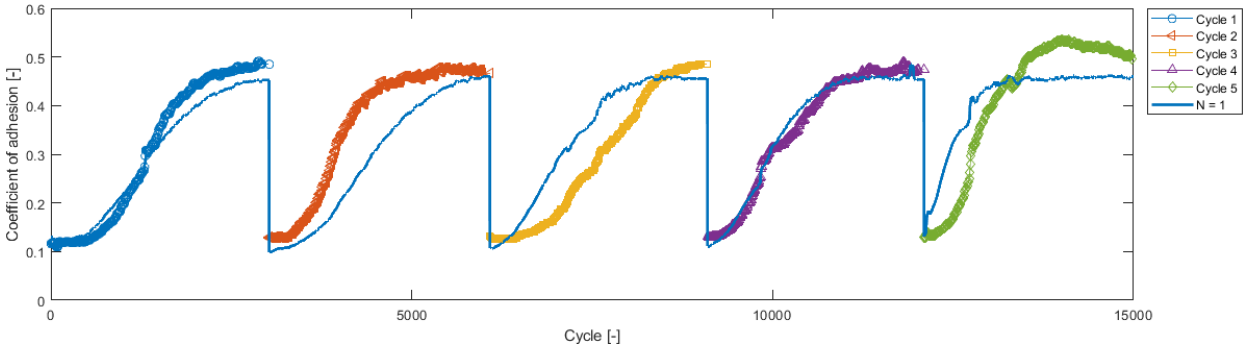

Figure 66. TOR-oil, condition 1; symbols: SUROS experiment, application 1 to 5; line: TOR product model result

Note: Experimental adhesion data were increased by 29 percent to match the coefficient of adhesion of uncontaminated conditions.

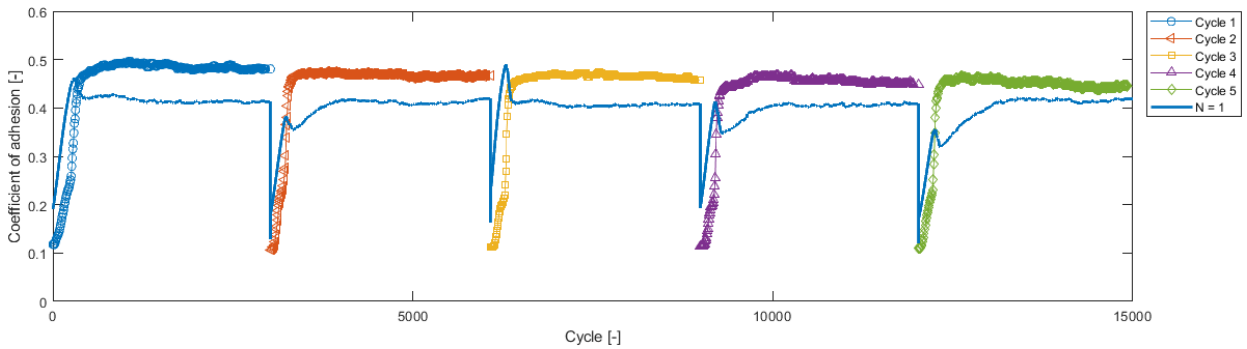

Figure 67. TOR-oil, condition 2; symbols: SUROS experiment, application 1 to 5; line: TOR product model result

Note: Experimental adhesion data were increased by 29 percent to match the coefficient of adhesion of uncontaminated conditions.

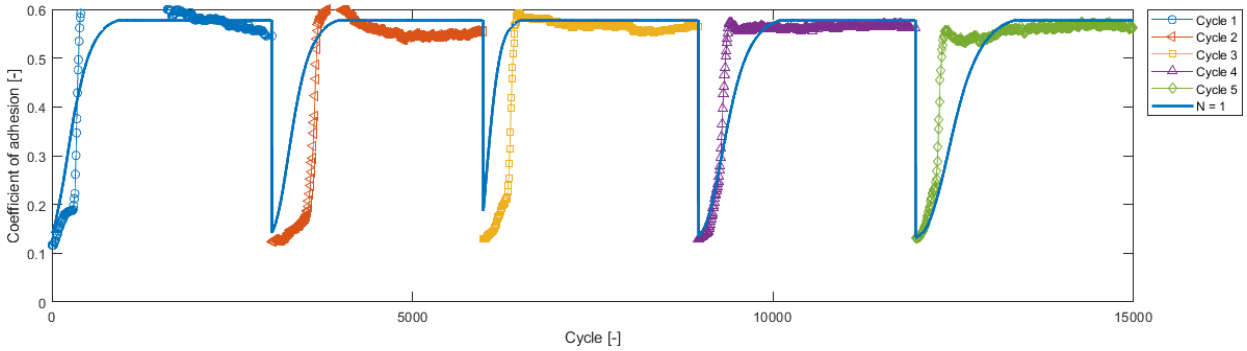

Figure 68. TOR-oil, condition 3; symbols: SUROS experiment, application 1 to 5; line: TOR product model result

Note: Experimental adhesion data were increased by 29 percent to match the coefficient of adhesion of uncontaminated conditions.

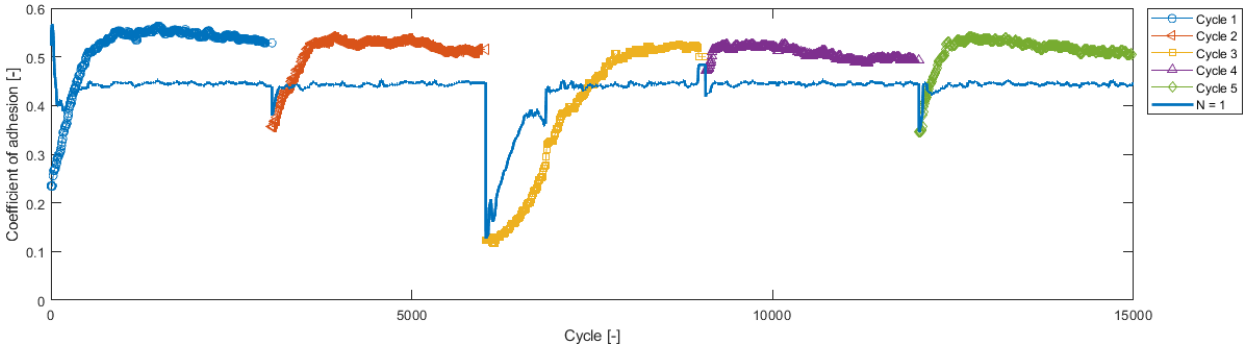

Figure 69. TOR-oil, condition 4; symbols: SUROS experiment, application 1 to 5; line: TOR product model result

Note: Experimental adhesion data were increased by 29 percent to match the coefficient of adhesion of uncontaminated conditions.

(d) FM-Grease

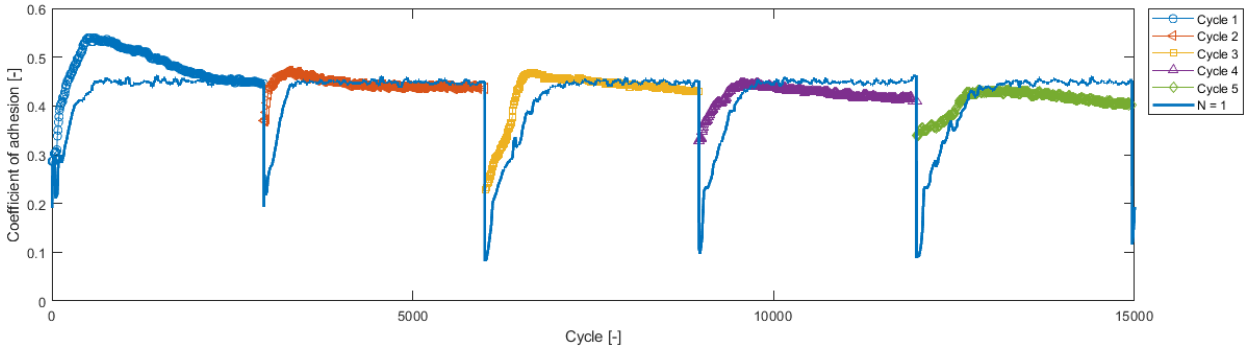

Figure 70. TOR-grease, condition 1; symbols: SUROS experiment, application 1 to 5; line: TOR product model result

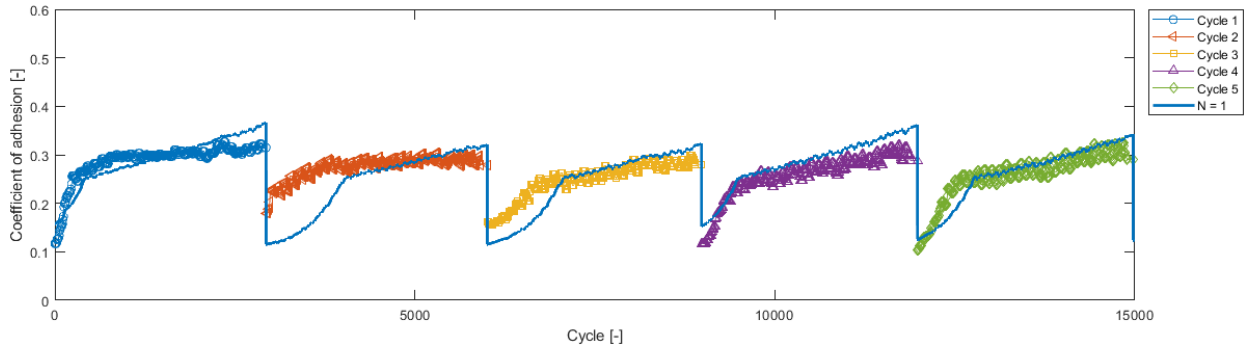

Figure 71. TOR-grease, condition 2; symbols: SUROS experiment, application 1 to 5; line: TOR product model result

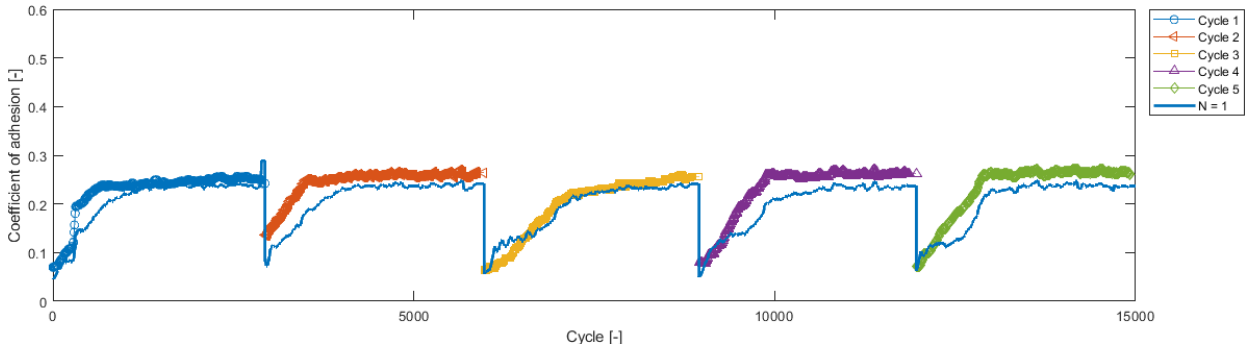

Figure 72. TOR-grease, condition 3; symbols: SUROS experiment, application 1 to 5; line: TOR product model result

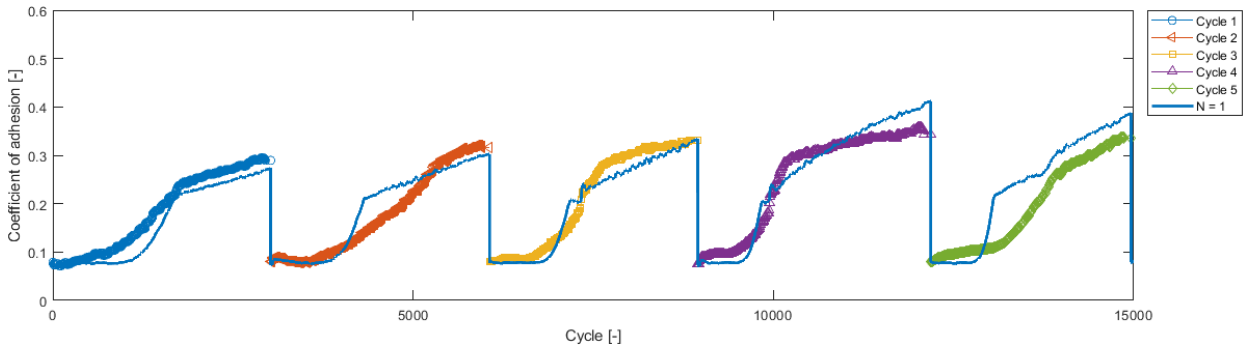

Figure 73. TOR-grease, condition 4; symbols: SUROS experiment, application 1 to 5; line: TOR product model result

(e) FM-Hybrid

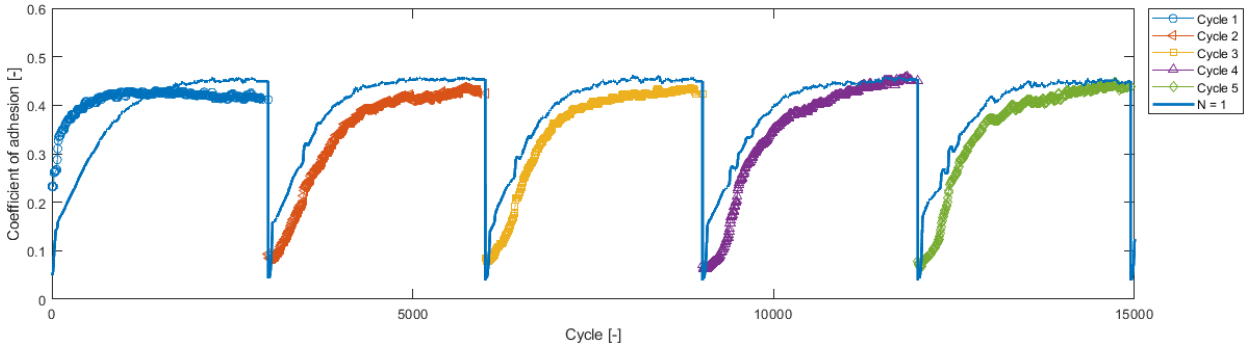

Figure 74. TOR-hybrid, condition 1; symbols: SUROS experiment, application 1 to 5; line: TOR product model result

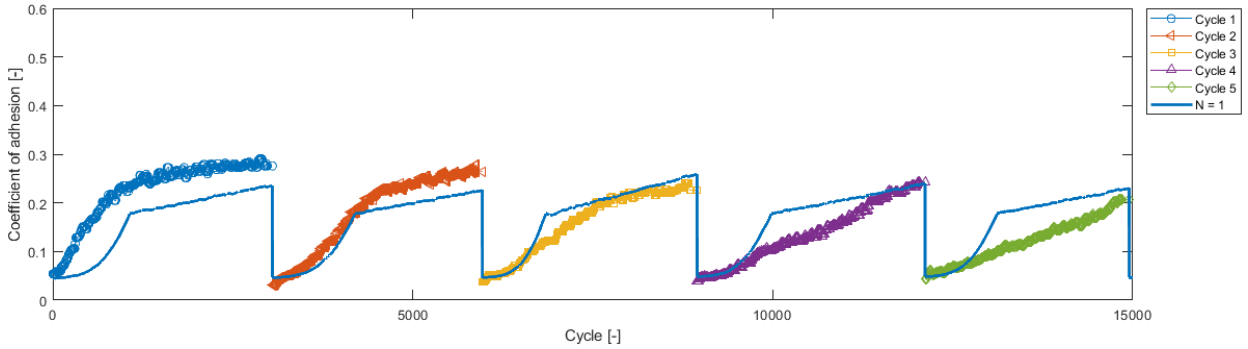

Figure 75. TOR-hybrid, condition 2; symbols: SUROS experiment, application 1 to 5; line: TOR product model result

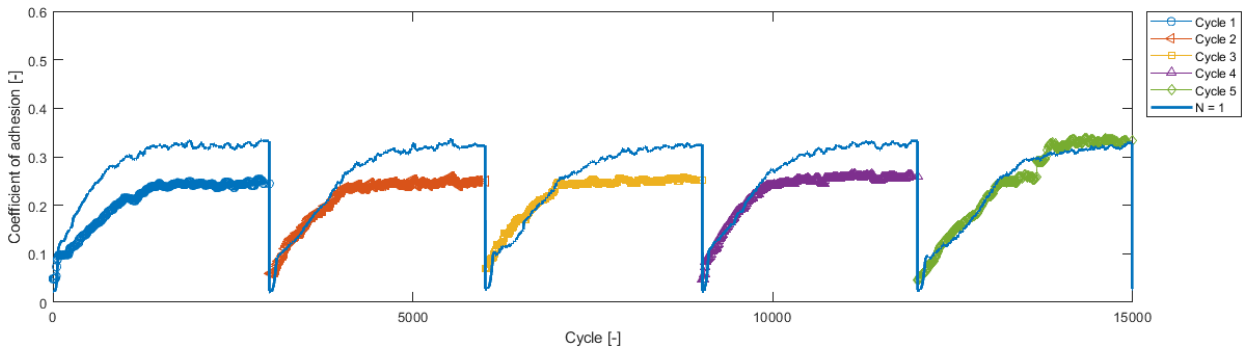

Figure 76. TOR-hybrid, condition 3; symbols: SUROS experiment, application 1 to 5; line: TOR product model result.

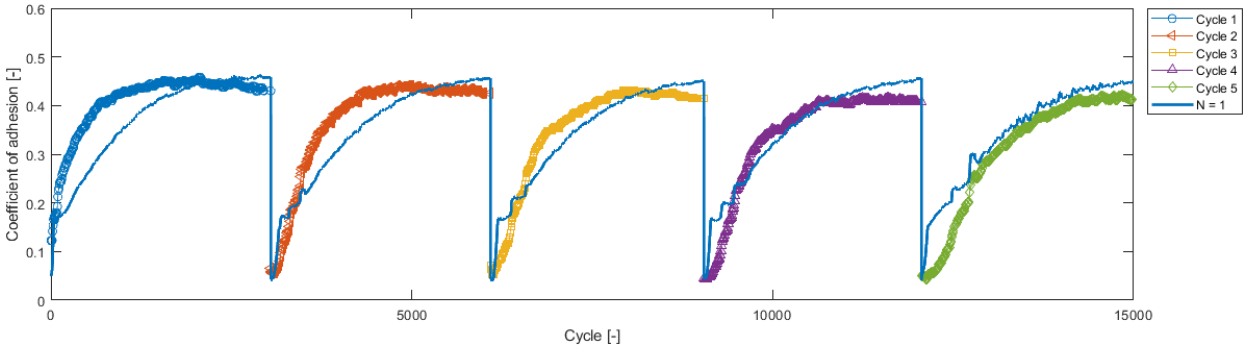

Figure 77. TOR-hybrid, condition 4; symbols: SUROS experiment, application 1 to 5; line: TOR product model result

Appendix F.
Model parameterization: Full-Scale Experiments

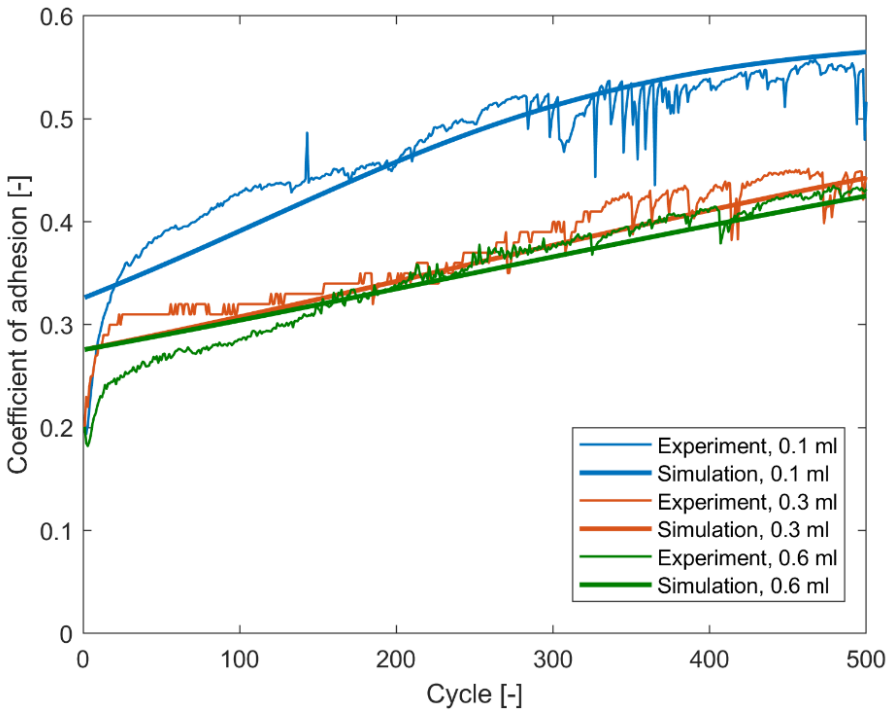

Figure 78. TOR-FM A, thin lines: FSR experiments; thick lines: TOR product model result

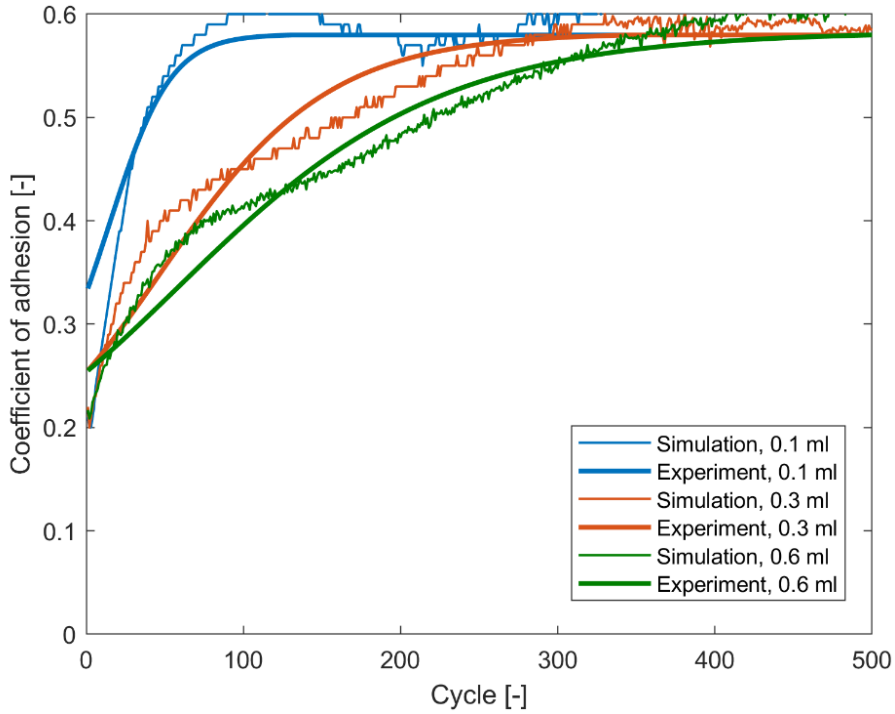

Figure 79. TOR-FM B, thin lines: FSR experiments; thick lines: TOR product model result

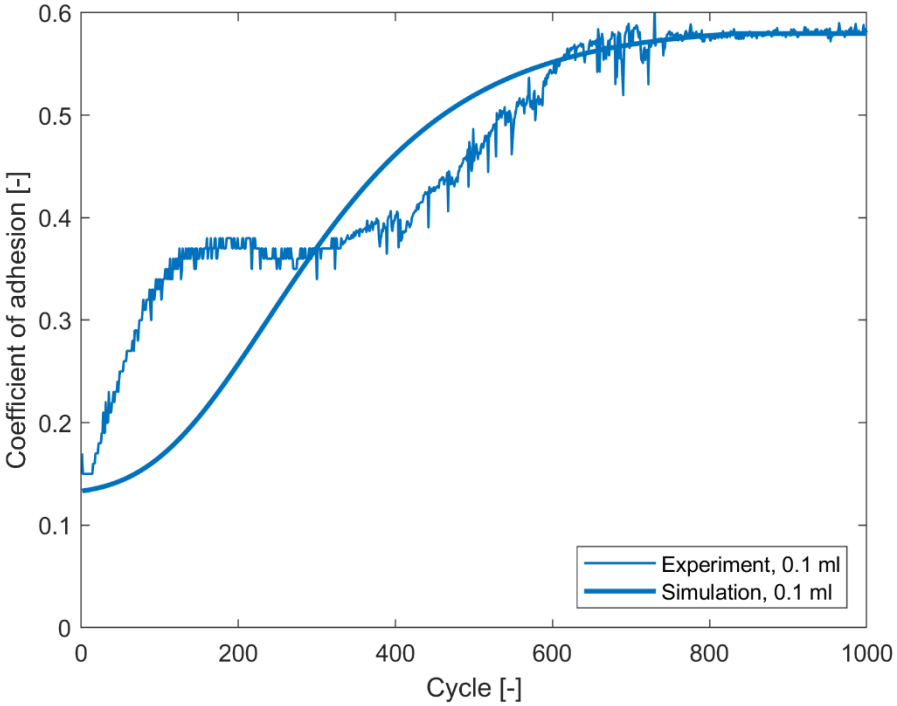

Figure 80. TOR-oil, thin lines: FSR experiments thick lines: TOR product model result

Abbreviations and Acronyms

ACRONYM	EXPLANATION
CoT	Coefficient of traction
FM	Friction modifier
FSR	Full-scale rig
GUI	Graphical user interface
ICRI	International Collaborative Research Initiative
RCF	Rolling contact fatigue
SUROS	Sheffield University rolling sliding
SWR	Scaled wheel rig
TOR	Top-of-rail
VTI	Vehicle-track interaction